universität wien

DIPLOMARBEIT

DNS-Demethylierungs Effekte in normalen humanen Fibroblasten

angestrebter akademischer Grad

Magister/Magistra der Naturwissenschaften (Mag. rer.nat.)

Verfasser:	Lucas Johannes Rudigier
Matrikel-Nummer:	a0304392
Studienrichtung /Studienzweig:	Biologie/ Mikrobiologie-Genetik
Betreuerin / Betreuer:	Denise P. Barlow, Ph.D.
Wien, am 27.05.2009	

universität wien

Diploma Thesis

DNA demethylation effects in normal human fibroblasts

The work presented in this thesis was undertaken in the lab of Dr. Denise Barlow from April 2008 to May 2009 at the Ce-M-M- Research Center for Molecular Medicine of the Austrian Academy of Sciences; c/o Institute of Genetics, Max F. Perutz Laboratories, Vienna Biocenter, Dr. Bohr-Gasse 9/4, 1030 Vienna, Austria

Author:	Lucas Johannes Rudigier
Student-Number:	a0304392
Department:	Biology/ Microbiology-Genetics
Supervisor:	Denise P. Barlow, Ph.D.
Vienna, 27th of May 2009	

Table of Contents

A. Zusammenfassung

Die DNS-Methylierung ist eine epigenetische Modifikation, die in der Ausprägung des Phänotyps mitwirkt ohne die DNA Sequenz zu verändern und somit eine bedeutende Rolle in der Entwicklung als auch bei Krankheiten spielt. Die genomische Prägung wird definiert als parental-spezifische monoallelische Expression. Eine wesentliche Eigenschaft der genomischen Prägung ist, dass geprägte Gene geclustert vorliegen und innerhalb dieses Clusters ein Gen für eine makro-nicht-kodierende RNS kodiert. Es wurde bereits gezeigt, dass makro-nicht-kodierende RNS durch DNS-Methylierung kontrolliert werden können. In der Maus wird beispielsweise die nicht kodierende RNS *Airn* ausschließlich vom paternalen Allel exprimiert, da dieses keine DNS-Methylierung („der Imprint“) am Promotor aufweist. Das maternale Allel hingegen weist eine DNS-Methylierung am Promotor auf und sorgt somit für die Unterdrückung der Expression von *Airn*. *Airn* sorgt für die Stilllegung von *Igf2r* in cis und führt weiters dazu, dass der Promotor von *Igf2r* methyliert wird. Dadurch wird *Igf2r* nur vom mütterlichen Allel exprimiert. Aufgrund dessen stellt sich die Frage, ob die DNS-Methylierung die Expression von makro-nicht-kodierenden RNS(s) in allen geprägten Clustern von Säugern kontrolliert. Ich setzte ein *in vitro* System für die Demethylierung von humanen Vorhaut-Fibroblasten (Hs-27) auf. Für diesen Zweck verwendete ich einen S-Phasen abhängigen DNS Methyltransferaseinhibitor namens 5-aza-2’-deoxycytidin (Decitabine), der die „Erhaltungs“-DNS Methyltransferase DNMT1 abfängt und somit deren enzymatische Reaktion verhindert. Dies führt dann zu einem passiven Verlust der DNS Methylierung. Um den DNS-Methylierungszustand zu überprüfen, verwendete ich DNS Blot Analyse in Kombination mit methyl-sensitiven Restriktionsenzymen. Die Genexpression überprüfe ich mittels qPCR und RNS Expressions-Tiling-Arrays. Das Resultat zeigt, dass die Behandlung von Hs-27 Zellen mit Decitabine zu einem geringen Verlust der DNS-Methylierung in den untersuchten Regionen führt. Die Expression der nicht-kodierende RNS *H19* und des *MAGE-A1* Gens wurde durch die Decitabine Behandlung induziert. Es kann jedoch nicht ausgeschlossen werden, dass die induzierte Expression aufgrund eines sekundären Effektes von Decitabine zustande kam anstatt ein direkter Effekt der DNS-Demethylierung zu sein, da diese nicht komplett war.

B. Abstract

DNA methylation is an epigenetic modification that contributes to the phenotype without changing the DNA sequence, and has a high impact on development and disease. Genomic imprinting is defined as parental-specific monoallelic gene expression. A key feature of genomic imprinting is that most imprinted genes are clustered and contain at least one macro non-coding RNA (ncRNA). It has been shown that macro ncRNAs can be controlled by DNA methylation. For instance, the mouse *Airn* ncRNA is exclusively expressed from the paternal allele due to the absence of a methylation mark ("the imprint") on its promoter. The maternal allele instead contains a methylated *Airn* promoter, which prevents *Airn* expression from this allele. *Airn* silences the *Igf2r* protein-coding gene *in cis* and triggers methylation of the *Igf2r* promoter. *Igf2r* is therefore only expressed from the maternal allele. Therefore it is tempting to hypothesize whether DNA methylation controls macro ncRNA expression in all mammalian imprinted gene clusters. I set up an *in vitro* system to demethylate human foreskin fibroblasts (Hs-27 cells). For this purpose I used the S-phase dependent DNA methyltransferase inhibitor 5'aza-2'-deoxycytidine (Decitabine) that leads to the trapping of the maintenance DNA methyltransferase DNMT1 during replication, thus inhibiting its enzymatic properties and resulting in a passive loss of DNA methylation. To check the cells DNA methylation status, I used Southern blot analysis with methylation-sensitive restriction enzymes. Gene expression was assayed by qPCR and by RNA expression tiling array. These results reveal that the treatment with Decitabine leads to a slight partial loss of DNA methylation on the regions subjected to investigation. The *H19* ncRNA and the *MAGE-A1* gene showed an induction of gene expression upon DAC treatment. However, as the loss of DNA methylation was not complete, it can not be excluded, that the observed expression of DNA methylation associated genes was due to secondary effects of the DAC treatment rather than a reduction of DNA methylation.

1. Introduction

1.1 DNA methylation

1.1.1 Overview

DNA methylation is an epigenetic modification whose correct setting is essential for normal development. In mammals, the target is a 5' cytosine located next to a guanine, separated by a phosphate group, and is called CpG dinucleotide. This mark, once established during development, is stable propagated through subsequent cell divisions. DNA methylation plays pivotal roles in genomic imprinting, X-inactivation, formation of centromers and silencing of retroviral elements (retrotransposons). Besides its contribution to develop a healthy organism, DNA methylation is a fundamental player in a variety of disease for instance Rett-, ICF-syndrome (immunodeficiency, centromere instability, facial abnormalities) and cancer. Although a number of studies have shown that DNA methylation correlates with transcriptional repression, up to now evidence proving that DNA methylation is responsible for gene silencing is lacking. However, genomic imprinting states the exception and illustrates that DNA methylation can be the key player for transcriptional repression of macro ncRNAs.

1.1.2 DNA methyltransferases

The first DNA methyltransferase to be identified was *Dnmt1*, the maintenance methyltransferase (Bestor and Ingram 1983; Bestor 1988). The hypothesis of a maintenance mechanism dates back to the 1970s. Holliday, Plugh and Riggs proposed a model by which an, at that time unidentified, enzyme is involved in a replication dependent manner to inherit the marks onwards to the unmethylated, newly synthesized strand (Holliday and Pugh 1975; Riggs 1975). The CpG dinucleotide is a palinodromic sequence. Through semiconservative replication one parental strand remains methylated at the CpG site whereas the newly synthesized strand contains unmethylated CpG sites. In agreement with this model, it was shown that the main targets for Dnmt1 are CpG sites (Bestor and Ingram 1983). In more detail it was reported, that Dnmt1 has a 5-30 fold higher preference for hemimethylated DNA, al-

though this does not exclude any *de novo* activity (Yoder, Soman et al. 1997; Bestor 2000). Knock out of *Dnmt1* is embryonic lethal at E9.5 showing abnormal imprinted gene expression and reactivation of retrotransposons (see Table 1) (Li, Bestor et al. 1992; Li, Beard et al. 1993; Lei, Oh et al. 1996). A question considered with high curiosity was to elucidate if Dnmt1 is the sole protein that is involved in DNA methylation. The key experiment was conducted by Lei et al and brought the final evidence: Upon deleting *Dnmt1*, *de novo* methylation marks were not impaired (Lei, Oh et al. 1996). This demonstrated that additional enzymes are involved in the DNA methylation process. Importantly, annotations of expressed sequence tags served as a profound tool for the characterization and identification of the *de novo* enzymes. The first candidate, Dnmt2 showed no DNA methyltransferase activity, instead it is responsible for methylation of the $tRNA^{Asp}$ anticodon loop at cytosine 38 (Yoder and Bestor 1998; Goll, Kirpekar et al. 2006; Rai, Chidester et al. 2007). Therefore knock out of this protein had no effect on the DNA methylation status. Identification, through EST search, of Dnmt3a and Dnmt3b followed (Okano, Xie et al. 1998). Dnmt3a is responsible for setting imprints during spermatogenesis or oogenesis. The lack of this enzyme or an additional factor Dnmt3L which lacks methyltransferase activity but enhances the activity of Dnmt3a and Dnmt3b leads to failure in the establishment of imprints (Hata, Okano et al. 2002; Kaneda, Sado et al. 2004). The disruption of Dnmt3a is lethal and embryos die 4-8 weeks after birth (see Table 1). In addition, the major function mediated by Dnmt3b is the silencing of repetitive elements. Knock out experiments have shown that *Dnmt3b*$^{-/-}$ embryos display demethylated satellite repeats and die at E14.5. Moreover, in humans a point mutation in the catalytic motif of DNMT3B leads to the hypomethylation of satellite repeats that are primarily located at the pericentromeric region of chromosome 1, 9 and 16. This observation is called the ICF syndrome: **i**mmunodeficiency, **c**entromere instability and **f**acial abnormality (Ehrlich 2003). Further, the structural motifs outline their relationship to each other and highlight that DNA methylation is a conserved mechanism, not restricted to eukaryotes. In prokaryotes DNA methylation exerts its function as a host immune system by defending the organism from invading parasitic elements. Besides preventing the transposition of transposons in eukaryotes, in this way also acting as a defense system, DNA methylation has also an important impact on development.

enzyme	main activity	phenotype
Dnmt1	maintenance methyltransferase preference for hemimethylated DNA	genome wide loss of DNA methyaltion, activation of retrotransposons, ectopic X-inactivation and impaired expreeion of imprinted genes, embryonic lethal at E9.5
Dnmt2	no DNA methyltransferase activity, methyaktion of $tRNA^{Asp}$ anticodon loop	no effect
Dnmt3a	de novo methyltransferase	aberrant establishment of imprints in oogeneis or spermatogenesis, postnatal lethality at 4-8 weeks, male sterility
Dnmt3b	de novo methyltransferase	hypomethylated minor satellite repeats, embryonic lethal at E 14.5
Dnmt3L	lacks methyltransferase activity supports the activity of Dnmt3a and Dnmt3b	fail to establish imprints, sterility, hypomethylation of retrotransposons and pericentromeric repeats

Table 1: Functional aspects of the DNA methyltransferases

This illustrates that the process of DNA methylation is not restricted to a certain kingdom and conservation is reflected in the structure of all DNA methyltransferases, mainly the catalytic domain. In all eukaryotic DNA methyltransferases (Dnmt1, Dnmt2, Dnmt3a, Dnmt3b) this domain is highly related to bacterial methyltransferases (Bestor 1988). DNA methyltransferases contain up to 10 motifs whereby 6 of them are highly conserved and involved in the enzymatic reaction. In contrast, the N-terminal domain fulfils regulatory functions and thus differs in function and length between the different Dnmts. Dnmt1, a 1620 amino acid long protein, contains an N-terminal domain that is separated from the catalytic domain by a Glycin-Lysine repeat region. It exhibits certain specific functional motifs. For instance it contains a nuclear localization signal and can interact with PCNA. The RFT motif is responsible for replication foci targeting and thus provides the ability to discriminate for hemimethylated DNA. Additionally, a cysteine-rich domain for interaction with DNA sequences and a BAH motif for protein-protein interactions are also present. Dnmt2 is 415 amino acids in length and completely lacks the N-terminal domain. Therefore no maintenance function would be predicted. It was shown that this enzyme also completely lacks *de novo* DNA methyltransferase activity (Okano, Xie et al. 1998).

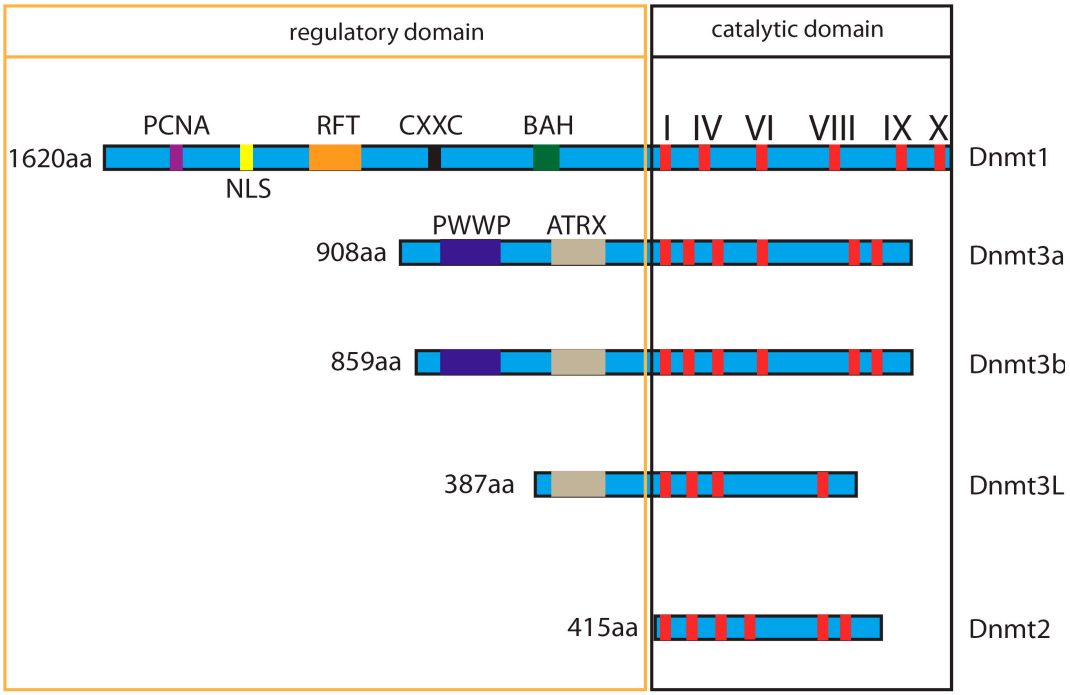

Figure 1: The structure of the eukaryotic DNA methyltransferases: black box includes the catalytic domains of Dnmt1, Dnmt3a, Dnmt3b, Dnmt2 and Dnmt3L that are conserved and mediate the enzymatic reaction with the exception of Dnmt3L and Dnmt2. Orange box includes the regulatory N-terminal domain, that is different in length between the different Dnmts. (PCNA) domain for the interaction with PCNA during replication, (NLS) nuclear localization signal, (RFT) replication foci targeting, (CXXC) cysteine-rich domain for DNA sequence binding, (BAH) protein-protein interaction domain, (PWWP) heterochromatin association domain, (ATRX) C2-C2 zinc-finger domain involved in protein-protein interactions (Cheng and Blumenthal 2008)

The N-terminal structure of Dnmt3a, a protein of 908 amino acids in length, contains a PWWP domain and a cysteine rich domain (ATRX). The former one is responsible for DNA binding and the latter one mediates protein-protein interactions. The same motifs are present in the structure of Dnmt3b, an 859 amino acid long enzyme. It has been shown that the activity of *de novo* enzymes is enhanced by the Dnmt3L protein (Hata, Okano et al. 2002). With 387 amino acids it is much shorter in length and shows no methyltransferase activity (Figure 1).

1.1.3 The enzymatic mechanism of DNA methylation

The covalent “Michael addition” is the main reaction mechanism of how the DNA methyltransferase modify CpG sites in the double helix, which then reside in the major groove of the B-DNA. As mentioned above, the catalytic domain is conserved between eukaryotes and prokaryotes and is involved in the enzymatic reaction. All DNA methyltransferases (Dnmts) share an IV and VI motif in their catalytic

domain. The Dnmt targets the cytosine on carbon 6 via motif IV, which provides a reactive thiol group. As a consequence a covalent bond at position 6 between the Dnmt and cytosine is formed, thereby converting the carbon 5 into a highly reactive carbanion. The carbanion at position 5 is then able to a nucleophil attack of the methyl donor, which is for all Dnmts *S*-adenosyl-L-methionin. This leads to the addition of a methyl group to position 5 of the cytosine. The base is additionally targeted by the motif VI, which stabilizes the enzyme-cytosine intermediate via hydrogen bonds to the amino group on position 4. Subsequently, the enzyme is released through proton abstraction at position 5 and the double bond between carbon 5 and 6 is reverted. This step is also known as β-elimination (Figure 2). A major mainly unsolved issue that needs further investigation is to find out how Dnmts are targeted to their sites. It has been shown that Dnmt1 interacts during replication with PCNA (Leonhardt, Page et al. 1992). More recently, it has been reported that the UHRF1 protein is able to interact via the SRA domain with hemimethylated DNA. Thereby the methylated cytosine undergoes base flipping by rotating around the phosphate backbone breaking up the hydrogen bonds with guanin and reaching out of the double helix. In this way UHRF1 is able to interact stably with the DNA and recruits Dnmt1 to their target sites (Arita, Ariyoshi et al. 2008; Hashimoto, Horton et al. 2008). How *de novo* Dnmts target sites subjected to DNA methylation still remains elusive.

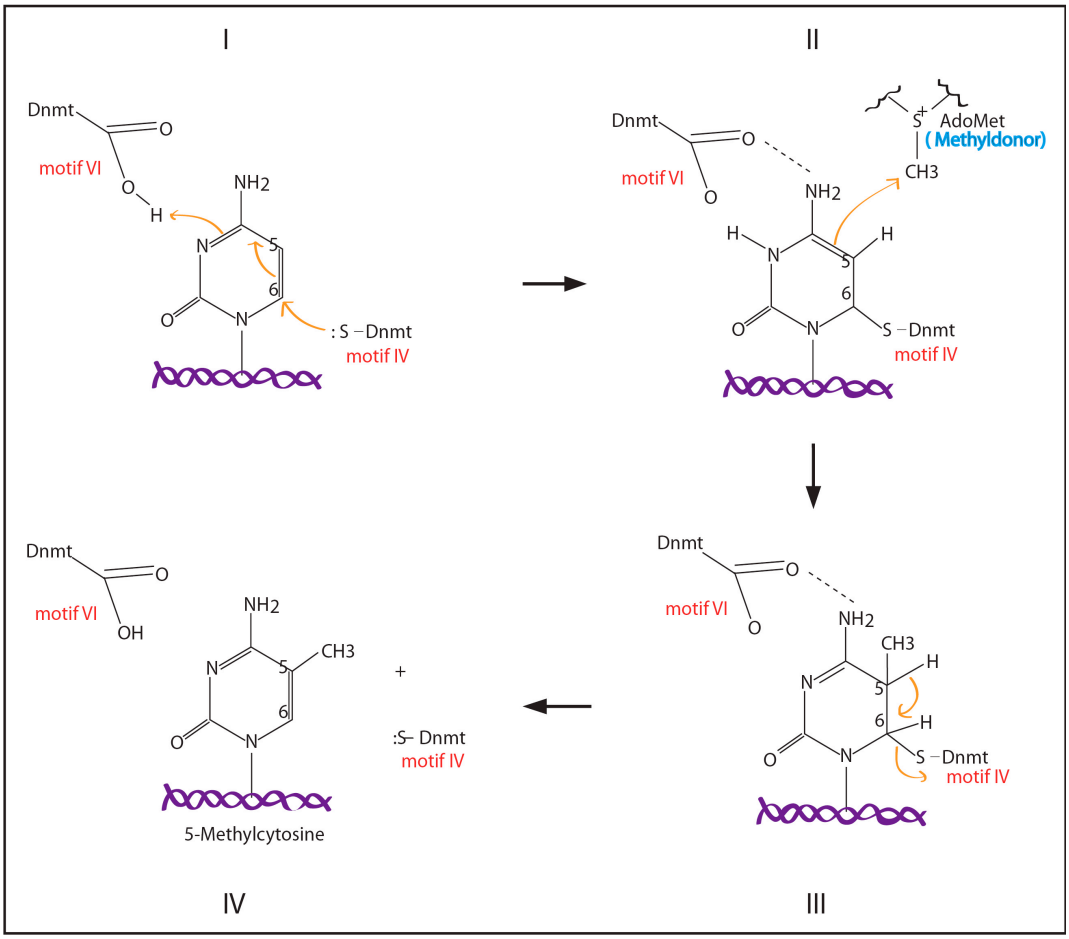

Figure 2: Covalent "Michael addition" reaction of the DNA methyltransferase: (**I**) The Dnmt targets carbon 6 via the motif IV that provides a thiol group and via motif VI nitrogen at position VI. (**II**) A covalent bond is formed between the Dnmt and cytosine and this intermediate is in addition stabilized via hydrogen bonds between a proton of the amino group at position 4 and oxygen of motif VI. The active carbanion at position 5 attacks the methyl group from the donor *S*-adenosyl-L-methionin (**III**). Proton abstraction at position 5 (β-elimination) leads to the release of the Dnmt from 5-Methylcytosine (**IV**).

1.1.4 CpG islands vs. CpG sites

70% of all CpG sites throughout the human genome are methylated (Ehrlich, Gama-Sosa et al. 1982). Most of these methylated CpG sites are located in repetitive elements residing in intergenic and/or intronic regions (Miranda and Jones 2007). Interestingly, the CpG dinucleotide is underrepresented in the human genome due to the ease of subjecting methylated CpG sites to a deamination reaction. Methylated CpG sites are a mutational hotspot and are converted to a thymine thus leading to a permanent inactivation of retrotransposons. Nevertheless, a small proportion of CpG dinucleotides has accumulated to a high density in certain promoter regions. In this context the CpG sites are called CpG islands. A general definition

states these stretches as CpG sites longer than 500bp with CpG content greater than 55% (Takai and Jones 2002). CpG islands are located at the 5' region of a gene and can spread through the first exon (Bird 1986). Promoters of approximately 50% of the human genes contain CpG islands including housekeeping genes and a restricted number of tissue specific genes. The hallmark of a CpG island is that they are free of DNA methylation in a healthy cell, with exceptions like the inactive X-chromosome in females and CpG island promoters of imprinted genes.

A common hallmark of cancer is aberrant DNA methylation. A cancer cell often reflects this by hypomethylated repetitive elements and hypermethylated CpG islands on tumor suppressor genes or housekeeping genes. In this context DNA methylation contributes strongly to chromosomal instability (Esteller 2008).

1.1.5 DNA methylation and gene expression

DNA methylation can affect the transcription of genes. This is primarily by the fact that methylated CpG sites are located in the major groove, the place were transcription factors bind to their target sequence and initiate the transcription of a gene. However when the CpG sites are methylated the binding of transcription factors can be prevented as it was shown for the insulator CTCF in case of the *Igf2* cluster (Bell, West et al. 2001).

In addition, of all epigenetic modifications DNA methylation is the only one that can modify the nucleotide sequence directly. In this context it should be noted that the DNA sequence in eukaryotes is packaged into chromatin. Chromatin contains the nucleotide sequence and associated proteins. The sole unit of the chromatin is the nucleosome that consists of basic histone proteins. One single nucleosome is made up of 8 histone proteins namely two of each H2A, H2B, H3 and H4. Roughly 146bp of DNA are wrapped around one nucleosome. Of great importance is that chromatin is either present in a densely packed conformation, that is referred to as heterochromatin or in a less densely packed conformation, named euchromatin. Both of these stages, heterochomatin and euchromatin correlate with chemically modified residues in the amino-terminal tails of histone proteins that protrude out of

the nucleosome. The most prominent ones are histone-methylation, -acetylation and -phosphorylation. Euchromatin-associated active marks are acetylation of histone 3 and 4 (H3ac/H4ac), methylation of lysine 4 of histone 3 (H3K4me). Heterochromatin-associated repressive marks are histone methylation of lysine 9 of histone 3 (H3K9me), H3 trimethylation of lysine 27 (H3K27me3), H4 methylation of lysine 20 (H4K20me) (Jenuwein and Allis 2001). Importantly, DNA methylation and histone modifications are linked to each other. Methylated DNA can serve as a target for certain proteins. For instance it was shown in a study of Jones et al that the methyl-CpG binding protein MeCP2, a repressor of transcription, binds to methylated CpG sites. MeCP2 interacts with the Sin3a complex that has histone deacetylase activity. Thereby acetylation marks are removed and an altered closed chromatin structure is established. Consequently, initiation of the transcription is prevented (Jones, Veenstra et al. 1998).

1.1.6 DNA methylation has 4 main roles

DNA methylation has an essential role in genomic imprinting (definition see in 1.2) and X-inactivation. An initial study of Li et al pointed out that mice which lack the Dnmt1 on both alleles show biallelic repression of the Igf2 (normally expressed only from the paternal allele) and Igf2r gene (normally expressed only from the maternal allele) as well as biallelic expression of the H19 ncRNA (normally expressed only from the maternal allele). Therefore, this shows that DNA methylation is essential for genomic imprinting (Li, Beard et al. 1993). X-inactivation is a developmental dosage compensation process in females by which one of the two X chromosomes gets inactivated. The role of DNA methylation in X-inactivation is to regulate expression of the macro ncRNA *Xist*. On the inactive chromosome the *Xist* promotor is unmethylated leading to *Xist* expression. On the active X chromosome the *Xist* promotor is hypermethylated, thus preventing the expression of *Xist* on the active X chromosome (Norris D.P. 1994). DNA methylation also plays an important role in the formation of centromers. Segregation of the chromosomes during mitosis is achieved through the attachment of microtubules to the centromere, a highly heterochromatic region. The centromere consists of repetitive DNA elements that are tandemly arranged and the basic unit is the satellite repeat. The correct formation of the centromere and accu-

rate chromosome segregation relies on DNA methylation. For instance, it has been shown that a point mutation in the DNMT3B enzyme correlates with hypomethylated satellite repeats that are located within the pericentromeric regions of chromosome 1, 9 and 16 causing the ICF syndrome (immunodeficiency, centromere instability and facial abnormality) (Ehrlich 2003). Another feature that highlights the importance of DNA methylation is the silencing of retroviral relicts that inserted in the human genome through evolution. Transposons can be subdivided into two classes: retrotransposons (class I) which move via an RNA intermediate into new sites or DNA transposons (class II) which copy themselves via a “cut and paste” mechanism with the help of the transposase into a new genomic location. These elements are subject to DNA methylation to prevent their transposition. Therefore DNA methylation contributes strongly to chromosomal stability and prevents translocation and DNA rearrangements (Bourc'his and Bestor 2004; Goll and Bestor 2005).

1.2 Genomic imprinting as a model for studying epigenetic mechanisms

1.2.1 Genomic imprinting – overview

Uniparental disomy (UPD) is a phenomenon in which an organism contains a duplication of a chromosome or parts of it from one parent and lacks this or these parts from the other parent. In addition to uniparental duplications also uniparental deletions can happen. Individuals that carry a deletion on a chromosome, which was inherited from one parent and the respective wild type chromosome inherited from the other parent have uniparental deletions. This laid the foundation for studying the phenomenon of genomic imprinting. Key experiments were conducted in the 1980s. Through nuclear transfer experiments diploid uniparental embryos in different combinations of the genomes were set up. Androgenetic embryos contain two paternal genomes whereas gynogenetic embryos harbor twice the maternal genome, in contrast to wild type embryo that contains a paternal and maternal genome. The results showed that the only viable combination is the embryo that received a paternal and maternal chromosome set (McGrath and Solter 1984; McGrath and Solter 1984; Surani, Barton et al. 1984). These results pointed out that gynogenetic embryos have defects in the tissues that contribute to development of placenta and androge-

netic embryos had defects in embryonic tissues, resulting in the death of the embryo (Barlow and Bartolomei 2007). Experiments with some UPDs in mice have shown that opposite outcomes are the results when single chromosomes or pieces are present either twice from the mother or from the father (Cattanach and Kirk 1985). These outcomes were manifested in the size of the offsprings. These experiments pointed out that for a proper development of an organism both genomes, the maternal and the paternal, are essential. However, inbred mice with the identical sequence on both alleles are also subjected to genomic imprinting, thus indicating that the mechanism is not restricted to the DNA sequence itself. However, more likely an epigenetic mechanism must operate to treat the alleles differentially. In this way the only time point to distinguish between the identical maternal and paternal allele is when they are separated during gametogenesis.

The discovery of the first imprinted genes is dated back in the early 1990s, when the imprinted *Igf2r* gene on mouse chromosome 17 was observed (Barlow, Stoger et al. 1991). The discovery of the imprinted *Igf2* on mouse chromosome 7 followed (DeChiara, Robertson et al. 1991) with the imprinted non-coding RNA *H19* (Bartolomei, Zemel et al. 1991).

1.2.2 Characteristics of genomic imprinting

Genomic imprinting is defined as parental-specific monoallelic gene expression. Diploid organisms contain a set of chromosomes inherited from the mother and from the father. Thus, each gene is present twice in the organism and the majority of genes show biallelic expression. For a small subset of genes this is not the case. Their expression is either restricted to the maternal or the paternal copy, and these genes are so-called imprinted genes.

Up to now approximately 90 imprinted genes have been identified and most but not all of them reside in clusters (http://www.mgu.har.mrc.ac.uk/research/genomic_imprinting) (Verona, Mann et al. 2003). The length of an imprinted cluster is variable, can be up to 4000kb and can harbor up to 12 protein coding genes but at least one gene encodes for a macro

ncRNA (Koerner, Pauler et al. 2009). A hallmark of imprinted genes is that most of them are associated with CpG islands (Paulsen, El-Maarri et al. 2000). Within or juxtaposed these CpG islands direct repeats are often present and it is hypothesized that they might be the attractors for the de novo methylation during gametogenesis, since repeats are subject to DNA methylation as a response of a defense mechanism (Neumann, Kubicka et al. 1995).

The imprint is a DNA methylation mark set on a differentially methylated region (DMR) either during spermatogenesis or oogenesis on the paternal or maternal chromosome, respectively. Such a DMR is called a gametic DMR, (Ferguson-Smith, Sasaki et al. 1993; Stoger, Kubicka et al. 1993). Furthermore, also somatic DMRs are found within imprinted genes, but those acquire the imprint later during development, when the embryo is diploid (Stoger, Kubicka et al. 1993; Olek and Walter 1997). The unmethylated gametic DMR is the regulatory element that controls the cluster in *cis*. This differs from *trans*-acting mechanisms in the way that the regulatory function is restricted to the same chromosome and can not act on other chromosomes (Barlow and Bartolomei 2007). If deletion of an unmethylated DMR results in loss of imprinted expression of all genes in a cluster, this DMR can be defined as an imprint control element (ICE) because it acts on the whole imprinted cluster and is pivotal for proper parental specific expression (Spahn and Barlow 2003).

Chromatin modifications have also been shown to be involved in modifying the ICE. The methylated ICE carries focal repressive histone marks for instance H3K9me3, the associated HP1 protein and H4K20me2 (Mikkelsen, Ku et al. 2007; Regha, Sloane et al. 2007). On the contrary, the unmethylated ICE is marked with active histone marks like H3/H4 acetylation and H3K4me. As described above chromatin is either present as euchromatin or heterochromatin and is associated with active or repressive histone marks. However, the observation of focal heterochromatin marks demonstrated that for instance repressive histone marks can be present in the body of a gene without constraining the elongation of polymerase II that runs through an actively transcribed gene.

Imprinted genes have a high functional impact in the development of an embryo ranging from the growth of the embryo or placenta to behavioral aspects after

birth including diseases like autisms and schizophrenia (Reik and Walter 2001). Up to now, six imprinted cluster in mouse have been intensively characterized with two paternally imprinted clusters - *Igf2* and *Dlk1* - and four maternally imprinted clusters *PWS, Gnas, Kcnq1* and *Igf2r*. The Igf2r cluster will be described in detail later.

1.2.3 The imprint life cycle and reprogramming

DNA methylation marks on DMRs are erased in primordial germ cells, established in mature germ cells and maintained after fertilization throughout the life of an organism. Primordial germ cells undergo a genome wide demethylation event at around embryonic day 12-13 (Brandeis, Kafri et al. 1993; Tada, Tada et al. 1998), and the DMRs of imprinted genes are subjected to *de novo* methylation at late fetal stage (Figure 3A) (Kafri, Ariel et al. 1992; Brandeis, Kafri et al. 1993). A second wave of genome wide DNA demethylation occurs immediately after fertilization. Thereby the paternal genome undergoes an active demethylation event (Oswald, Engemann et al. 2000) and later the maternal genome looses its methylation marks passively (Howlett and Reik 1991). Interestingly, imprinted genes escape somehow this second demethylation event and therefore they maintain their imprints (reviewed (Reik and Walter 2001; Li 2002). How imprinted genes are protected remains an unanswered question up to now (Monk, Boubelik et al. 1987). At the blastocyst stage around E3.5 most of the genome is demethylated but the DNA methylation marks will be established newly during implantation by the action of *de novo* enzymes. Throughout implantation the ectoderm and mesoderm become hypermethylated contrasting the primitive endoderm and trophoblast (Figure 3B).

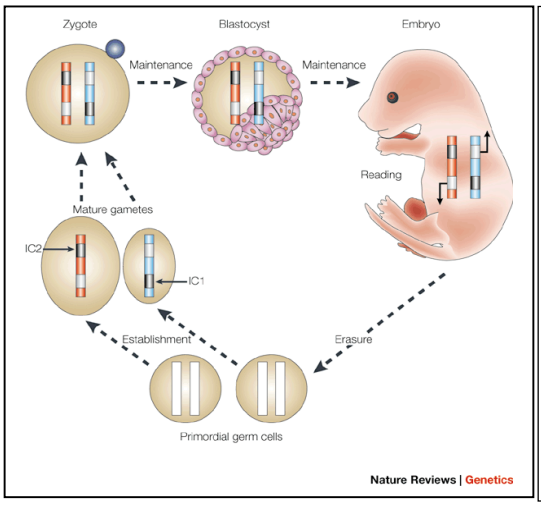

Figure 3A: The imprint life cycle: As an example, the imprint control element 1 (ICE1) and ICE2 are shown: the black box carries a methylation mark and the white box is unmethylated leading to imprinted expression in the embryo. During gametogenesis the imprints are erased in early primordial germ cells (PGCs) and restablished in mature gametes. When the embryo becomes diploid the imprints are maintained (Reik and Walter 2001).

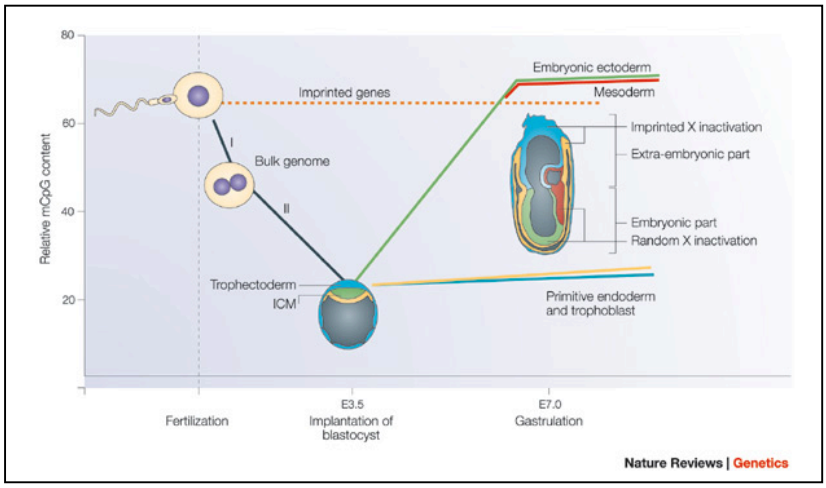

Figure 3B: Reprogramming during embryonic development: Immediately after fertilization a second demethylation event takes place. First, the paternal genome undergoes an active demethylation process (I) followed by a passive event (II) of the maternal genome. At embryonic day 3.5 (E3.5) the blastocyst displays a genome wide demethylation pattern followed by *de novo* methylation after implantation in the embryonic ectoderm and mesoderm, contrasting the primitive endoderm and trophoblast. In terms of X-inactivation in the extraembryonic part an imprinted mode is favored whereas in the embryonic part X-inactivation occurs randomly random (Li 2002)

1.2.4 The Insulin-like growth factor type 2 receptor (*Igf2r*)-cluster

In general, the *Igf2r* cluster harbors genes that underlie either biallelical or monoallelical expression that can be further manifested in a tissue- specific manner and expression of some genes is specific to a certain developmental stage. The genes *Mas1* and *Slc22a1* (solute carrier family 22 member 1) are expressed from both alleles. *Igf2r* (Barlow, Stoger et al. 1991), *Slc22a2* and *Slc22a3* are expressed exclusively from the maternal allele, contrasting *Airn* (Lyle, Watanabe et al. 2000) that is expressed only from the paternal allele. Imprinted expression of *Igf2r* and *Airn* is nearly present in all tissues of mice with a few exceptions like preimplantation embryos, undifferentiated ES cells, testes and neurons (Wang, Fung et al. 1994; Szabo and Mann 1995; Szabo and Mann 1995; Lerchner and Barlow 1997; Yamasaki, Kayashima et al. 2005). *Slc22a2* and *Slc22a3* show imprinted expression only in extraembryonic tissues. Imprinted expression of *Slc22a3* is restricted to a certain developmental stage. It shows imprinted expression at 11.5 dpc (days per coitum) and switches to biallelic expression at 15.5 dpc. On the other hand, *Slc22a2* is imprinted in both of these stages (Verhaagh, Schweifer et al. 1999; Zwart, Sleutels et al. 2001).

In more detail, the mouse *Igf2r* cluster spans 490kb on chromosome 17 and contains three protein-coding genes (*Igf2r*, *Slc22a2* and *Slc22a3*) that are exclusively expressed from the maternal chromosome. While silencing of these 3 protein-coding genes takes place on the paternal allele, the macro ncRNA *Airn* is expressed from a promotor residing in intron 2 of *Igf2r*, known as region 2, in antisense orientation with respect to *Igf2r* from the paternal allele. However, the ncRNA *Airn* is responsible for the repression of *Igf2r, Slc22a2* and *Slc22a3* on the paternal allele (Figure 4). This was shown by truncating *Airn* from 108kb to 3kb resulting in loss of silencing of the imprinted genes (Sleutels, Zwart et al. 2002). Moreover, it was also shown that if DNA methylation is missing, *Igf2r* is biallelically repressed (Li, Beard et al. 1993). Importantly this cluster contains a germline DMR (gDMR) and a somatic DMR (sDMR). The former one comprises the promoter of the macro ncRNA *Airn*. *Igf2r* and the macro ncRNA *Airn* have an overlap of ~29kb with each other (Lyle, Watanabe et al. 2000). The germline DMR (DMR2), the imprint control element of this cluster, has a length of 3.7kb and harbors a 2kb CpG island (Stoger, Kubicka et al. 1993; Wutz, Smrzka et al. 1997). The somatic DMR (DMR1) is located at the *Igf2r* promoter and gains DNA methylation, only on the paternal allele during development (Sleutels, Zwart et al. 2002). Furthermore, the 3' end of the *Airn* transcript overlaps with the non-imprinted *Mas1* gene (Lyle, Watanabe et al. 2000). The macro ncRNA *Airn* is mostly unspliced, nuclear localized, only a minority of 5% is spliced and cytoplasmatic located (Seidl, Stricker et al. 2006). Whereas in mice the imprinted *Ifg2r* cluster shows strict imprinted expression, it only shows polymorphic imprinted expression in humans (Xu, Goodyer et al. 1993; Smrzka, Fae et al. 1995; Oudejans, Westerman et al. 2001; Monk, Arnaud et al. 2006).

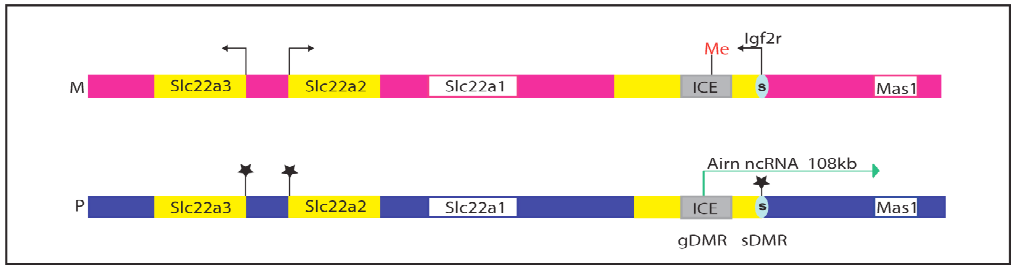

Figure 4: The *Igf2r* cluster: the imprint control element (ICE) in intron 2 of the *Igf2r* gene is unmethylated on the paternal allele leading to expression of the macro ncRNA *Airn* (108kb). *Airn* initiates the silencing of the three protein-coding genes (*Igf2r*, *Slc22a2* and *Slc22a3*) in *cis*. On the contrary, the ICE on the maternal allele harbors a methylation imprint which hinders the expression of ncRNA *Airn* and prevents the silencing of the 3 protein coding genes. *Slc22a1* and *Mas1* gene are monoallelicaly expressed. (*yellow box*) imprinted genes, (*white box*) biallelicaly expressed genes, (*s*) somatic DMR, (*ICE*) imprint control element or gametic DMR, (black *arrow*) expressed allele of an imprinted gene, (black star) repressed allele of an imprinted gene, (*green arrow*) expression of the ncRNA *Airn.*

1.2.5 Macro non-coding RNAs

"DNA makes RNA makes protein" states the central dogma of modern biology. Besides protein-coding genes, which make up 1-2% (Kapranov, Willingham et al. 2007) of the genome, a large fraction of the genome is transcribed but not translated into a protein and this fraction is designated as non-coding RNAs (ncRNAs). Well investigated classes of ncRNAs are involved in processes such as splicing and translation, by excerpting introns like the small nucleolar (sno) RNAs or by converting the messenger RNA (mRNA) into a protein, namely the transfer RNA (tRNA) and ribosomal RNA (rRNA). However, this is not all. The class of ncRNAs is much bigger then expected. Powerful tools like genome-wide tiling arrays and cDNA sequencing made it visible that the transcriptome encodes more non-coding transcripts then coding transcripts (Kapranov, Cheng et al. 2007). A possible way to classify them is by their length (small vs. macro ncRNAs) or the way they mediate their functions, in respect to *cis* or *trans* (Koerner, Pauler et al. 2009). The class of small ncRNAs comprises micro (mi) RNAs (22nt), short interfering (si) RNAs (21nt) and piwi interacting (pi) RNAs (26-31nt). Their main function is dedicated to inhibit translation or, in respect to piRNAs, to silence transposons, and they act in *trans*. On the other hand large ncRNAs are defined as 200nt or longer (Kapranov, Cheng et al. 2007) and are the only ncRNAs up to now that exert their functions also in *cis* (Koerner, Pauler et al. 2009). Macro ncRNAs have a pivotal role in genomic imprinting. They can occur in antisense or sense direction with respect to protein coding genes in the cluster and can overlap a protein coding gene or lie in intergenic regions. *Airn* (108kb), *Kcnq1ot1* (91kb) and *Nespas* (30kb) are antisense macro ncRNAs, which are transcribed from a promoter contained in the ICE. In this way the unmethylated ICE leads to the expression of the ncRNA and its deletion results in loss of imprinting as described above.

1.3 Hypothesis

Although genomic imprinting is conserved in mice and humans, most of the knowledge on how the imprinting mechanism is working is provided by using the mouse as a model system. In the mouse a bulk of data suggests that imprinted macro ncRNAs are directly controlled by DNA methylation (Li, Beard et al. 1993; Shemer, Birger et al. 1997; Seidl, Stricker et al. 2006). Based on this we want to untangle the question if the same is true in humans thus making a necessity to demethylate the nucleotide sequence. In this way I will investigate if Decitabine, a DNA methyltransferase inhibitor, is able to demethylate the human genome, using human foreskin fibroblasts (Hs-27 cells) as a model system and methylsensitive-restriction enzymes combined with Southern blot as a technique. In addition I analyzed the effect of DAC on gene expression by qPCR and by RNA-chip that contains all imprinted human regions.

1.4 DNA Demethylation

1.4.1 Ways for DNA demethylation

There are several ways to achieve a DNA demethylation effect. One would be by targeting the DNMTs through homologous recombination. Rhee and colleagues have shown that the DNA methylation pattern upon deletion of DNMT3B in human cancer cell line decreases by 3%. Remarkably, the concordant deletion of *DNMT1* and *DNMT3B* reduced the DNA methylation pattern approximately 95-fold (Rhee, Bachman et al. 2002). A second approach that could lead to a DNA demethylation effect is upon RNAi mediated knock down of the DNMT enzymes (Fournel, Sapieha et al. 1999). The third approach for achieving such an effect is upon the usage of DNA methyltransferase inhibitors. In the end, all three approaches are able to be taken in consideration using the mouse as a model system. To demethylate the genomic sequence in humans the RNAi and the usage of DNA methyltransferase inhibitors would come into consideration. In my thesis I stress on the latter point, using DNA methyltransferase inhibitors.

1.4.2 Classes of DNA methyltransferase inhibitors

Inhibitors of the DNA methyltransferase can be subdivided into either S-phase dependent or independent. Chemical compounds that are S-phase independent target the active site of the DNA methyltransferase leading to a loss of DNA methylation (Brueckner, Garcia Boy et al. 2005). Examples are: Procainamide, Hydralazine, Psammaplin A, EGCG, MG98, RG108 (Stresemann, Brueckner et al. 2006; Yoo and Jones 2006). On the other hand, S-phase dependent inhibitors are incorporated into the DNA and mimic a cytosine. Zebularine, 5,6-Dihydro-5-azacytidine, 5-azacytidine and 5-aza-2'-deoxycytidine are examples of base analogues that can be either incorporated into RNA or DNA, with the exception of the DNA restricted 5-aza-2'deoxycytdine. These fraudulent bases are modified cytosines and differ from normal base in a way that the enzymatic reaction of the DNA methyltransferase is inhibited (Figure 5A).

1.4.3 5-azacytidine (5-aza)

5-azacytidine was one of the first compounds that were synthesized 40 years ago as a cytotoxic chemotherapeutic agent (Sorm, Piskala et al. 1964). 5-azacytidine is able to induce differentiation of mouse embryonic cells to muscle cells, fat cells and chondrocytes (Taylor and Jones 1979). Roughly 20 years after the invention of this compound Jones et al reported that 5-azacytidine also has demethylation activity at low concentrations (Jones and Taylor 1980). Importantly, 5-azacytidine has a ribose as a sugar moiety and thus to work as an inhibitor of the DNA methyltransferase it has to be converted by the ribonucleotide reductase to the deoxyribose for incorporation into DNA. It has been shown that roughly 90% of 5-azacytidine will be incorporated into RNA and only a small portion of 5-azacytidine gets incorporated into DNA (Li, Olin et al. 1970). The incorporation into RNA mediates the cytotoxic effects by affecting RNA biosynthesis.

1.4.4 5-aza-2'deoxycytdine (Decitabine, DAC)

5-aza-2'deoxycytdine (DAC) was originally synthesized as a cytotoxic chemotherapeutic agent at the same time as 5-aza (Sorm, Piskala et al. 1964). Contrasting 5-azacytidine, DAC is less toxic and has a higher efficiency for DNA methylation inhibition. This is due to the fact that DAC is only incorporated into DNA and not into RNA. To be functional, DAC has to be activated. This involves several metabolic steps. First, DAC has to be taken up into the cell via membrane transporters whereby in humans 4 classes are involved in this transport: ABC transporters, equlibrative uniporters (SLC29A), concentrative dependent transporters (SLC28A family) and substrate exchange transporters (SLC22/15 families) (Pastor-Anglada, Cano-Soldado et al. 2005; Stresemann and Lyko 2008). After cellular uptake DAC has to be metabolized to the triphosphate level and upon competing with the cellular CTP (cytidine triphosphate) pool, DAC is incorporated into DNA by DNA polymerase (Figure 5C). The main difference that exists between DAC and cytosine is the presence of nitrogen instead of a carbon on position 5, which exerts the inhibitory effect on the DNMT1. This is primarily due to the fact that DNMT1 recognizes hemimethylated DNA. During replication, a semiconservative process, the parental strand remains present with methylated cytosine contrasting the newly synthesized strand that exhibits DAC in the DNA (this happens upon competition with the CTP pool, so it should be taken in account that not all cytosines are replaced by DAC). DNMT1 targets hemimethylated DNA but fails to fulfil the last step of the enzymatic reaction. The DNMT1 targets carbon 6 of cytosine, that flips out of the DNA and thus a covalent bond gets formed leading to the trapping of the DNMT1. Due to the presence of nitrogen on position 5 the last reaction step the β-elimination fails and DNMT1 is trapped in the DNA helix (Santi, Norment et al. 1984; Christman 2002) (see Figure 5C). Accordingly, through subsequent replication cycles this leads to a passive loss in DNA methylation. In terms of the metabolism, deoxycytidine-kinase is the main enzyme that catalysis the phosphorylation steps for DAC in contrast to 5-azacytidine (Stegmann, Honders et al. 1995), were Uridine-Cytidine kinase or different enzymes might be involved. This shows that the activation of these compounds is mediated through different enzymes.

It is known that DAC as well as 5-azacytidine are unstable in aqueous solutions. A study by Stresemann and Lyko 2008 has determined by capillary electrophoresis experiments the difference in the half-life of 5-azacytidine and Decitabine. The result shows that DAC exhibits a half-life of 21 hours at 37°C at a pH 7 and 5-azacytidine of 7 hours (Stresemann and Lyko 2008).

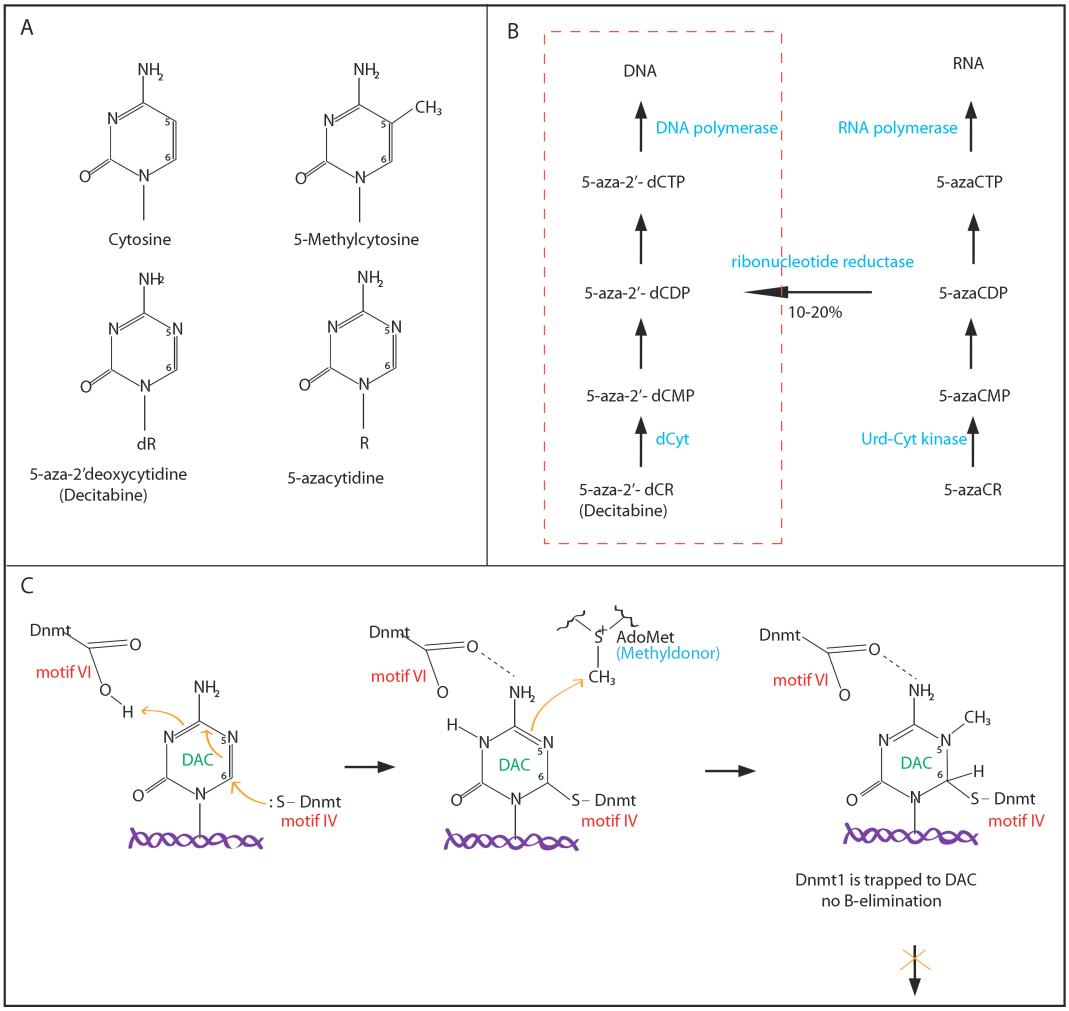

Figure 5: Metabolism of DAC and enzymatic reaction: (**A**) chemical structure of cytosine, 5-methylcytosine, Decitabine and 5-azacytidine are shown. (**B**) Dashed red box: Decitabine has to be activated by conversion by the deoxycytidine kinase to the triphosphate level before the incorporation into DNA by DNA polymerase. 5-azacytidine is activated by the Uridine–Cytidine kinase to the triphosphate level and incorporated into RNA by the RNA polymerase. For incorporation into DNA it is necessary that 5-azacytidne is at the diphosphate stage reduced to the deoxyribose by the action of ribonucleotide reductase. Note that only a low amount is incorporated into DNA (Stresemann and Lyko 2008). (**C**) Enzymatic mechanism of Dnmt1 in respect to DAC. The reaction is described in Figure 2 with the exception that DAC contains a nitrogen at position 5 thus leading to the trapping of Dnmt1 due to the prevention of the β-elimination.

It should also be noted that DAC can be inhibited by cytidine deaminase. This problem can be circumvented upon the usage of Zebularine, which is a newly derived DNA methyltransferase inhibitor and also known to inhibit cytidine deaminase.

A previous study pointed out that V5 cells (cell line transduced with a vector carrying cytidine deaminase) showed a reduced response upon DAC treatment in contrast to 3T3 cells. However, if the cells were treated in a combinatorial manner with Zebularine and DAC, they showed an enhanced response to DAC compared to 3T3 cells. This concludes that Zebularine inhibits cytidine deaminase and increases thereby the responds of DAC (Lemaire, Momparler et al. 2009).

1.4.5 Decitabine – differentiation, cytotoxicity and DNA demethylation

DAC, residing in the DNA, is able to induce differentiation, cytotoxicity and DNA demethylation of cells (Jones and Taylor 1980; Creusot, Acs et al. 1982; Pinto, Attadia et al. 1984). The cytotoxicity effect is primarily mediated upon the formation of DNMT1-DAC adducts (Juttermann, Li et al. 1994), which have been shown to induce DNA damage (Palii, Van Emburgh et al. 2008). Furthermore, a recent study has reported that the cytotoxic effect is primarily mediated through *de novo* DNA methyltransferases Dnmt3a and Dnmt3b (Oka, Meacham et al. 2005). At high concentrations DAC induces DNA double strand breaks thus activating repair proteins like ATM/ATR, in addition the histone variant H2AX is recruited to the damaged site and phosphorylated. Consequently, the cell enters into cell cycle arrest and apoptosis by the p53/p21 pathway (Ewald, Sampath et al. 2008). However, at low concentration the main effect upon DAC treatment is DNA demethylation. This makes DAC a potential compound to reactivate tumour suppressor genes e.g. p16 (Merlo, Herman et al. 1995).

An interesting issue is the remethylation of certain genes after the exposure to DAC. A study by Bender et al has investigated the demethylation and remethylation process upon DAC treatment in respect to the p16 promotor region. They found that upon DAC treatment for 24 hours the DNA methylation on the p16 promoter gets reduced from 95% to 35%, analyzed 72 hours after the treatment. However, the methylation marks were restablished after DAC withdrawn followed by a reduction in the expression level (Bender, Gonzalgo et al. 1999).

2. Results

2.1 DNA Blot Probe design and Synthesis

2.1.1 Probe design:

To analyze loss of methylation in Hs-27 cells I designed in total 10 DNA-blot probes from regions that were previously published as DNA methylated. The mitochondrial DNA is not methylated and the designed probe is used as a loading control. Table 2 lists all probe names as well as the region they detect.

Probe name	Chromosomal position of the probe	Element under analysis	Additional info
hH19mp	chr11:1979862-1980453	*H19* DMR	-
hDLK1mp	chr14:100343689-100344270	*DLK1* DMR	-
hPWSmp	chr15:22620491-22621106	*PWS* DMR	-
hOCT4mp	chr6:2388804-2389335	*OCT-4* TSS	no CpG island
hMAGEA1mp	chrX:152140930-152141536	*MAGE-A1* TSS	no CpG island
hHERV(gag)mp	chr19:20728192-20728765	5'LTR of HERV	probe is placed in gag region
hAluJbmp	chr6:160311736-160312147	SINE (AluJb)	-
hL1P3mp		LINE (L1P3)	5'UTR under the investigation
hSat2mp	chr10:41799625-41800157	Satellite 2 repeat	pericentromeric region
hMTmp	chrM:6119-6662	mitochondrial probe	loading control, no DNA methylation
Bx	chr6:160348427-160349007	*AIRN* DMR probe	from Irena Vlatkovic
hKCNQ1OT1mp	chr11:2676050-2676907	*KCNQ1OT1* DMR	from Renping Qiao
HB	chr6:160309497-160310015	CpG island of *IGF2R*	-

Table 2: Probe names are shown: h (X) mp= *h*uman(X)*m*ethylation *p*robe; TSS= Transcription start site.

2.1.2 PCR reactions

DNA blot probes for the regions listed in Table 2 were constructed using PCR. For each PCR reaction $MgCl_2$ optimization was conducted, with the best $MgCl_2$ concentration the PCR was repeated shown on the right side of Figure 6A-J. Additionally, a Betaine optimization (0/ 0.4/ 0.8/ 1.2M) including the best achieved $MgCl_2$ concentration was carried out, for achieving a better result for hDLK1mp,

hMAGEA1mp and hPWSmp. The bands on the right side (Figure 6A-I) were cut out for cloning.

For the human H19 methylation probe (hH19mp), the best result of the PCR was achieved with 1.2mM $MgCl_2$ in lane 7, shown by a visible band at 592bp (Figure 6A, left). Figure 6B illustrates the $MgCl_2$ optimization for the human Dlk1 methylation probe (hDLK1mp) and a band appeared in lane 8 (1.6mM $MgCl_2$) at 582bp. The $MgCl_2$ optimization for the human PWS methylation probe (hPWSmp) reveals the best result in lane 7 (1.2mM $MgCl_2$) showing a band at 616bp (Figure 6C, left). In Figure 6D the $MgCl_2$ optimization of the human OCT-4 methylation probe (hOCT4mp) shows the best result in lane 7 (1.2mM $MgCl_2$) by the appearance of a band at 532bp. The $MgCl_2$ optimization of the MAGE-A1 methylation probe (hMAGE-A1mp), shown in Figure 6E, reveals a band in lane 7 (1.2mM $MgCl_2$), at a length of 607bp. Figure 6F shows the design of a human endogenous retrovirus methylation probe (hHERV(gag)mp) and reveals the best result in lane 6(1mM $MgCl_2$) showing a band at 574bp. The $MgCl_2$ optimization according to the human AluJb methylation probe (hAluJbmp) reveals a band at 411bp in lane 7 (1.2mM $MgCl_2$) (Figure 6G). The human sat2 methylation probe (hSat2mp), shown in Figure 6H, reveals the best result according to $MgCl_2$ optimization within lane 8 (1.6mM $MgCl_2$), showing a band at 533bp. In Figure 6I the PCR for human mitochondrial methylation probe (hMTmp) is shown and the best result was achieved in lane 6 (0.8mM $MgCl_2$) showing a band at 544bp. At last, the design of a human LINE (L1P3) methylation probe (hL1P3mp) reveals for the $MgCl_2$ optimization a band in lane 8 (1.6mM $MgCl_2$) at 606bp (Figure 6J). The PCR reaction was then conducted with 1.6mM $MgCl_2$ (data not shown).

In summary, PCR for probes to 10 specific regions were successfully conducted amplifying fragments of the expected length. All fragments were cut out gel purified and cloned into the pGEM –T-Easy vector.

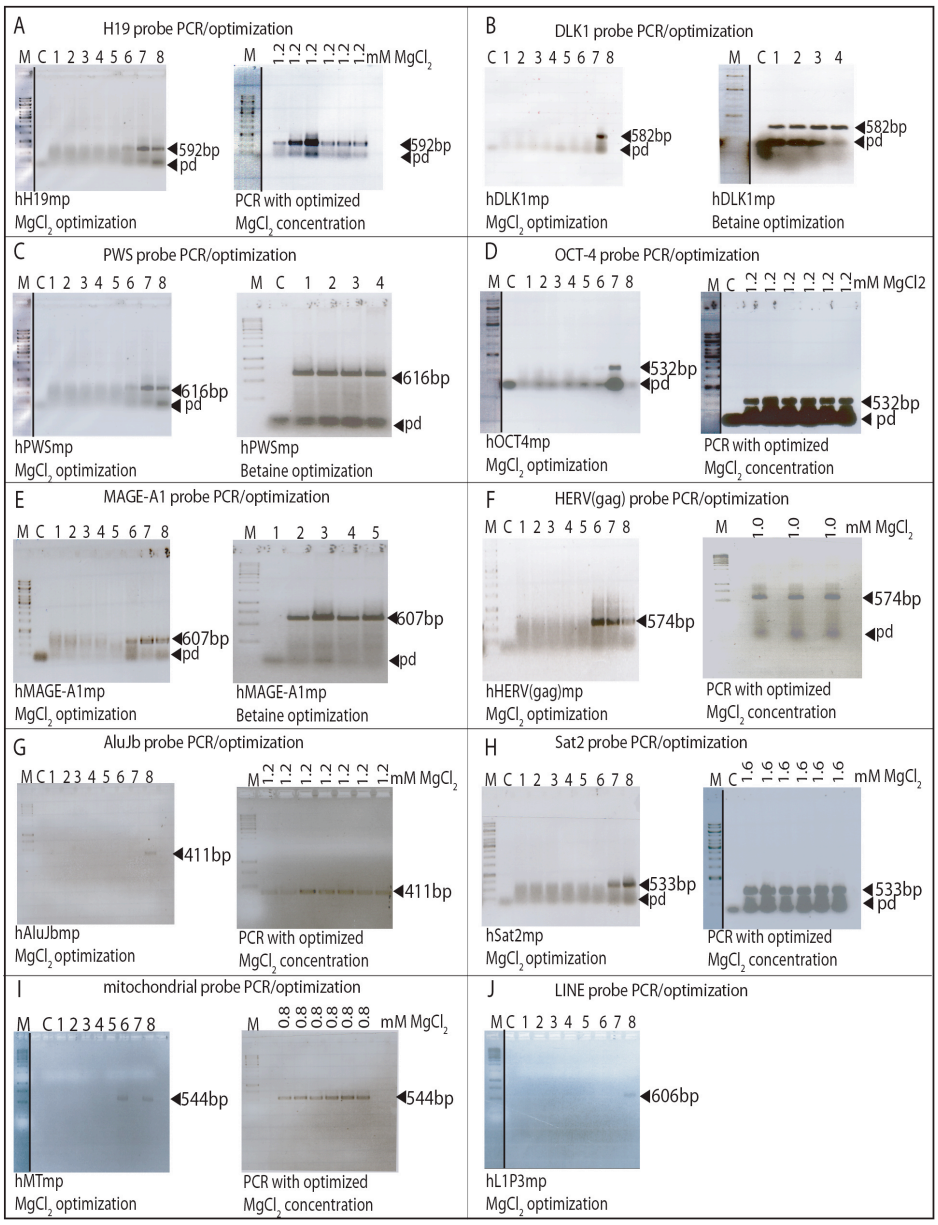

Figure 6: $MgCl_2$ and/or Betaine optimization / PCR reactions for constructing DNA blot probes to analyze DNA methylation status of methylated regions. A-J: M= 1kb DNA ladder, the marker in A-D and H-J was modified with Photoshop CS2, C=control (no template), for $MgCl_2$ optimization: Betaine: 0.8M, Lane 1-8 (0.4/ 0.48/ 0.60/ 0.70/ 0.80/ 1.0/ 1.2/ 1.6mM $MgCl_2$), pd= primer dimers, for Betaine optimization Lane 1-4 (0/ 0.4/ 0.8/ 1.2M Betaine) **A:** hH19mp left: $MgCl_2$ optimization: A fragment in lane 7(1.2mM $MgCl_2$) and lane 8 (1.2mM $MgCl_2$) is visible at 592bp in addition to primer dimers (pd). right: The PCR was repeated with 1.2mM $MgCl_2$ and the bands were cut out. **B:** hDLK1mp left: as in A, left: The size of the fragment is 582bp (lane8, 1.6mM $MgCl_2$). right: The Betaine optimization was conducted with 1.6mM $MgCl_2$, showing no effect. **C:** hPWSmp left: as in A, left: The size of the fragment is 616bp. right: as in B, right ($MgCl_2$ =1.2mM). **D:** hOCT4mp left: as in A, left: The size of the fragment is 532bp (lane7, 1.2mM $MgCl_2$); right: as in A, right ($MgCl_2$ =1.2mM) **E:** hMAGEA1mp left: as in A, left: The size of the fragment is 607bp (lane 6, 7, 8 with 1.0/ 1.2/ 1.6mM $MgCl_2$). right: as in B, right ($MgCl_2$ =1.2mM) **F:** hHERV(gag)mp left: as in A, left: The size of the fragment is 574bp (lane 6,7,8 with 1.0/ 1.2/ 1.6mM $MgCl_2$). right: as in A, right: ($MgCl_2$ =1.0mM) **G:** hAluJbmp left: as in A, left: The size of the fragment is 411bp (lane7, 1.2mM $MgCl_2$). right: as in A, right: ($MgCl_2$ =1.2mM) **H:** hSat2mp left: as in A, left: The size of the fragment is 533bp (lane7, 8 with 1.2/ 1.6mM $MgCl_2$); right: as in A right: ($MgCl_2$ =1.6mM) **I:** hMTmp left: as in A, left: The size of the fragment is 544bp (lane 6, 8 with 0.8/ 1.6mM $MgCl_2$); right: as in A, right: ($MgCl_2$ =0.8mM) **J:** hL1P3mp left: as in A, left: The size of the fragment is 606bp (lane 8 with 1. 6mM $MgCl_2$).

2.1.3 Control digestion of the cloned PCR fragments

After transformation into $CaCl_2$-competent bacteria and blue/white selection, the insert sequence for each construct was checked by enzyme digestion (Figure 7A-J). The theoretical sequence of the vector plus insert was created *in silic*" with the software Gene Constuction Kit using publically available DNA sequence and the theoretical digestion pattern was determined.

In all cases the predicted digestion pattern, on the right for each construct, fits to the obtained digestion pattern on the left. In Figure 7A the digestion pattern of the cloned PCR product hH19mp, digested with Cfr421, is shown. The *in silico* predicted digestion pattern indicates 3 bands 3320bp, 404bp and 120bp and all three bands were obtained, although the band at 120bp is very faint. In the uncut control (C) lane higher molecular bands are present. These bands are different conformations of the uncut vector ranging from supercoild plasmids that move fast through the agarose to an open circle confirmation that moves slower and are also seen in other gels in this figure. In Figure 7B the digestion of the cloned hDLK1mp with RsaI is shown. Three bands are visible at 1982bp, 1363bp and at 251bp that match the predicted pattern. In Figure 7C the AluI digestion pattern of the hPWSmp pGEM-T-Easy construct is shown. The *in silico* digestion predicts 16 bands in total, although 10 bands are of small size and were not visible. However, the obtained digestion pattern shows a thick band that indicates a band at 671bp as well as 655bp, a smaller band at 520bp as well as thick, smeary band at approximately 200bp (indicated as a red dot 1) and one at approximately 120bp (indicated as a red dot 2). The PvuII digestion pattern of the pGEM-T-Easy vector containing the hOCT4mp product is shown in Figure 7D. The *in silico* digestion pattern predicts four bands: at 2563bp, 491bp, 312bp 179bp, which are present in the obtained digestion. The cloned hMAGE-A1mp fragment, digested with RsaI, displays 2 bands with a size of 2207bp and 1425bp that match the predicted bands. In Figure 7F the cloned hHERV(gag)mp was digested with DraIII or RsaI. Similarly, on RsaI digestion produced the predicted bands at 2196 and 1313bp. Figure 7G shows the digestion the coned hAluJbmp fragment, digested with PvuII or BstXI. The predicted PvuII bands at 2563bp, 574bp and 289bp were seen. Similarly, the predicted BstXI fragments at 3077bp and one at 349bp were obtained. In Figure 7H the hSat2mp cloned fragment was digested with revealing the

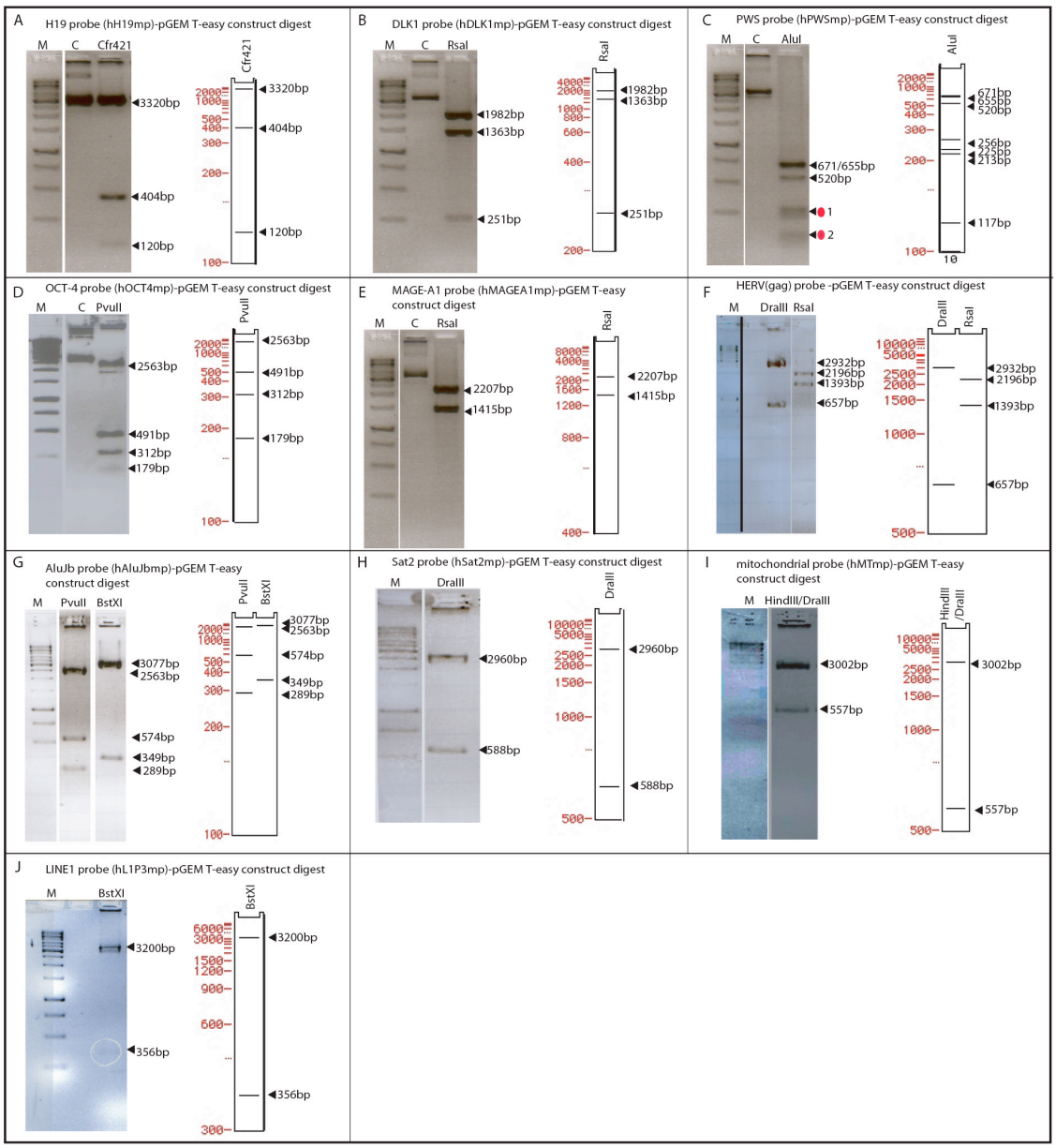

Figure 7: Restriction fragment patterns confirming cloning of correct PCR fragments into p GEM-T-Easy M= 1kb DNA ladder, C= Control (no enzyme), visible in different conformations ranging from supercoild, nicked circle to multimere. The *in silico* predicted pattern fits in all cases to the obtained digestion pattern. **A**: The hH19mp pGEM-T-Easy construct was digested with Cfr421. The right side shows the *in silico* predicted digestion pattern with 3 bands present (3320bp, 404bp, 120bp). The left side indicates the obtained digestion pattern with the same bands present. **B:** The hDLK1mp pGEM-T-Easy construct digested with RsaI. The fragment sizes are: 1982bp, 1363bp and 251bp **C:** The hPWSmp pGEM-T-Easy construct digested with AluI. The fragment sizes are: 671bp, 655bp, 520bp, 256bp, 225bp, 213bp, 117bp plus 10 more, that were not visible due to their small size. **D:** The hOCT4mp pGEM-T-Easy construct digested with PvuII. The fragment sizes are: 2563bp, 491bp, 312bp, 179bp. **E:** The hMAGE-A1mp pGEM-T-Easy construct was digested with RsaI. The fragment sizes are: 2207bp and 11425bp. **F:** The hHERV(gag)mp pGEM-T-Easy construct was digested with DraIII or RsaI. The fragment sizes for DraIII are: 2932bp and 657bp and for RsaI: 2196bp and 1393bp. **G:** The hAluJbmp pGEM-T-Easy construct was digested with PvuII or BstXI. The fragment sizes are for PvuII: 2563bp, 574bp and 298bp and for BstXI: 3077bp and 349bp. **H:** The hSat2mp pGEM T-Easy construct was digested with DraIII. The fragment sizes are: 2960bp and 588bp. **I:** The hMTmp pGEM-T-Easy construct was digested with HindIII and DraIII. The fragment sizes are: 3002bp and 557bp. **J:** hL1P3mp pGEM-T-Easy construct: digested with BstXI. The fragment sizes are: 3200bp and 356bp.

predicted bands at 2960bp and 588bp. In Figure 7I the hMTmp construct was digested with HindIII plus DraIII. The predicted bands at 3002bp and 557bp were seen. The last construct is shown in Figure 7J and was digested with BstXI to confirm that the vector contains the hL1P3mp. The predicted bands at 3200bp and 356bp were seen, although the smaller fragment at 356bp is very faint.

To summarize up, all PCR fragments were cloned successfully into the pGEM-T-Easy vector as shown by the predicted restriction fragments being seen. Additionally, the inserts were sequenced confirming they were the correct sequence.

2.1.4 Probe preparation

In the next step, the constructs were digested with EcoRI to cut out and gel purify the DNA-blot probes (Figure 8 A-K). Upon digestion with EcoRI all cloned PCR fragments were extended in their length by 18bp due to the fact that EcoRI cuts at the flanking edge either side of the insert in the vector. In the EcoRI digests shown in Figure 8A-I the band at 2996bp is the vector backbone. In Figure 8A one can see the digestion of the hH19mp pGEM-T-Easy construct with EcoRI resulting in the desired fragment of 610bp in length. Figure 8B shows the digestion of hDLK1mp pGEM-T-Easy construct with EcoRI resulting in the predicted fragment at 600bp. The red star indicates an extra higher molecular weight band that maybe the uncut pGEM-T-Easy vector. The hPWSmp pGEM-T-Easy construct digest shown in Figure 8C reveals the expected fragment of 624bp. The hOCT4mp pGEM-T-Easy construct digest is shown in Figure 8D. Upon digestion with EcoRI the expected band of 550bp was seen. The hMAGE-A1mp digestion of the pGEM-T-Easy construct with EcoRI is shown in Figure 8E. The desired fragment was is present at 625bp. Figure 8F shows the hHERV(gag)mp pGEM-T-Easy construct digested with EcoRI and the predicted fragment was visible at 592bp. In Figure 8G the probe preparation of hAluJbmp is shown. The pGEM-T-Easy construct was digested with EcoRI revealing a very faint band at 429bp as the DNA blot probe. The EcoRI digestion of hSat2mp pGEM-T-Easy construct is shown in Figure 8H. The predicted band was present at 551bp. In Figure 8I the EcoRI digestion of the hMTmp pGEM-T-Easy construct is shown. The digestion reveals a band at 562bp representing the DNA blot probe. The hL1p3mp

pGEM-T-Easy digestion with EcoRI is illustrated in Figure 8J and confirms the presence of the DNA blot probe at a length of 625bp. The next DNA blot probe preparation was conducted for the digestion of the pE3Up plasmid with BstXI, shown in Figure 8K. This construct contains the Bx probe that detects the upstream region of the *AIRN* DMR. Upon digestion with BstXI 4 fragments were present, with the fragment at 577bp representing the DNA blot probe. Figure 8L shows the digestion of the pEX1 construct with HindIII and BstEII for the preparation of the HB probe, that detects an upstream region of the *IGF2R* CpG island. The DNA blot probe (HB) was present at 500bp.

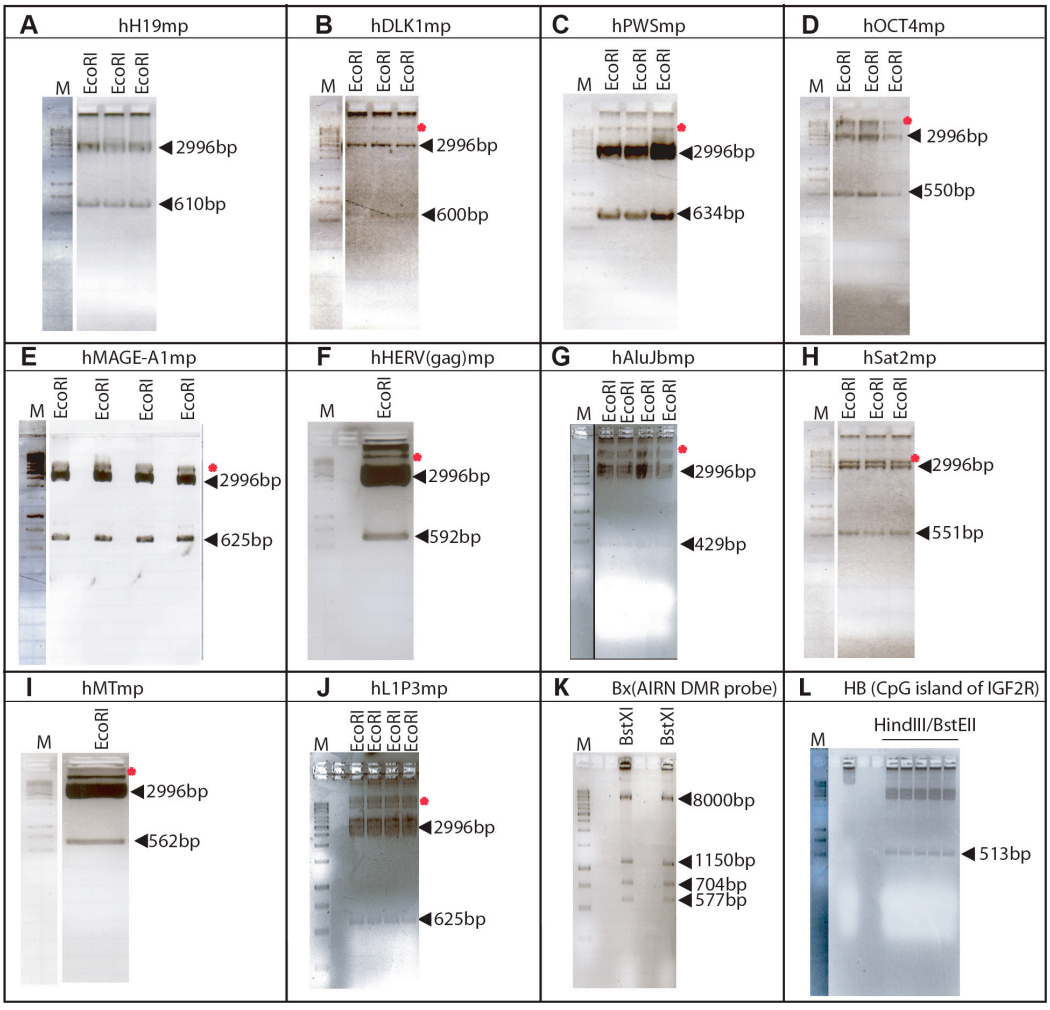

Figure 8: DNA blot probe preparation M=1kb DNA ladder, red asterix= uncut vector. (A-J) Digest was conducted with EcoRI resulting in the vector backbone at 2996bp and the probe size indicated in the respected legend. (A) hH19mp: 610bp **B:** hDLK1mp: 600bp. **C:** hPWSmp: 634bp. **D:** hOCT4mp: 550bp. **E:** hMAGEA1mp: 625bp. **F:** hHERV(gag)mp: 592bp. **G:** hAluJbmp: 429bp; **H:** hSat2mp: 551bp. **I:** hMTmp: 562bp; **J:** hL1P3mp: 625bp; **K:** Bx(AIRN DMR) probe: pE3Up construct was digested with BstXI and revealed the DNA blot probe at a length of 577bp as well as additional restriction fragments at 8000bp, 1150bp and 704bp, respectively. **L:** HB probe: digestion of the pEX1 construct was conducted with HindIII and BstEII and showed the DNA blot probe at 500bp as well as two other fragments at approximately 3000bp.

Taken together, all the digestions worked and the DNA blot probes at the expected length were cut out, gel purified and then used to detect the specific chromosomal under investigation and to analyze their methylation status.

2.2 The normal DNA methylation status of the control regions

In order to determine the normal methylation status of the regions in Table 1 in human fibroblasts (Hs-27) cells, DNA from these cells were analysed by Southern blotting for their methylation status. For this purpose I used the DNA blot probes, which I have designed as described above. Genomic DNA isolated from Hs-27 cells was digested with specific enzymes. The methyl sensitive restriction enzyme HpaII was used that recognizes a CCGG motif and can only cut at these sites when the CG in this motif is unmethylated. Furthermore, the isoschizomere MspI was used which recognizes the same restriction site, but is able to cut at these sites whether CG is methylated or unmethylated.

2.2.1 DNA methylation status of 5 imprinted clusters

Previous studies have shown that the *H19* DMR is always methylated on the paternal allele and unmethylated on the maternal allele (Bartolomei 1993, Ferguson Smith, 1993). The normal methylation state of the *H19* DMR in Hs-27 cells is shown in Figure 9. On the left side (9B) the ethidium bromide stained gel is shown after the digestion with BglII (Lane 1) alone or in combination with either HpaII (Lane 2) or MspI (Lane 3). The gel was blotted on a Hybond-Nylon membrane and then hybridized with the hH19mp probe. The digestion with BglII alone results in a visible fragment at 3888bp. Lane 2 displays a complex methylation pattern, which is due to the variable methylation state of the HpaII sites in Hs-27 cells. Upon digestion with the isoschizomere MspI three bands were visible in lane 3. According to the digestion map in Figure 9A, two MspI restriction sites are present inside the probe region flanked by one BglII restriction site on the right site and additional MspI sites on the left side. Upon double digest with BglII and MspI all CCGG sites will be cut by MspI resulting in a fragment visible at 284bp, one at 962bp and one at 1111bp. The diges-

tion pattern in lane 2 is not the result of the incomplete HpaII digestion as shown by rehybridization of the membrane with the HB probe that recognizes the unmethylated CpG island of *IFG2R* (Figure 9C and D). The result shows two bands for the digestion with BglII and HpaII, which can be explained by three additional HpaII sites that are present outside of the CpG island. These results show that these three HpaII sites are in some cells unmethylated, resulting in a band recognizable at a length of 911bp, whereas in most other cells they remain methylated resulting in a visible band at 1529bp. The MspI digestion pattern results in the 911bp fragment.

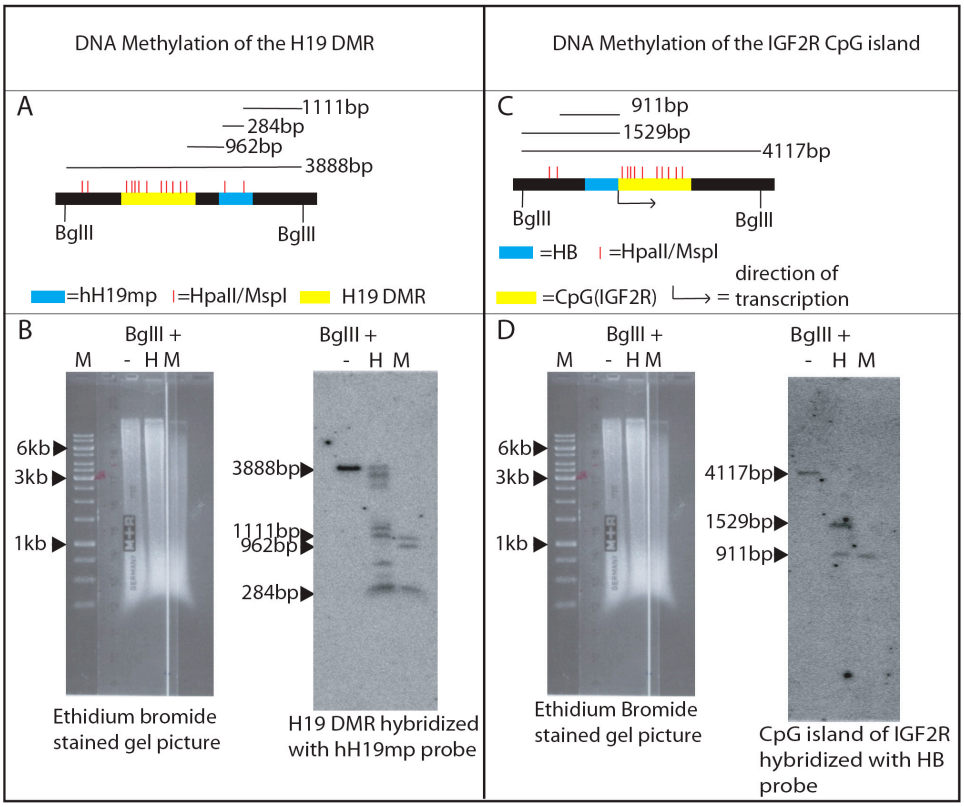

Figure 9: DNA Methylation status of the *H19* DMR in Hs-27 cells; A: The Restriction map of the *H19* DMR region is shown. DNA is shown as a black bar, the *H19* DMR as a yellow bar, the probe (hH19mp) as a blue bar, methyl- in/sensitive enzymes (MspI/HpaII) are indicated by a vertical red slash on top of the DNA and the restriction fragments upon digestion are illustrated as horizontal bars. BglII sites are as block lines below the DNA **B:** left: The ethidium bromide stained gel after the digestion of 10-20µg Hs-27 DNA with BglII alone (lane1) or in combination with HpaII (lane2) or MspI (lane3). right: DNA blot: Hybridization with hH19mp results in a fragment at 3888bp with BglII alone. In combination with HpaII a variable methylation pattern is visible or in combination with MspI three bands are visible: at 1111bp, 962bp and 284bp. **C:** Same as in A except that it is the restriction map of *IGF2R* CpG island. The arrow shows the direction of transcription. **D:** left: same ethidium bromide stained gel as shown in B. right: DNA blot: rehybridization of the membrane in B with the HB probe. The result upon digestion with BglII alone displays a band at 4117bp, in combination with HpaII two bands are visible: at 1529bp and at 911bp, or in combination with MspI one fragment at 911bp is present.

In case of the *IGF2R* cluster it was shown in earlier studies that the *AIRN* DMR is always methylated on the maternal allele whereas the paternal allele re-

mains always unmethylated (Smrzka, Fae et al. 1995). Figure 10 shows the normal occurring methylation state of the *AIRN* DMR in Hs-27 cells. On the left side of Figure 10B the ethidium bromide stained gel after digestion with EcoRI (Lane 1) alone or in combination with HpaII (Lane 2) or MspI (Lane 3) is shown. The gel was blotted on a Hybond-Nylon membrane and then hybridized with the Bx probe, as shown on the right side of in Figure 10B. The Bx probe detects a 5757bp fragment upon digestion with EcoRI alone. Due to the double digestion with EcoRI and HpaII two bands were visible, one at 5757bp and one at 2988bp. This pattern was interpreted as 50%

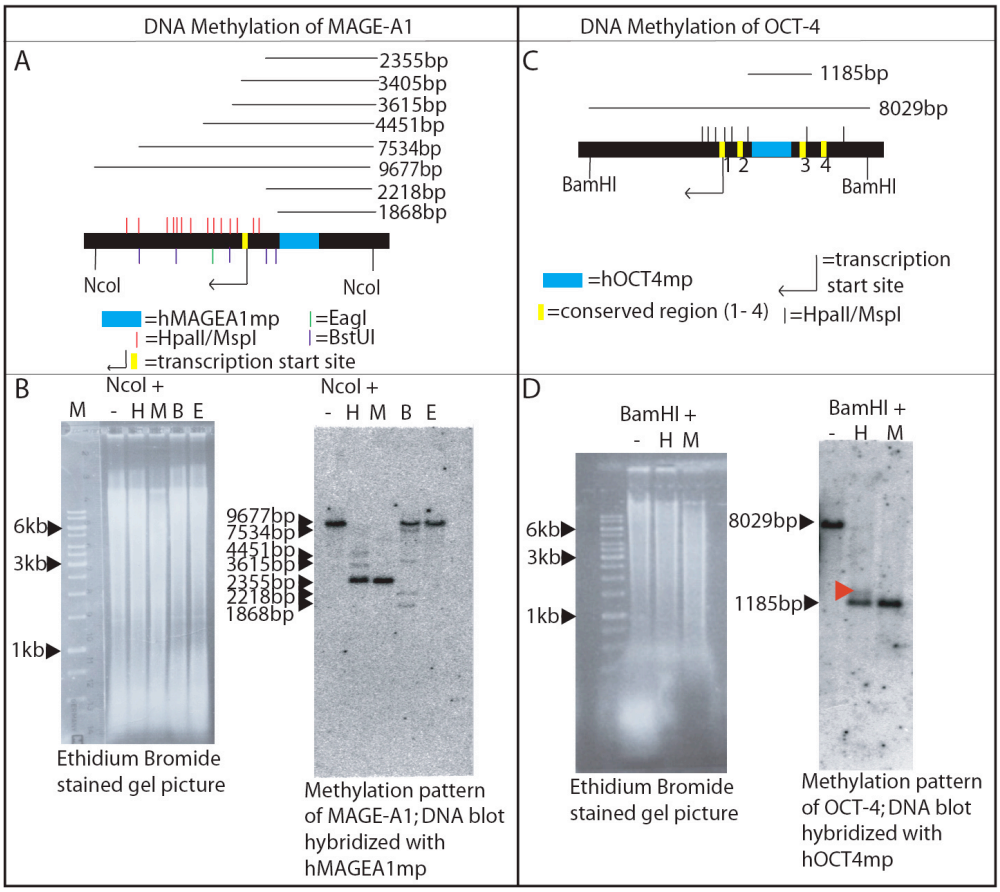

Figure 10: Methylation status of the *AIRN* DMR in Hs-27 cells; A: restriction map of the *AIRN* DMR is shown. DNA is shown as a black bar, the *AIRN* DMR as a yellow bar and the Bx probe is shown as a blue bar. Methyl- in/sensitive enzymes (MspI/HpaII) sites are indicated by a vertical red slash on top of the DNA, and the resulting fragments upon digestion are illustrated as horizontal bars. Below the DNA EcoRI sites are indicated. **B:** Left: ethidium bromide stained gel after the digestion of 10-20µg Hs-27 DNA with EcoRI alone (lane1), or in combination with HpaII (lane2) or MspI (lane3). Right: DNA blot: hybridization with Bx probe resulted in a fragment at 5757bp with EcoRI alone, in combination with HpaII two fragments appeared, one at 5757bp and one at 2988bp, while in combination with MspI one band is visible at 2988bp. An open arrowhead points towards the faint band. **C:** Same as in A except that it is the restriction map of *IGF2R* CpG island. **D:** Left: the same ethidium bromide stained gel as shown in B. Right: DNA blot: rehybridized the HB probe. The result upon digestion with EcoRI alone displayed a band at 7935bp. In either case EcoRI in combination with HpaII or MspI, resulted in a band at 684bp. Open arrowhead points towards the faint bands (7935bp and 684bp).

methylated and 50% unmethylated, as previously described (Smrzka, Fae et al. 1995). The control digestion with MspI revealed a fragment visible at 2988bp, which was very faint due to the unequal loading of DNA as visible in the ethidium bromide stained gel. To assess whether the digestion pattern, obtained in lane 2 of Figure 10B, is due to the incomplete digestion of HpaII the membrane was rehybridized with the HB probe that recognizes the unmethylated CpG island of *IGF2R* (Figure 10D). This resulted in a fragment visible at 684bp for both EcoRI/HpaII and EcoRI/MspI according to the restriction map of the *IGF2R* CpG island (Figure 10C). This confirmed that the EcoRI/HpaII digestion in 10B was complete.

It has also been reported that the DMR of *DLK1*, *PWS* and *KCNQ1OT1* are differentially methylated (Zeschnigk, Schmitz et al. 1997; Beatty, Weksberg et al. 2006; Geuns, De Temmerman et al. 2007). At these loci it is always the maternal allele that is methylated and the paternal allele that is unmethylated.

The normal methylation status of the *DLK1* DMR is shown in Figure 11B. On the left side the ethidium bromide stained gel picture is shown after digestion with SphI alone (Lane 1) or in combination with either HpaII (Lane 2) or MspI (Lane 3). This gel was then blotted on a Hybond-Nylon membrane and then hybridized with hDLK1mp as illustrated in Figure 11B on the right. The digestion with SphI alone reveals more than one band, an unexpected result. This might be explained by the hDLK1mp probe cross-hybridizing with other regions. Moreover, upon the digestion with SphI together with HpaII multiple bands are shown. This indicates a variable methylation pattern. Lane 3 showing the digestion of SphI together with MspI shows the three expected bands at 2638bp, 1019bp and 302bp predicted by the restriction map in Figure 11A.

The normally occurring methyation status of the *PWS* DMR in Hs-27 cells is shown in Figure 11D with the restriction map shown in Figure 11C. The DNA was digested with EcoRI plus HpaII or MspI. The ethidium bromide gel after restriction digest is shown in Figure 11D on the left side. This gel was then blotted onto a Hybond-Nylon membrane and hybridized with hPWSmp probe. This is shown in Figure 11D on the right side. Lane 1 shows the predicted 9244p fragment upon the digestion with EcoRI alone. Upon digestion with EcoRI together with HpaII a broad, but

faint band is visible indicating a variable methylation pattern, since two HpaII sites are present in the *SNRPN* DMR and multiple HpaII sites are outside of the *SNRPN* DMR. The digestion with EcoRI and MspI results in the expected 5136bp fragment. In Figure 11E the restriction map of the *KCNQ1OT1* DMR is shown and in Figure 11F the normal methylation state of the *KCNQ1OT1* DMR was analyzed. The ethidium bromide stained gel (left) illustrates the DNA after digestion with HindIII alone (Lane 1) or in combination with methylsensitive (Lane 2: HpaII (H), Lane 4: BstUI (B) and Lane 5: EagI (E)) or insensitive (Lane 3: MspI (M)) restriction enzymes. After gel blotting and hybridization with hKCNQ1OT1mp (right) the digestion with HindIII alone showed the expected fragment at 24274bp. The digestion with HindIII together with HpaII indicates that some of the HpaII sites are methylated (Lane 2). In comparison to that the digestion with HindIII together with MspI (Lane 3) reveals a single fragment at a length of 4065bp. An additional indication that the *KCNQ1OT1* DMR is methylated is seen upon digestion with HindIII plus BstUI, as shown in lane 4. In this case, 4 bands are present. The longest band at 24274bp indicates that in some cells all BstUI sites are methylated and therefore BstUI will not cut. The fragments present at 2221bp, 5136bp and 3632bp indicated that some cells have variable methylated BstUI sites. Additionally the digestion with EagI shows one fragment present at 24274bp and one at 5130bp.

Taken together these results revealing the normal methylation status of the imprinted regions indicating that the *H19* DMR, the *AIRN* DMR and the *KCNQ1OT1* DMR can be used as controls for analyzing the possible loss of DNA methylation. This is because these regions show clearly a differentially methylation pattern (*AIRN* DMR), or a variable methylation pattern (*H19* DMR, *KCNQ1OT1* DMR). The methylation status of *PWS* DMR and *DLK1* DMR was not clearly visible with the probes and restriction enzymes used, so these loci were not used as controls.

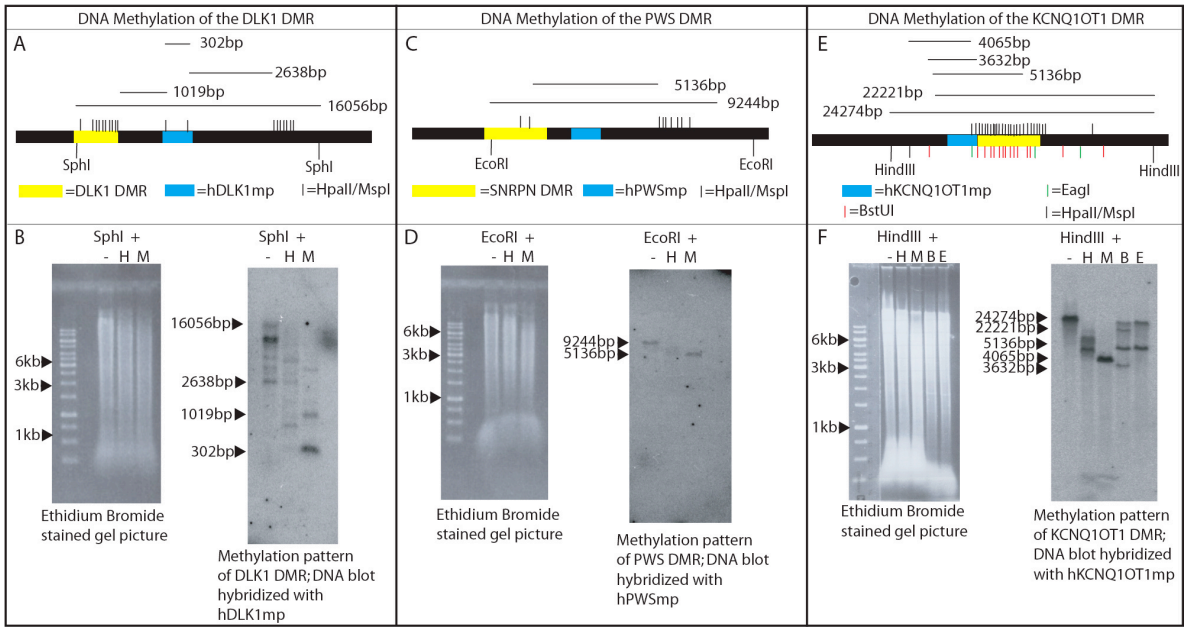

Figure 11: Methylation status of the *DLK1*-, *PWS*- and *KCNQ1OT1* DMR A: Restriction map of the *DLK1* DMR is shown. DNA is shown as a black bar, the *DLK1* DMR as a yellow bar and the hDLK1mp is shown as a blue bar. Methyl- in/sensitive enzymes (MspI/HpaII) sites are indicated by a vertical black slash on top of the DNA as well as the resulting fragments upon digestion are shown as horizontal bars. Below the DNA, enzymes are indicated which were used in combination with HpaII and MspI, in this case SphI. **B:** Left: Ethidium bromide stained gel after the digestion of 10-20µg Hs-27 DNA with SphI alone (lane1) or in combination with HpaII (lane2) or MspI (lane3). Right: DNA blot: hybridization with hDLK1mp probe resulted in multiple fragments with SphI alone or in combination with HpaII. SphI together with MspI revealed three visible bands at a length of 2638bp, 1019bp and 302bp, respectively. **C:** Same as in A except that this is the *PWS* DMR. **D:** Same as in B expect the hPWSmp probe was used and DNA was digested with EcoRI alone or in combination with HpaII and MspI. The observed fragments were 9244bp and 5136bp. **E:** Same as in A with the exception that this is the *KCNQ1OT1* DMR and HindIII plus HpaII, MspI, BstUI or EagI were used. Below the DNA EagI is shown by the green slash and BstUI by the vertical blue slash. **F:** Same as in B except the hKCNQ1OT1mp probe was used for hybridization. The hybridization resulted in one fragment at 24274bp upon digestion with HindIII alone and together with HpaII in a variable methylation pattern. HindIII together with MspI revealed one band at 4065bp. HindIII together with BstUI resulted in 4 bands: at 24274bp, 22221bp, 5136bp and 3632bp. HindIII together with EagI resulted in two bands: at 24274bp and 5136bp.

2.2.2 DNA methylation status of *MAGE-A1* and *OCT-4*

Besides imprinted genes there is a subset of genes, which show a repressed transcription status associated with promoter DNA methylation. For instance, a member of the cancer/ testis antigen family, *MAGE-A1* and the stem cell transcription factor *OCT-4*. For the *MAGE-A1* gene, it was shown that DNA demethylation correlates with transcriptional activity (De Smet, Lurquin et al. 1999) thus making it a potential control for my experiment. The *OCT-4* gene transcriptional start site was shown to become methylated during differentiation (Freberg, Dahl et al. 2007). It

should be noted that both genes presented in here lack a CpG island but are CpG rich.

I assessed the methylation status of the *MAGE-A1* and *OCT-4* promoter region. In Figure 12B the DNA blot with methylsensitive restriction enzymes for *MAGE-A1* is shown. On the left side the ethidium bromide gel is presented after digestion with NcoI alone or in addition with methylsensitive restriction enzymes (HpaII, BstUI or EagI) and the insensitive restriction enzyme MspI. The result after blotting the gel on a Hybond-Nylon membrane and hybridizing with hMAGEA1mp is shown on the right side in Figure 12B. A clear band of 9677bp is visible in lane 1 upon digestion with NcoI alone. The digestion pattern in lane 2 is the result of the double digest with NcoI and HpaII. Here a clear band is present at 2355bp matching the unmethylated band present in lane3 (NcoI + MspI). In addition, two faint bands are shown at a length of 3615bp and approximately 4500bp indicating methylated HpaII sites according to the restriction map shown in Figure 12A. This indicates that in most Hs-27 cells the majority of HpaII sites are unmethylated, but in a minority of cells HpaII sites are present. The digestion with NcoI together with BstUI displays 4 bands. A strong band at 9677bp indicated that most of the BstUI sites were methylated whereas some of them remained unmethylated and therefore additional bands appeared. These bands were at a length of 7523bp, 4451bp, 2218bp and 1868bp, respectively, as shown in Figure 12B on the right side. The digestion with NcoI together with EagI revealed one band at 9677bp, thus indicating that the EagI site was methylated.

In Figure 12D the normal methylation status of the *OCT-4* promoter is shown. The left side shows the ethidium bromide gel after digestion with BamHI alone, together with HpaII or together with MspI. The gel was then blotted onto a Hybond-Nylon membrane and hybridized with hOCT4mp. This probe analyzes the flanking CpG sites between the conserved element 2 and 3. The result of this hybridization is shown on the right side of Figure 12D. According to the restriction map in Figure 12C a 8029bp fragment is expected and was seen in lane 1 upon digestion with BamHI alone. Further, the double digest of BamHI/HpaII (lane 2) displayed a band at a length of 1185bp which matched the only band present in the BamHI and MspI double digest (lane 3). Above this fragment a faint band, indicated by the red arrowhead, is visible and this correlates with some methylated HpaII sites. However

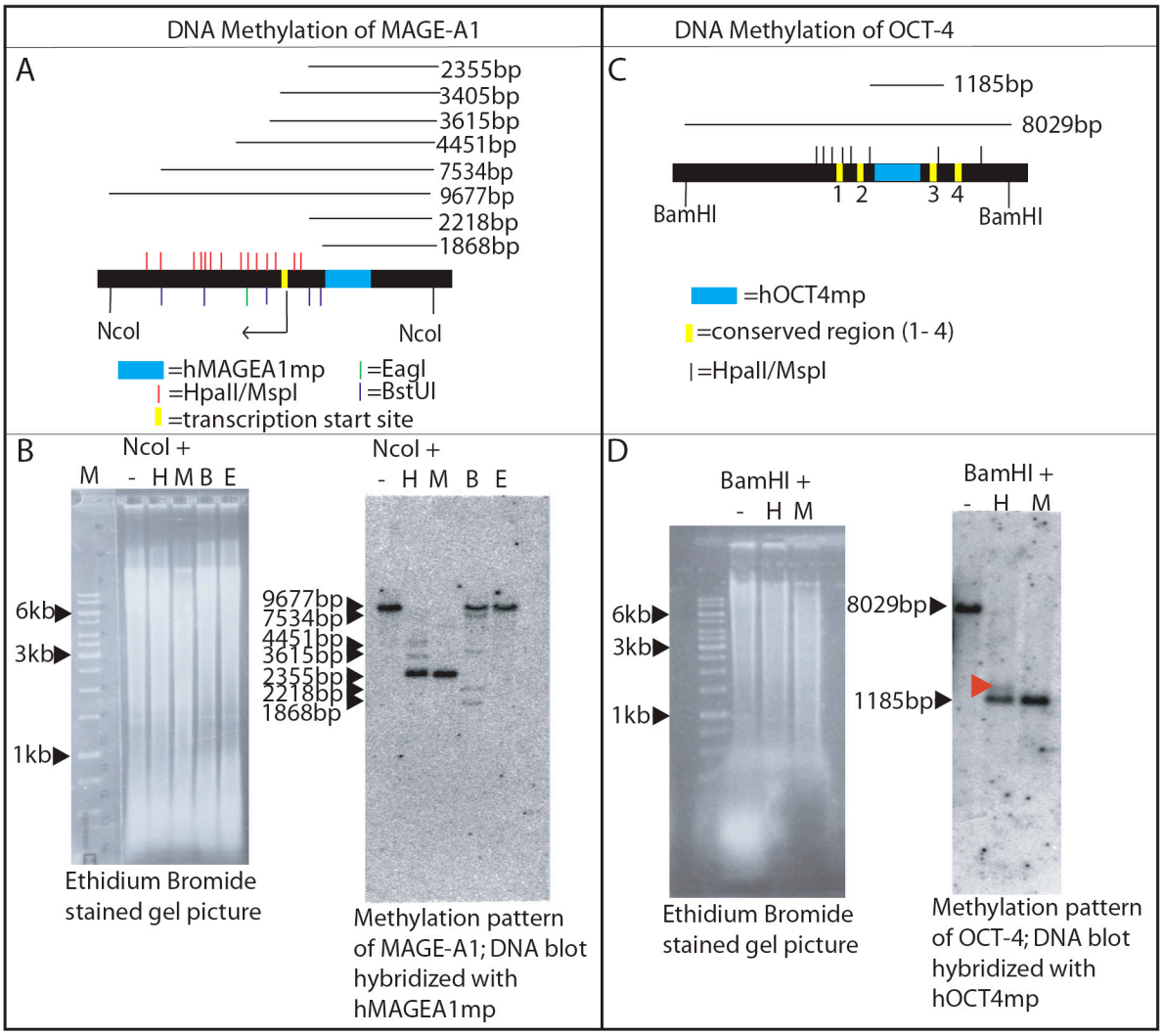

Figure 12: Methylation status of *MAGE-A1* and *OCT-4* A: Restriction map of the *MAGE-A1* is shown. DNA is shown as a black bar, the transcription start site (TSS) as a yellow bar and the hMAGEA1mp is shown as a blue bar. Methyl- in/sensitive enzymes (MspI/HpaII) sites are indicated by a vertical red slash on top of the DNA as well as a green and blue vertical slash below the DNA. Black vertical bar shows the NcoI restriction enzyme sites and restriction fragments are shown as horizontal bars above the DNA. The black arrow from the TSS shows the direction of the transcription. **B:** Left: Ethidium bromide stained gel after the digestion of 20µg Hs-27 DNA with NcoI alone (lane1), in combination with HpaII (lane 2), MspI (lane 3), BstUI (lane 4) or EagI (lane 5). Right: DNA blot hybridization with hMAGEA1mp probe resulted in a 9622bp band for the digestion with NcoI alone. NcoI together with HpaII resulted in a strong 2355bp band and faint bands at 3615bp and 4500bp (lane 2). A digestion with NcoI and MspI showed only the 2355bp band. Digestion EagI + NcoI revealed a single fragment at 9677bp. **C:** Same as in A with the exception that this is the *OCT4* promoter region. CR1-4 indicates conserved regions 1-4. BamHI is indicated below the DNA. Digestion with BamHI alone reveales a band at 8029bp and together with MspI at 1185bp. **D**: Same as in B with the exception of the used enzymes and the obtained restriction fragments. used enzymes: The digestion with BamHI alone reveled a fragment at 8029bp (lane1), BamHI together with HpaII (lane2) resulted in a fragment at 1185bp and a faint band above (indicted by the red arrow head). The digestion with BamHI together with MspI revealed a fragment at 1185bp.

it appears that most of the CpG sites in the majority of cells remain unmethylated at CR2 and CR3.

Concluding, both the *MAGE-A1* and *OCT-4* promoter regions, by DNA blot were not clearly methylated in Hs-27 cells as analyzed with the probes and restriction enzymes described. Therefore these regions were not included as controls in further experiments.

2.2.3 DNA methylation status of repetitive elements

As pointed out in the introduction DNA methylation is also involved in preventing the transposition of transposable elements (Bourc'his and Bestor 2004). It is known, that repetitive elements like SINEs, LINEs and a Satellite repeats containing a large fraction of the methylated CpG sites throughout the human genome (Weisenberger, Campan et al. 2005). These studies suggest that the methylation status of repetitive elements could also be used as controls in my experiment. Firstly, I assessed their normal methylation state in Hs-27 cells as shown in Figure 13. On the left side of Figure 13A the ethidium bromide stained gel after digestion with HpaII (methylation sensitive-lane 1) and MspI (methylation insensitive-lane 2) is shown. The gel was then blotted onto a Hybond-Nylon membrane and hybridized with hL1P3mp that detects LINE repeats as is shown on the right. The results indicated that most of the CpG sites were methylated, since a higher molecular fragment was present in lane 1 upon the digestion with HpaII (black arrow) compared with the MspI digestion (lane 2). Additionally, smaller fragments were present in lane 1 with fainter signal intensity. This indicated that in some cells some of the LINE HpaII sites were not methylated whereas the majority of the CpG dinucleotides were methylated or that some LINE repeats were not methylated but the majority were. In lane 2 the digestion with MspI revealed a shift from a higher molecular fragment (closed arrow, in lane 1) to a lower molecular sized band (open arrow). This shift was also visible on the ethidium bromide gel. Since MspI is methylation insensitive also smaller sized fragments were visible at a higher intensity as well as an additional band appears that was not present in the HpaII lane (green arrow).

The satellite 2 repeats are located in the pericentromeric region and are highly associated with DNA methylation, as published earlier (Weisenberger, Campan et al. 2005). Figure 13B examines the normal methylation state of satellite 2 repeat in Hs-

27 cells. On the left side of Figure 13B the ethidium bromide stained gel is shown after digestion with HpaII (methylation sensitive-lane 1) or MspI (methylation insensitive-lane 2). The comparison of the HpaII digestion and MspI digestion shows already in the ethidium bromide gel a shift from a higher band to a lower molecular band as may also seen in Figure 13A. This gel was blotted on a Hybond-Nylon membrane and hybridized with hSat2mp to detect Satellite 2 repeats as shown on the right side of Figure 13B (after 2 hours of exposure). If we consider the HpaII digestion in lane 1 a higher molecular band was present as indicated by the black arrow and no defined additional bands appeared at a smaller size (although there was a smear over a large size range). This indicated that most HpaII sites were methylated. However, upon the digestion with MspI (lane 2) the higher molecular band shifted towards a lower molecular size as shown by the open arrows. In addition 3 other bands were present at a smaller size (green arrows), albeit at a very low intensity.

The normal methylation status of the AluJb element that belongs to the SINE family is illustrated in Figure 13C. On the left side the ethidium bromide gel is present after the digestion of DNA with HpaII (lane 1) and MspI (lane 2). The ethidium bromide gel indicated the methylation sensitive HpaII gave larger digestion fragments than the methylation insensitive MspI that both recognize the same restriction site. After DNA blotting on a Hybond-Nylon membrane and hybridization with hAluJb in the HpaII digestion (lane1) the black arrow indicated a higher molecular weight smear compared to the MspI digestion (lane 2) (Figure 13C, right side). This indicated that most of the HpaII sites are methylated in AluJb Sine repeats in Hs-27 cells.

Finally, I analyzed the methylation state of long terminal repeats (5'LTR) from human endogenous retrovirus (HERV). It was published previously that retroviral elements are highly methylated in normal cells (Walsh, Chaillet et al. 1998), but hypomethylated in cancer cells (Menendez, Benigno et al. 2004). In Figure 13E the methylation state of 5'LTR elements in Hs-27 cells is shown. On the left side the ethidium bromide gel is depicted after the digestion with EcoRI alone or in combination with HpaII or MspI. The gel was then blotted onto a Hybond-Nylon membrane

and hybridized with hHERV(gag)mp. The results are shown in Figure 13E on the right side. The digestion with EcoRI alone shows multiple bands.

This was expected since the DNA blot probe was designed for covering a repetitive region and therefore recognizes not only one HERV. Nevertheless, the digestion pattern obtained upon double digest (EcoRI+ HpaII) showed 3 broad thick bands. The longest band was approximately 5000bp, a second at 3000bp and the smallest band at approximately 1200bp. Overall this was an indication that the 5'LTR element of HERVs were highly methylated, since in the MspI digestion in lane 3 the 5000bp and 3000bp largely disappeared at a remarkable level. However, smaller bands with a strong intensity appeared instead.

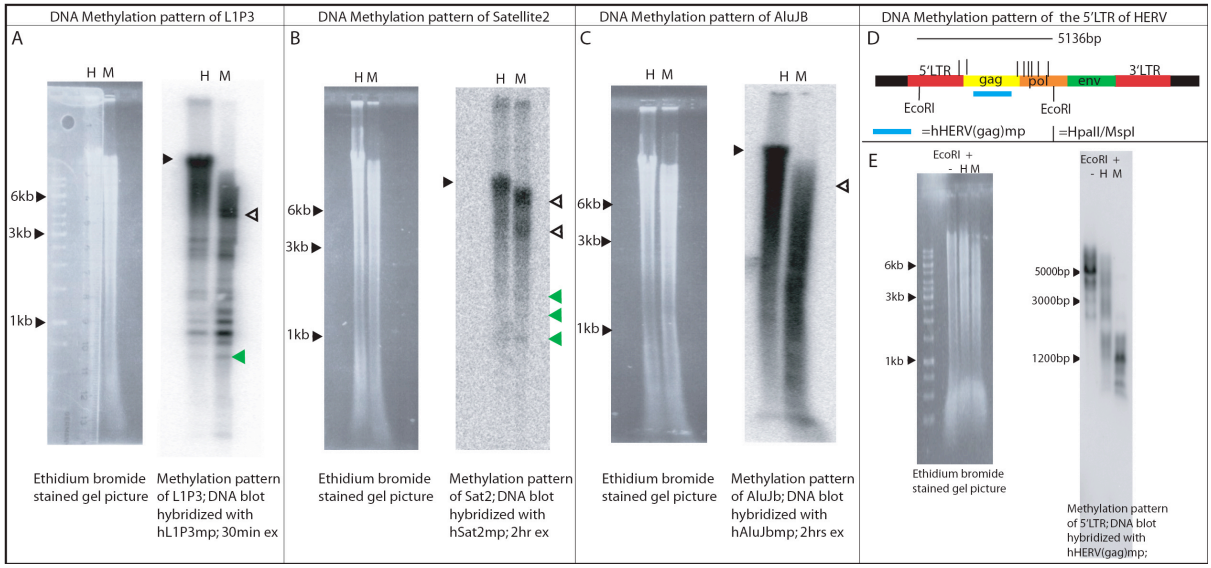

Figure 13: Methylation status of repetitive elements: LINE (L1P3), Satellite2, SINE (AluJb) and of HERVs: In all digestions HpaII (methyl-sensitive) or MspI (methyl- insensitive) was used. HERV was digested in combination with EcoRI. **A:** LINE (L1P3): Left: ethidium bromide stained gel. Right: DNA blot hybridized with hAluJbmp. Black arrow shows higher molecular band. Open arrow shows smaller molecular band and the green arrow shows an additional band that is not present in the HpaII digestion. **B:** same as in A, except it was hybridized with hSat2mp. **C:** same as in A, except it was hybridized with hAluJbmp. **D:** Restriction map of a HERV: black bar: DNA, red bar: 5'LTR or 3'LTR, yellow bar: gag region, orange bar: pol region and green bar: env region. Methylsensitive and methylinsensitive enzymes (HpaII and MspI) are shown as vertical bars above the DNA. A 5136bp restriction fragment is shown as a horizontal bar, below the DNA the probe is shown as a blue bar covering the gag region. Flanking restriction enzyme EcoRI **E:** same as in A, except: enzymes as described in D**.** DNA blot hybridized with hHERV(gag)mp.

In summary, the methylation status of L1P3 elements and the 5'LTR of HERVs could serve as controls in my further experiments because a clear methylation pattern was observed. On the contrary, the methylation status observed for the AluJb and Satellite2 repeat was excluded from further experiments. Although, it was

shown that these elements were methylated, the difference in the Southern blot banding pattern was not so dramatic as for L1P3 and the 5' LTR of HERV and therefore it would be difficult to quantify subtle changes in the DNA methylation status.

2.3 DAC Treatment of Hs-27 cells and analysis of Loss of Methylation

Previous studies have shown that 5-aza-2'deoxycytidine (DAC) can induce differentiation (Creusot, Acs et al. 1982), cytotoxicity (Juttermann, Li et al. 1994), DNA demethylation and reactivation of silenced genes (Jones and Taylor 1980) at micro-molar concentrations. My initial experiments focused on determining the optimal DAC dose in Hs-27 cells that demethylated DNA but had low enough cytotoxicity to allow the cells to still proliferate.

2.3.1 Continuous DAC treatment over 5 days (L1P3)

The first DAC treatment regime that I used was continuous treatment. I treated the cells in total for 5 days, changed the media every day as well as with new drug supply. I used a DAC concentration range from 0-20μM based on previous studies (Juttermann, Li et al. 1994). In Figure 14A the ethidium bromide stained gel is shown after the digestion with HpaII or MspI. In the ethidium bromide gel the methylation sensitive HpaII digest from the control untreated sample appeared slightly larger than the treated samples. The gel was then blotted on a Hybond-Nylon membrane and hybridized with hL1P3mp, as shown in Figure 14B. The result showed the appearance of small molecular weight bands in the treated samples upon digestion with HpaII (Figure 14B green box and 9C the blow up of the green box), although these bands are only visible at 0.05-0.5μM. At higher concentrations this faint band is not visible anymore. DNA loading was assessed upon the rehybridization of the membrane with hMTmp. The red box marks the 1.2kb fragment, which was used for quantification of the signal intensity between HpaII and MspI bands. The quantification is shown in Figure 14D. A slight increase at middle concentration range was detectable.

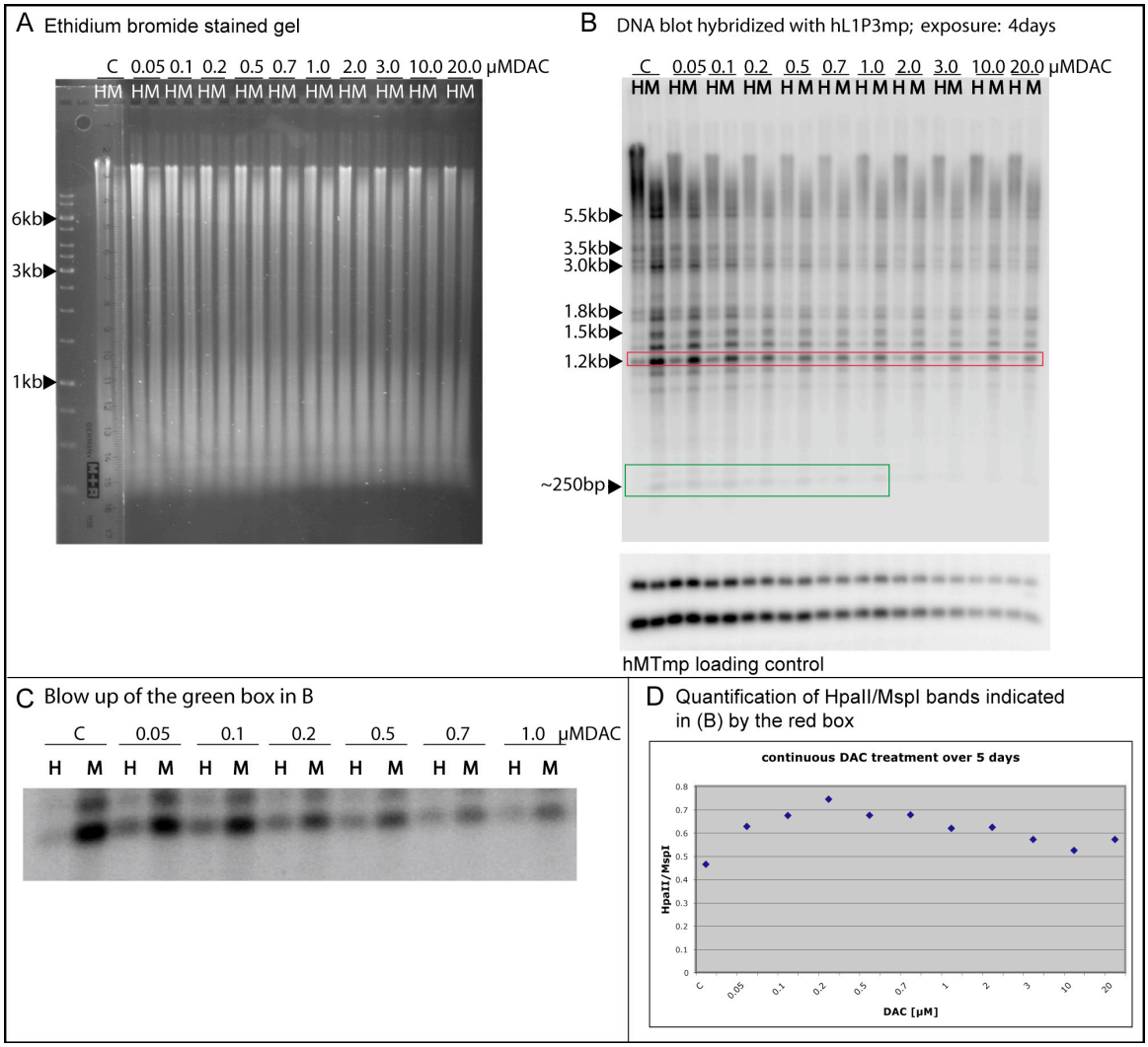

Figure 14: Continuous DAC treatment of Hs-27 cells for 5 days (DNA preparation 12.11.08) For each concentration 3 x 10^5 cells were seeded in a 10cm dish and the media and drug supply was changed every 24 hours. The concentration range: 0.05, 0.1, 0.2, 0.5, 0.7, 1.0, 2.0, 3.0, 10, 20 µM is indicated on the top in A and B. **A:** Ethidium bromide stained gel after DNA digestion with HpaII or MspI. A shift from a higher molecular fragment (C) to a smaller fragment (HpaII lanes in all treated samples) was observed. **B**: Top**:** DNA blot of hybridized with hL1P3mp, exposure time: 4days. The red box indicates the HpaII and MspI band that were consulted for quantification. The green box indicates a slight gain of a band in the HpaII lanes of concentration 0.05-0.2µM. Bottom: rehybridization of the membrane with hMTmp: this showed the unequal loading. **C:** Blow up of the green box shown in B. **D:** Quantification of the HpaII and MspI bands from B; no obvious change is detactable.

2.3.2 Viability assay of DAC treated Hs-27 cells

As mentioned above, DAC is not only a demethylation agent but can also induce cytotoxicity which occurs after G1 or G2 arrest initiated through the p53 pathway(Karpf, Moore et al. 2001; Zhu, Hileman et al. 2004; Palii, Van Emburgh et al. 2008). Therefore, I examined the effect of DAC on the viability of Hs-27 cells. The cells were treated with a dose ranging from 0-20µM. Every, second day the cell

number was counted for each concentration. The results are shown in Figure 15. After two days there was no obvious affect on the cell viability (Figure 15A). After 4 days, cell viability slowly declined with increasing concentrations of DAC (Figure 15B). The decline was first apparent at 0.5µM DAC and was greater at 20µM (Figure 15B). After 6 days treatment a decline in cell viability was visible at even the lowest DAC concentration (Figure 15C). The first decline was visible between a dose of 0 - 0.1µM, illustrated by a drop from 90% to ~75% viability. The second decline was present at concentrations between 0.1-20µM as a drop from 75% to ~65% viability. Although the experiment was conducted in one technical replica, the results indicate in here that DAC treatment has a negative effect on the viability of the cells with increasing concentration.

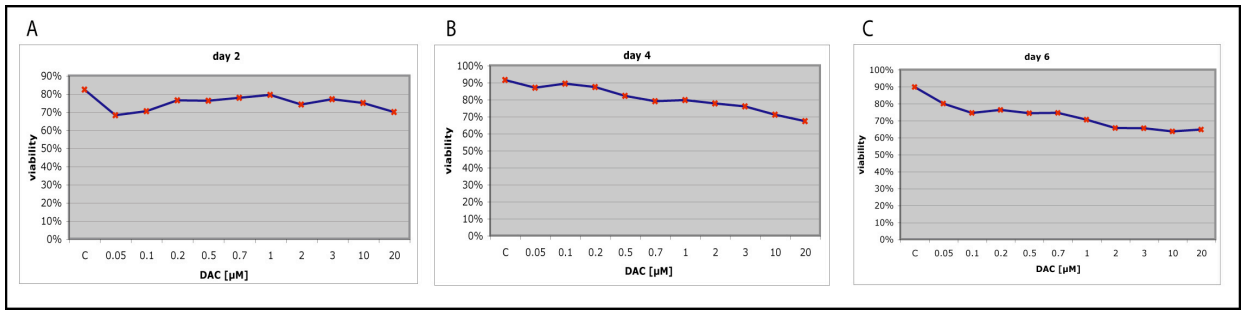

Figure 15: Viability of continuous DAC treated Hs-27 cells: for each concentration range 3 x 10^5 / 10cm dish were seeded, treated and then counted after 2, 4 and 6 days. The experiment was conducted in one technical replica. X-axis indicates the concentration range from 0-20µM and the y-axis indicates the viability in percent **A:** Hs-27 cells counted after 2 days **B:** counted after 4 days **C:** counted after 6 days

2.3.3 Continuous DAC treatment over 5 days (*H19* DMR)

To determine whether the effect of no obvious loss of DNA methylation was restricted to repetitive elements as shown in Figure 14, I examined with the same treatment strategy the effect on a single copy gene. I repeated the DAC treatment experiment, since I was unable to isolate enough DNA from the initial experiment presented in Figure 14. The results presented in Figure 16 show the analysis of the DNA methylation status of the *H19* gene after DAC treatment. The ethidium bromide stained gel (Figure 16A) showed no indication of a loss of DNA methylation in contrast to the ethidium bromide gel for the L1P3 repeat, where a slight shift of the HpaII lane compared to the MspI lane was visible (Figure 14). A slight decrease in the

amount of loaded DNA is visible already at a concentration of 0.1, which became more apparent with increasing concentrations of DAC (Figure 16A). The hybridization of the membrane with the hH19mp is shown in Figure 16C after a 24hr exposure and in Figure 16D after a 4day exposure. In the control lane a 3888bp band was present upon the digestion with BglII alone as expected according to the restriction map in Figure 16B. The double digestion with BglII and HpaII revealed a complex methylation pattern. Lane 3 showed the digestion with BglII together with MspI and resulted in 3 visible fragments at 1111bp, at 962bp and at 284bp. The double digestion with BglII and HpaII in the treated samples with DAC concentrations ranging

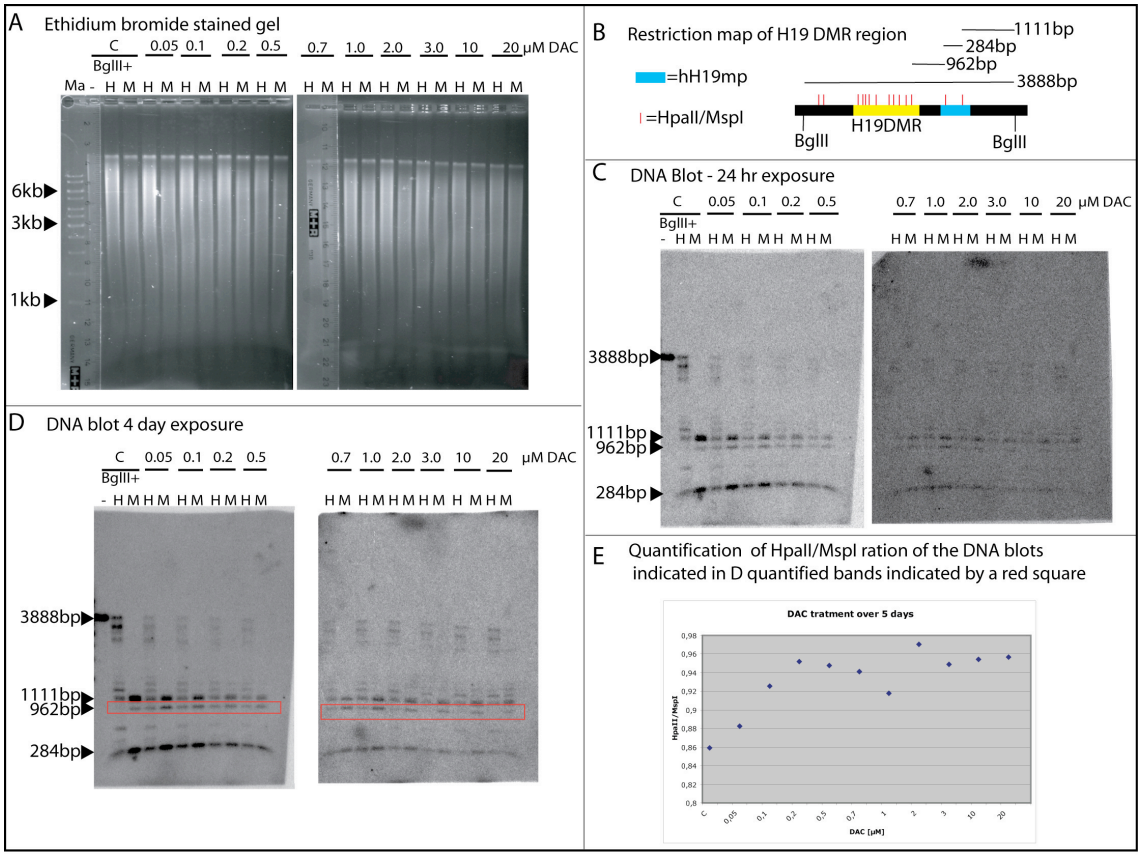

Figure 16: Continuous DAC treatment of Hs-27 cells for 5 days: (DNA preparation 18.11.08): A: Ethidium bromide stained gel after digestion with HpaII or MspI; Ma= Marker; C= untreated control. The concentration range 0.05-20µM is shown above the gel. A decrease in the loading of DNA was visible with increasing DAC concentrations. **B** Restriction map of the *H19* DMR region as described earlier (Figure 9). **C:** DNA blot hybridized with hH19mp after 24 hr exposure. In C (BglII-): 3888bp fragment was visible, (+HpaII): showed a complex methylation pattern, (+MspI): 1111bp, 962bp and 284bp fragments were visible: Higher molecular bands in (+HpaII) of the treated samples decreased in intensity and a band at 962bp appeared. Red box indicates the bands used for the quantification. D: same as in C with the exception of 4 day exposure. **E:** Quantification of the HpaII/ MspI ratio of bands shown in D on the right. X-axis indicates the DAC concentrations and the y-axis indicates the HpaII/MspI ratio. An increase of the signal intensity of the 962bp fragment in the BglII/HpaII lane with increasing DAC concentrations was detected.

from 0.05 until 2.0µM clearly showed a fragment present at a length of 962bp that was absent in the control (lane HpaII (H)), indicating a loss of methylation. The quantification was conducted between the gained BglII/HpaII fragment and the BglII/MspI fragment, indicated in Figure 16D by the red box. The results in Figure 16E revealed a slight increase in signal intensity for the 962bp fragment in the BglII/HpaII lane.

2.3.4 Continuous DAC Treatment over 9 days (L1P3)

Since there was no obvious loss of DNA methylation for L1P3 (Figure 14), and only a partial loss of DNA methylation for the *H19* DMR (Figure 16), I therefore extended the duration of the treatment from 5 to 9 days. Accordingly, I

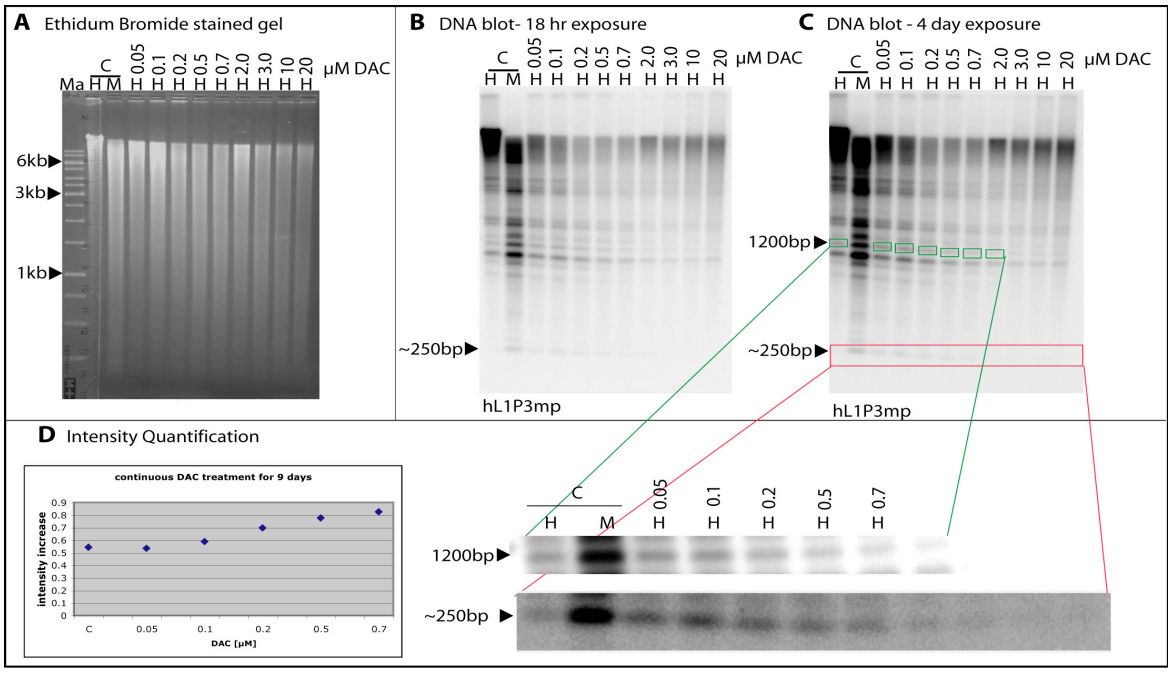

Figure 17: Continuous DAC treatment of Hs-27 cells for 9 days - L1P3 under investigation: (DNA preparation 27.11.08): For each concentration 3 x 10^5 cells were seeded in a 10cm dish and the media and drug supply was changed every 24 hours over 9 days. The concentrations used were 0.05, 0.1, 0.2, 0.5, 0.7, 2.0, 3.0, 10, 20 µM as indicated on the top of A, B, C; Ma=1kb DNA ladder; C=untreated control **A:** Ethidium bromide stained gel after DNA digestion with HpaII or MspI. Unequal loading of DNA was visible. **B**: DNA blot of hybridized with hL1P3mp: exposure time: 18 hours **C:** Exposure time 4 days. Red box indicates the HpaII bands that were consulted for quantification with comparison to a higher molecular HpaII band (green boxes); arrow= gain of a band; **D:** Top: blow up of the gained 200bp band (red box) which were quantified upon comparison with a higher molecular weight fragment, 1200bp (green box). Bottom: In the quantification a slight intensity increase for the 200bp band is detectable.

treated the cells in a continuous manner for 9 days and analyzed the DNA methylation status of the L1P3 repeat (Figure 17). In Figure 17A the ethidium bromide stained gel is shown after the digestion with HpaII or MspI. The gel picture indicated that DNA loading was unequal. Moreover, a slight shift from a higher molecular size in the control HpaII lane to a smaller molecular size in the treated samples was visible. The gel was then blotted on a Hybond-Nylon membrane and hybridized with hL1P3mp, as shown in Figure 17B and C. After 18 hours of exposure (17B) the signals appeared at a strong intensity in the control lane and to a lesser intensity in the treated samples, although no noticeable change in the DNA methylation pattern was detected. After 4 days exposure a faint band appeared at a small size (~ 250bp) matching a MspI band (see arrow, Figure 17C). This band was slightly present in the control digestion with HpaII, and appeared in the 0.05-0.7μM DAC treated cells stronger, becoming fainter with increasing DAC concentrations and disappeared after 2μM. This band was quantified in comparison with a higher molecular band, illustrated by the green boxes. The result of this quantification is illustrated in Figure 17D. The gain of this band was more obvious in the blow up. The quantification revealed a relative increase in the intensity of the smaller molecular fragment, with increasing DAC concentrations up until 0.7μM interpreted due to unequal DNA loading. These results showing the gain of a small molecular weight fragment were similar to that shown in Hs-27 cells treated for 5 days with DAC (Figure 14). In summary results indicated that although some CpG sites were demethylated, the majority of the CpG sites remain methylated. Therefore, no obvious loss in the DNA methylation pattern was detected.

2.3.5 Non-continuouse DAC treatment over 9 days (L1P3 and HERV)

DAC induces cytotoxicity, upon the trapping of the DNMT1 (Juttermann, Li et al. 1994) and activation of the p53 pathway (Karpf, Moore et al. 2001), as mentioned above. Therefore, in order to minimize the cytotoxicity effect (shown in Figure 15) I tested non-continuous DAC treatment. I treated the cells once every third day over 9 days. This gave the cells more time to recover from the cytotoxic stress and to replicate which is necessary for DAC induced DNA. The continuous treatment at low and at high concentrations could lead to a high level of DAC in the cells not allowing DNA

damage to be efficiently repaired and inducing apoptosis. With non-continuous treatment every three days, DAC levels should decline between treatments because the half-life is 21 hours at 37°C at pH 7.0 (Stresemann and Lyko 2008).

In this case I treated the cells over 9 days and the result of the DNA digestion with HpaII and MspI is shown in Figure 18A. From the ethidium bromide stained gel it appears that the amount of loaded DNA is unequal, compared between the samples (Figure 18A). After hybridization with the hL1P3mp probe the results show this more clearly (Figure 18B and C). In addition it appears that the MspI digestion from 0.5, 2.0, 10 and 50μM is incomplete because a thick higher molecular band is present, which the untreated control lacks (Figure 18B and C). Nevertheless, in the control sample the HpaII digestion compared to the MspI digestion revealed that most of the CpG sites were methylated and therefore signal intensity in the HpaII digestion was lower for the smaller sized fragments. On the contrary, if the HpaII and MspI lanes from the 1.0μM DAC treatment were compared to each other it appeared that some of the CpG sites were demethylated. For this purpose the MspI lanes and HpaII lanes, that are illustrated in Figure 18D by the red box, were quantified and compared to each other within the control as well as within each concentration from 0.1-10μM. This reveals, apart from unequal loading, that a partial decrease of DNA methylation is visible if e.g. upon comparing the quantification of the 1.0μM lane to the control lane.

The DNA methylation of the 5' LTR of human endogenous retrovirus (HERV) after non-continuous DAC treatment is shown in Figure 19. I digested the DAC treated DNA with EcoRI together with HpaII or MspI. The ethidium bromide stained gel indicated unequal loading. The gel was blotted on a Hybond-Nylon membrane and hybridized with the hHERV(gag)mp probe. The results are shown in Figure 19C and D after 24 hours or 48 hours of exposure, respectively. The DNA blot results showed firstly, that the amount of loaded DNA was unequal between the samples, although loading appeared equal between the HpaII and MspI lanes within a sample. This made the quantification of HpaII compared to MspI lanes possible. The red box showed the bands of the HpaII and MspI lanes and indicated that the HpaII band increased in intensity compared to the control. The quantification of these bands made this clearer. These results must be cautiously interpreted due to the unequal

DNA loading, but the treated samples appeared to show a partial decrease in the DNA methylation pattern, which appeared to be constant from 0.1 to 3µM DAC.

In summary, the results from the non-continuous (pulse) treatment suggested a partial loss of DNA methylation had occurred at L1P3 and HERV repetitive elements, but this finding was confounded by unequal DNA loading. To try to determine if loss of DNA methylation really can be induced by non-continuous DAC treatment I next examined the DNA methylation status of non-repetitive elements.

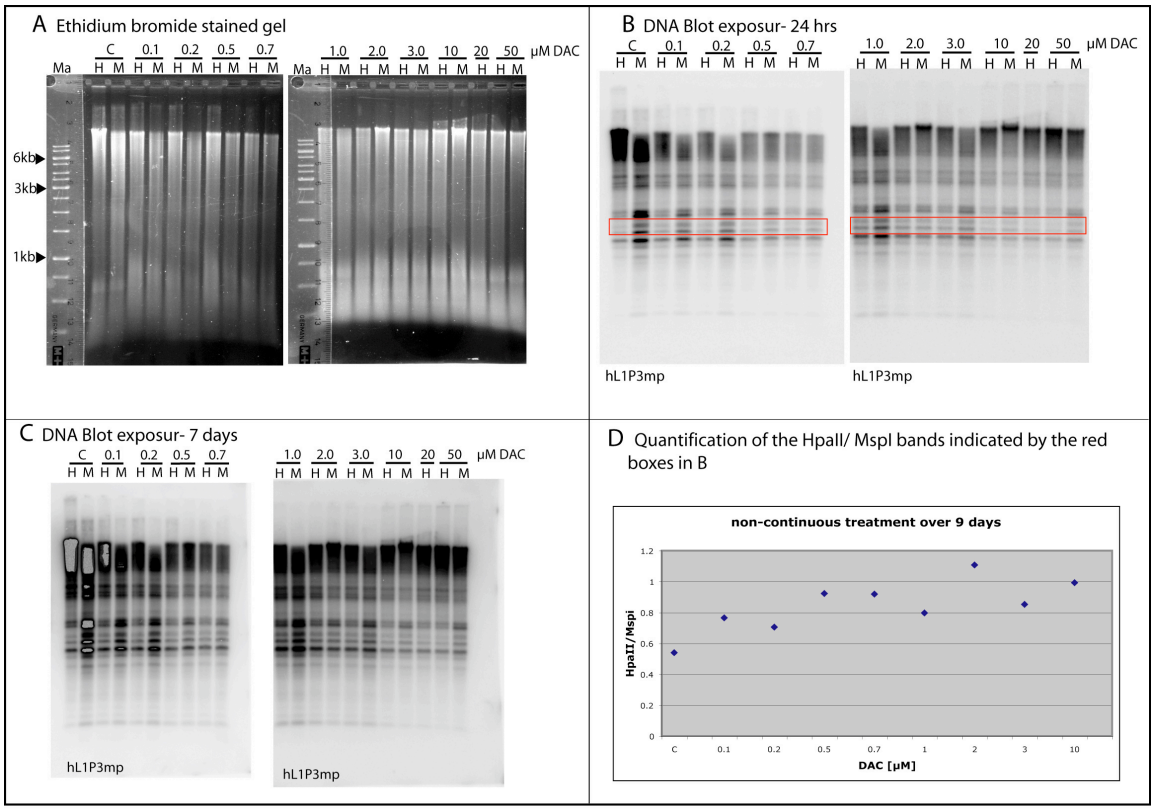

Figure 18: non- continuous treatment (pulse) DAC treatment of Hs-27 cells for 9 days- L1P3 under investigation (DNA preparation 11.12.09): for each concentration 3 x 10^5 cells were seeded in a 10cm dish. The media and drug supply was changed every 72 hours over 9 days. The concentration range was 0.1, 0.2, 0.5, 0.7, 1.0, 2.0, 3.0, 10, 20 and 50µM as indicated on the top of A, B, C; Ma= 1kb DNA ladder; C= untreated control **A:** ethidium bromide stained gel after DNA digestion with HpaII or MspI. Unequal loading of DNA was visible. **B**: DNA blot hybridized with hL1P3mp and exposed for 24 hours. Red box indicated the bands in HpaII and MspI which were consulted for quantification; **C:** same as in B except: exposure is 7 days. **D:** The bands that were consulted for quantification are shown by the red box. The MspI band intensity was divided by the HpaII band intensity. X-axis indicates the DAC concentrations; y-axis shows the average of MspI to HpaII. A partial loss of DNA methylation was seen compared to the control.

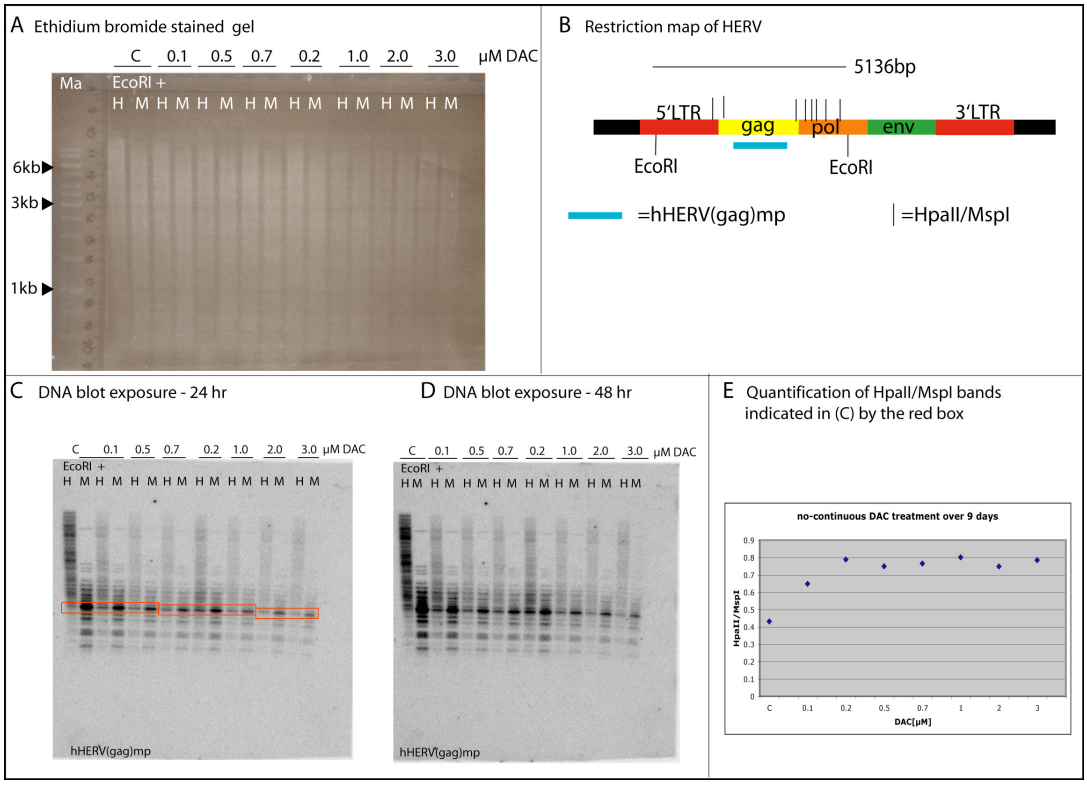

Figure 19: Pulse DAC treatment of Hs-27 cells for 9 days – HERV is under investigation (DNA preparation 11.12.09): For each concentration 3 x 10^5 cells were seeded in a 15cm dish, the media and drug supply was changed every 72 hours over 9 days. The concentration range was 0.1, 0.5, 0.7, 0.2, 1.0, 2.0, 3.0µM as indicated on the top of A, C, D. Ma= 1kb DNA ladder; C= untreated control **A:** DNA was digested with EcoRI together with HpaII or MspI. Unequal DNA loading was visible in the ethidium bromide stained gel. **B:** Restriction map of HERV as described earlier in Figure 13. **C:** DNA blot hybridized with hHERV(gag)mp and exposed for 24 hours. The red box shows the HpaII and MspI band that were consulted for the quantification. D: Same as in C with the exception that the exposure was 48 hours. **E:** Quantification by ImageJ of the bands from the red box in C.

2.3.6 Non-continuous DAC treatment over 9 days (*H19* and *AIRN* DMR)

In order to examine the effect of 9 days non-continuous DAC treatment on the DNA methylation state of the single copy *H19* and *AIRN* DMR, I used the 3 highest concentrations (1, 2, 3 µM DAC) from which previous experiments compared to untreated control cells. Accordingly, I treated the cells in the same way as described above. Firstly, I looked at the proliferation of the cells and pictured them. Figure 20 shows the cells under the control conditions as well as under the conditions with 1, 2, 3µM non- continuous DAC treatment, respectively. From these results, it was visible that the control had a higher cell density than the treated samples. Furthermore, between the treated sampled there seems to be a decline in the density from 1µM to 2 and 3µM.

The DNA from these cells was isolated for the digestion with BglII together with MspI or HpaII. The ethidium bromide stained gel of the three replicas showed no obvious evidence of the unequal loading of DNA between the treated samples, but compared to the DAC treatments the control HpaII digestion appeared to have more DNA loaded (Figure 21A). Indeed, after DNA blotting and the hybridization with hH19mp this became more apparent (Figure 21C). In all of the three replicas the signals in the treated samples were less intense compared to the control. Nevertheless, if one considers the control HpaII digests no 962bp fragment matching the MspI band was visible in all three replicas. This fragment only appeared after DAC treatment. Despite the unequal loading, this can be cautiously interpreted as a partial loss of DNA methylation. Moreover, the higher molecular fragments that present in the control HpaII digestion also disappeared in the treated samples. This might be on the one hand due to the unequal loading and on the other hand due to a partial loss of DNA methylation indicated by the fact that a 962bp fragment was gained. The quantification of the 962bp fragment between the HpaII and MspI lane within each sample was conducted with the ImageJ program and the results are shown in Figure 21D. These results do not show as great a difference between the control and the treated samples as seen by visual inspection perhaps due to background signals on the membrane.

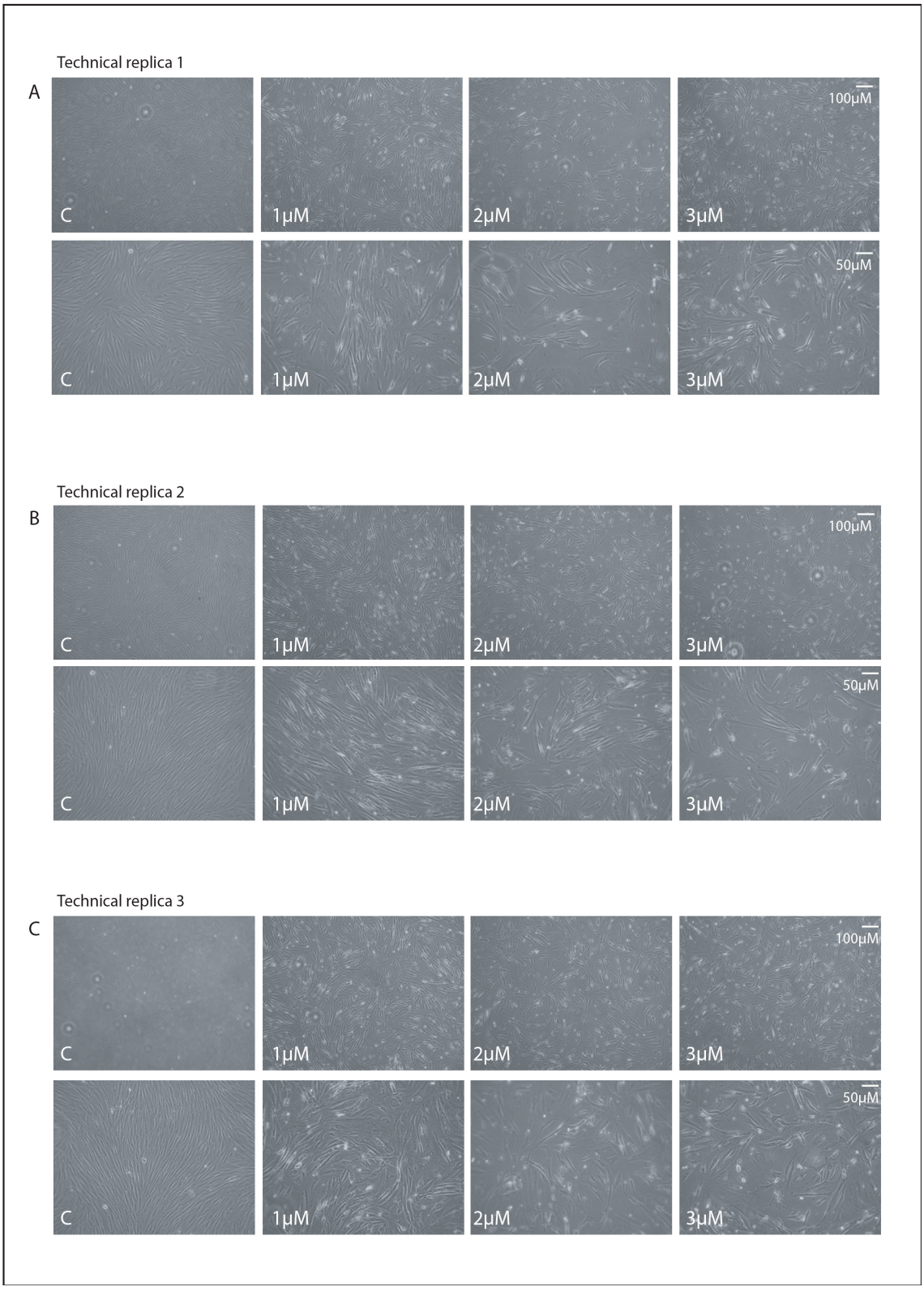

Figure 20: Proliferation of Hs-27 cells after 9 days of pulse treatment: Cells were treated under the same conditions as described in Figure 19 and were photographed. The experiment was conducted in three technical replica **A**: Technical replica 1: **B:** Technical replica 2 **D:** Technical replica 3. A decline on cell density was visible between the control and the treated cells as well as a decline in cell density between the treated samples with increasing DAC concentration.

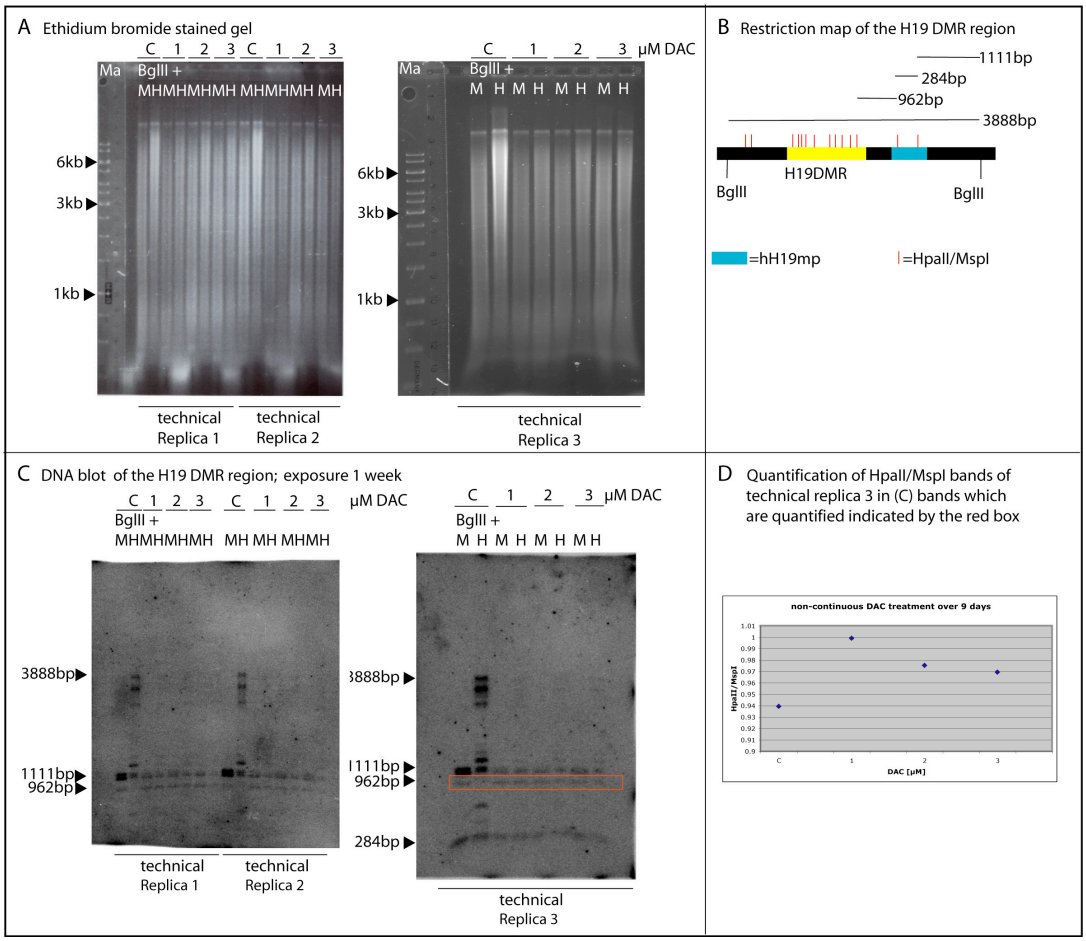

Figure 21: DNA methylation status of the *H19* DMR in Hs-27 cells after 9 days of pulse DAC treatment (DNA preparation: 25.01.09): For each concentration 3 x 10^5 cells were seeded in a 15cm dish and the media and drug supply was changed every 72 hours over 9 days. The concentration range was 1.0, 2.0, 3.0µM as indicated on the top of A, C, D; Ma= 1kb DNA ladder; C= untreated control **A:** Ethidium bromide stained gel of three technical replicas digested with BglII plus MspI or HpaII. Unequal DNA loading was visible. **B:** Restriction map of the *H19* DMR region as described earlier in Figure 9. **C:** DNA blot of 3 technical replicas hybridized with hH19mp. Replica 1 and 2: control MspI lane 2 fragments are visible, one at 1111bp and one at 962bp. Electrophoresis was conducted for 6V/cm (5-6 hours) therefore the 284bp fragment was not detectable anymore in contrast to technical replica 3. In all replicas the loading of the DNA was unequal, although in the HpaII lanes from 1-3µM a gain of the 962bp fragment was detected. **D:** Quantification (ImageJ) of the 962bp band (shown by the red box in C): for each sample the HpaII and MspI lane were compared to each other.

Next the methylation status of the *AIRN* DMR was analyzed in the untreated control and the treated samples (Figure 22). The ethidium bromide stained gel indicated more DNA was loaded in the control HpaII lane compared to the treated samples. This was visible in all three replicas Figure 22A. The effect became more apparent after the hybridization of the membrane with the Bx probe. The untreated control digestion with EcoRI and MspI revealed one band present at 2988bp. The digestion of EcoRI together with HpaII resulted in fragment present at 5757bp and one at 2988bp. These bands were visible from replica 1 to replica 3. In the treated

samples only the 2988bp fragment was visible, although it was very faint. In replica three the 5757bp fragment was also visible but very faint. The unequal DNA loading and faint bands in the treated samples makes interpretation of this data difficult. However, there were tentative indications that at least a partial loss of the DNA methylation pattern, in DAC treated samples had occurred. This was due to the fact that for example the 2988bp fragment in the HpaII lane of the 1µM sample in replica 3 appears to be stronger than the 5757bp fragment in the same lane. In comparison, in the untreated control, HpaII digestion, the fragments (5757bp and 2988bp) appear to have similar same intensity.

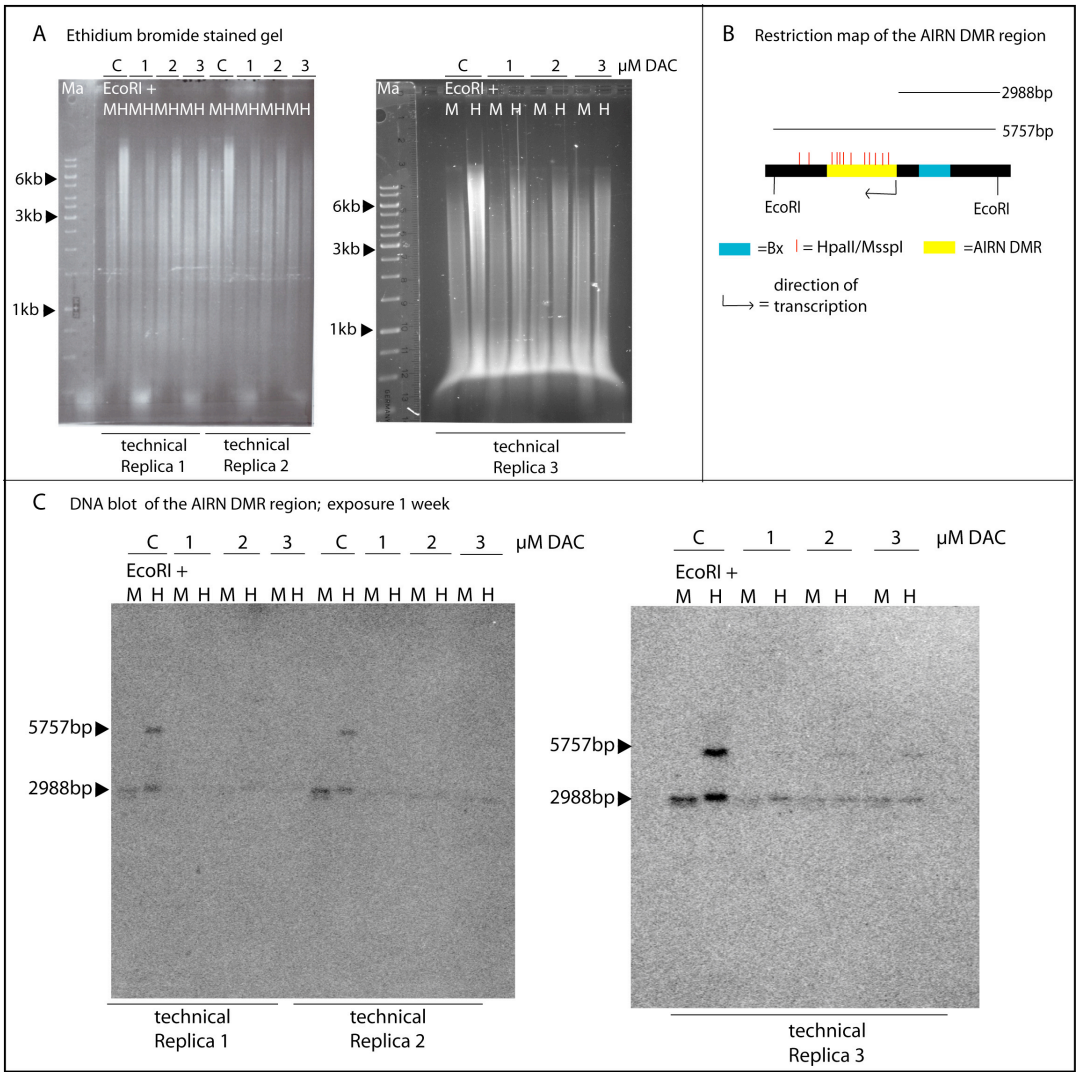

Figure 22: DNA methylation status of the *AIRN* DMR in Hs-27 cells after 9 days of non-continuous (pulse) DAC treatment (DNA preparation date: 25.01.09): Experimental procedure conducted as described in Figure 21. **A:** Ethidium bromide stained gel of the three replicas was visible after the digestion with EcoRI together with HpaII or MspI. Unequal loading was visible in comparison between the untreated control sample and the treated samples. **B**: Restriction map of the AIRN DMR as describe in Figure 10. **C:** DNA blot after 1 week exposure: The visible fragments are at 5757bp and 2988bp according to the restriction map in B. Signals of the treated samples are low in intensity due to unequal DNA loading.

Taken together, these results showed no obvious loss of the DNA methylation pattern, although it seems at least a partial loss of DNA methylation was achieved for the *H19* DMR since a gain of a band was visible. This interpretation has to be taken with care because the DNA loading was unequal.

2.4 Expression analysis

2.4.1 qPCR analysis of the *H19* ncRNA and *MAGE-A1* gene

As no dramatic loss of DNA methylation was detectable by Southern blot analysis, the effect of DAC upon the induction of gene expression of the *MAGE-A1* gene and the *H19* ncRNA was assessed in addition. The *MAGE-A1* gene is not expressed in somatic cells but expressed in a variety of tumors as well as in the testis of males (Simpson, Caballero et al. 2005). Moreover, the transcriptional repression was shown to be associated with CpG methylation of the transcriptional start site (De Smet, Lurquin et al. 1999). The *H19* ncRNA shows a differential expression pattern, as described previously. Previous studies have shown that the expression of the *H19* ncRNA and *MAGE-A1* gene is induced upon DAC treatment (De Smet, Lurquin et al. 1999; Lynch, Tycko et al. 2002). To assess this in Hs-27 cells I performed qPCR assys for these two genes. Figure 23A shows the induction of the *H19* ncRNA upon normalization to the ribosomal large protein A0 (RPLPO) and illustrates that *H19* ncRNA is induced upon treatment with DAC. The induction is between 10-100 fold. The result using GAPDH (TaqMan assay) for normalization showed an induction of 5-25 fold (Figure 23C). Note the large difference in the technical replicas for *H19*. In addition, the expression of the *MAGE-A1* gene was induced to a 15- fold level using RPLPO for normalization and a 5-10 fold level using GAPDH for normalization. The induction of the *MAGE-A1* expression compared to the *H19* ncRNA was more constant at different DAC treatment concentrations. Therefore, the expression of the *MAGE-A1* gene showed no concentration dependent induction as was visible in the normalization to RPLPO as well as to GAPDH.

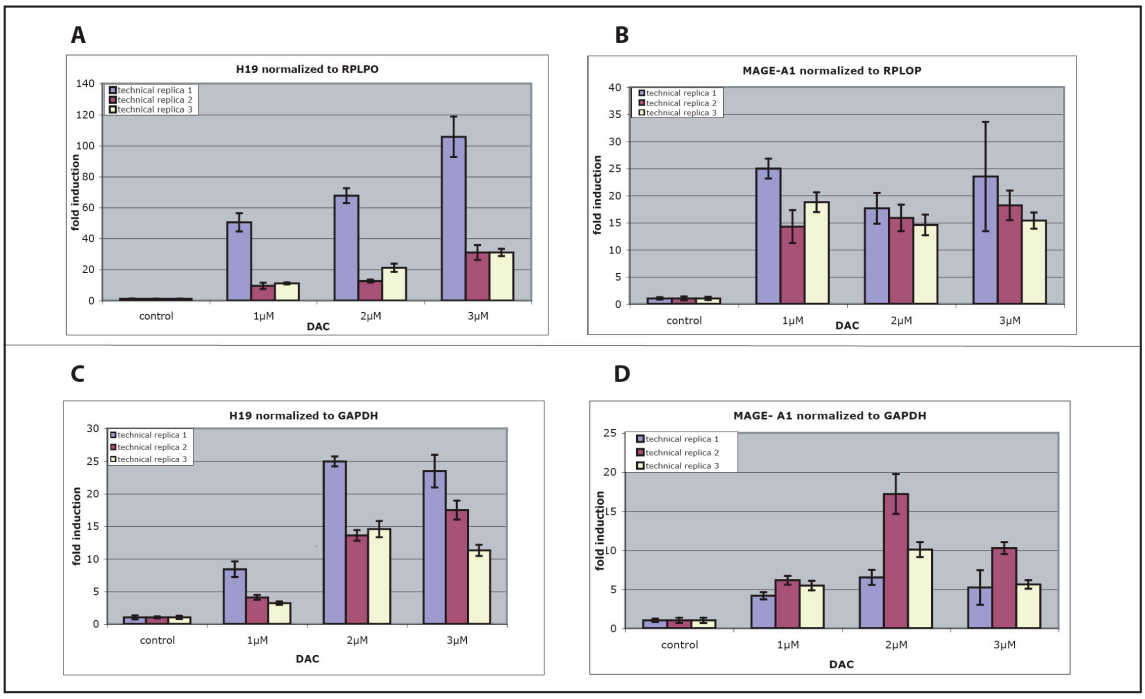

Figure 23: Expression levels of the MAGE-A1 gene and the H19 ncRNA of DAC treated Hs-27 cells: (RNA preparation day 25.01.09). qPCR of the *H19* ncRNA and the *MAGE-A1* gene normalized to RPLPO (A, B) in a SYBR green assay or to GAPDH (C,D) in a TaqMan assay. The assay was conducted in 3 technical replicas and the control was set to 1. The x-axis showed the DAC concentration range. The y-axis gives the fold induction. Both assays reveal an induction of the *H19* ncRNA and the *MAGE-A1* gene

2.4.2 RNA-expression tiling array

The effect of DAC on macro ncRNA expression was examined by using a NimbleGen custom tiling array. The HIRTA (Human Imprinted Tiling Array) (prepared by Irena Vlatkovic, a Ph.D. student in the lab) chip covers by 26 imprinted regions in human. Most of these regions are roughly 1MB in length. After the identification of repetitive sequences with the repeat masker, single copy regions were covered with 50bp oligo probes per 100bp.

In Figure 24 I show the expression of the *H19* ncRNA in WT Hs-27 cells and DAC treated cells. In WT Hs-27 cells the *H19* ncRNA is not expressed, However, upon treatment with 1µM DAC the expression of *H19* is induced (see Figure 24A and in the blow up of 24B).

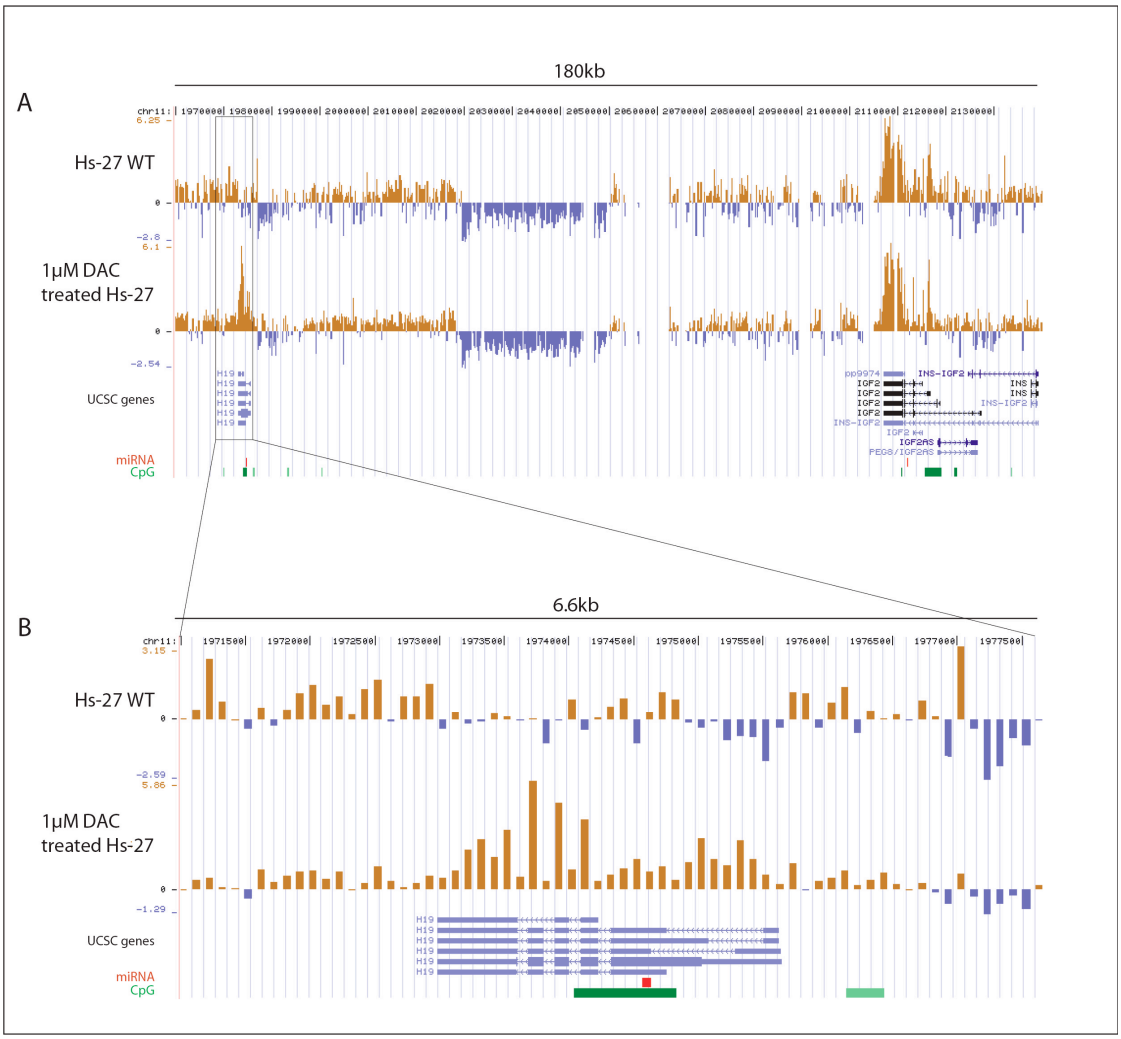

Figure 24: *H19* ncRNA expression was examined using HIRTA. RNA preparation day of DAC treated Hs-27 cells: 25.01.09. The y-axis displays the $\log_2$ ratio of cDNA normalized to genomic Hs-27 DNA. The x-axis displays the genomic position in the human genome. CpG islands are shown as green bars and miRNAs are in red. **A:** Custom tracks loaded onto the USCS browser display Hs-27 WT cells and 1μM DAC treated Hs-27 cells. **B:** Blow up of the H19 ncRNA from A. The results show that H19 ncRNA expression is induced upon 1μM DAC treatment (unpublished data from Irena Vlatkovic)

3. Discussion

It is known that DNA methylation in imprinted regions can control the expression of macro ncRNAs (Seidl, Stricker et al. 2006). To address the question if all macro ncRNAs in human of imprinted regions are regulated by DNA methylation it is necessary to demethylate the genomic sequence. A DNA demethylation effect in human is provided by using the DNA methyltransferase inhibitor, Decitabine. Therefore, this thesis illustrates, as a basis for further studies, the effect of Decitabine, on DNA methylation (Oki, Aoki et al. 2007). The results presented here indicate, DAC treatment induced a very slight loss of DNA methylation at some loci as well as the induction of gene expression, in particular the *H19* ncRNA and the *MAGE-A1* gene.

3.1 PCR reactions and Cloning

In order to test the DNA demethylation effect of DAC I designed 10 DNA blot probes using PCR (Figure 6). For each of them I conducted $MgCl_2$ concentration optimization in order to obtain a product. The reason for this is that $MgCl_2$ has an influence on all steps in the PCR: denaturation, annealing, product specificity, occurrence of primer dimers and the activity of the TaqPol. The optimal $MgCl_2$ concentration for my PCR reactions was in a range from 0.8 to 1.6mM. Moreover, I conducted for the hDLK1mp (Figure 6B), hPWSmp (Figure 6C) and hMAGE-A1mp (Figure 6E) probe PCRs, an optimization reaction for Betaine, to achieve a better result. Betaine has the capability to enhance the substrate specificity as well as the enhancement of amplification of GC rich regions. However, in these results Betaine did not improve PCR yield and specificity when the optimimal $MgCl_2$ concentration was used. Therefore optimization was sufficient to PCR amplify the probes in this case, but with more difficult PCRs, Betaine optimization may be useful.

There were some difficulties PCR amplifying repetitive LINE (L1P3) and SINE (AluJb) elements. I was unable to PCR amplify a LINE element which had been previously published as being methylated (Weisenberger, Campan et al. 2005). A study by Bourc'his et al (2004) analyzed the DNA methylation state of a LINE repeat (5'UTR) in mouse. Therefore, I used this sequence to BLAST against the human ge-

nome and detected a homologous LINE repeat on chromosome 9. Accordingly, I designed a set of PCR primers located in the 5'UTR, and this LINE was then able to PCR amplify it (Figure 6J).

In case of the SINE repeat I used a different approach. MY first set of primers designed against SINE (AluJb) repeats failed to amplify a product using Hs-27 genomic DNA or a BAC template. Therefore, I next identified a group of Alu repeats on the BAC2358 template and designed a new set of primers. The forward primer was flanking a single copy region and the reverse primer was designed to a repetitive region. Using the BAC2358 template I was able to PCR amplify the Alu repeat (Figure 1G).

Cloning of the probe templates into pGEM-T-Easy was successfully conducted according to the manufacturer's protocol. For the Maxi Prep procedure I used for the purification steps either the protocol "DNA purification by DNA Centrifugation" or "DNA purification by DNA Vacuum". DNA centrifugation technique was sufficient for most of the constructs, but for some of the constructs it failed to obtain a high enough yield. Thereafter, I used the protocol for the purification according to the vacuum procedure. A possible explanation for the better yield of the Vacuum procedure maxiprep might be that an additional centrifugation step after the neutralization procedure collecting the cell debris and preventing the purification column of being overloaded. An additional advantage of the vacuum purification protocol is that requires less time than the centrifugation maxiprep protocol.

In summary, the PCR reactions worked after $MgCl_2$ optimization, while Betaine optimization showed no effect. Moreover the cloning and maxiprep of DNA was successful once the optimal method was chosen. In this way I cloned 10 DNA blot probe templates for analyzing a possible loss in DNA methylation upon DAC treatment of Hs-27 cells.

3.2 Treatment strategies

The first aim of the analysis of loss of methylation was to find the optimal drug dose treatment strategy for Hs-27 cells. In general, a well-defined treatment strategy for DAC is not available. However, literature search revealed that the main dose schedule of DAC lies in the micro-molar range (Yoo and Jones 2006). To determine the optimal dose in Hs-27 cells I conducted experiments with a previous published dose range from 0-20µM (Juttermann, Li et al. 1994). Firstly, I needed to determine a dose range in which the cells still divide, since DAC is S-phase dependent. Secondly, published studies suggested I need more than two rounds of replication to see an effect of loss of DNA methylation. Therefore, the detection of loss of DNA methylation is dependent on the rounds of replication a cell undergoes. After one round of replication the DNA is hemimethylated, while in the second round of replication two demethylated strands and 2 hemimethylated strands are the result (Jones, Taylor et al. 1982). The duration of the treatment depends therefore on the doubling time of the cells which in the case of Hs-27 cells, is every 21 hours.

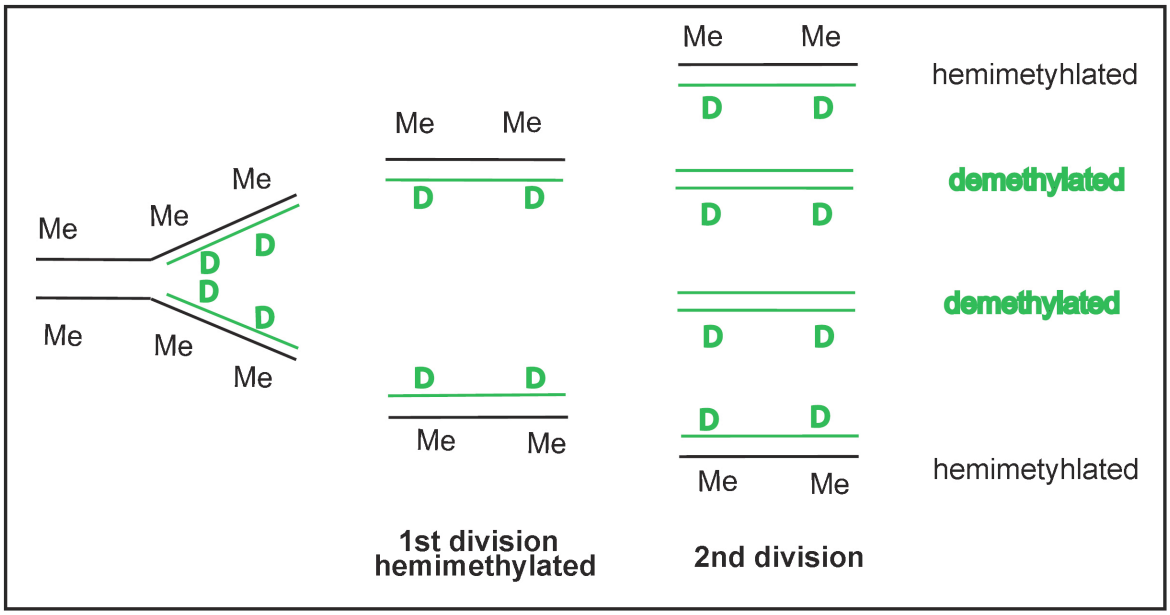

Figure 25: S-phase dependent mechanism of DAC (Jones, Taylor et al. 1982); Me=5-Methylcytosine, D= Decitabine. DAC gets incorporated during S-phase in the newly synthesized strand, which leads subsequently to the trapping of the DNMT1. After the 1st round of replication two hemimethylated DNA strands are the result. If DAC still present, after the 2nd division 50% hemimethylation and 50% demethylation is the result.

However, doubling time may also be affected by the drug. Moreover, the best dose for achieving a demethylation effect varies between the cell lines as published previously in case of cancer cell lines (Stresemann, Brueckner et al. 2006). Further, the main focus of previous literature was on DAC induced expression level in cancer cells (Herman, Latif et al. 1994; Herman, Jen et al. 1996; Salem, Markl et al. 2000; Lynch, Tycko et al. 2002) and only one paper I found analyzed DAC induced expression in comparison between normal cells and cancer cells (Liang, Gonzales et al. 2002). Therefore the knowledge on how normal cells respond to the effect of DAC treatment is poorly understood.

Accordingly, I tried two different strategies, continuous and non-continuous treatment, to achieve a possible loss of DNA methylation induced by DAC. In the case of the continuous treatment I treated the cells every day with the concentration range from 0-20μM. In the experiments (Figure 14, Figure 16) I conducted this approach over the duration of 5 days. To assess any of a possible loss of DNA methylation I looked first on a repetitive element, the L1P3 (Figure 14). This was due to the fact that this is not restricted to a single copy region so any demethylation effect could be observed throughout the genome with respect to a L1P3 repeat. The result revealed by this experiment was that some of the CpG sites are demethylated upon DAC treatment (Figure 14C, D). The highest decrease of CpG methylation in this context was achieved with a concentration of 0.05, 0.1 and 0.2μM. At 0.5μM and 0.7μM this band was still visible although to a fainter intensity. At the concentrations 1, 2, 3, 10, 20μM lower molecular bands were not visible anymore. This might be due to a difference in the loading of the DNA (explanation follows). The same effect was achieved upon the extension of the treatment duration over 9 days (Figure 17C, D). The quantification showed an increase in the intensity towards 0.7μM. Therefore the duration of the treatment showed no obvious affect on the DNA methylation status.

Further, the single copy region *H19* DMR (Figure 16) was assessed for the the loss of methylation. In this case a clear band at 962bp was visible in the HpaII lane from 0.05-2μM which was not present in the HpaII lane of the control. This was an indication of a partial loss of the DNA methylation in this region. The band intensity decreased at higher DAC concentrations also in this experiment. Compared to

the L1P3 element the decrease started at 2µM. Moreover the quantification in here has to be considered with care because to different blots exhibit different backgrounds.

In contrast, for the non-continuous treatment cells were treated every third day with DAC. This was conducted to decrease the DAC-induced stress to the cell. The result of the L1P3 (Figure 18) repeat revealed a partial loss of DNA methylation. A small molecular band appeared in the treated samples from 0.05- 3.0µM in the HpaII lane, which was very faint present in the control and in the samples with concentrations 10, 20 and 50µM. (Figure 26). Moreover, also the HERV element (Figure 20) revealed a partial decrease up to 3µM as examined upon quantification of the HpaII/ MspI bands. A common strategy in chemotherapy is that the optimal dose is determined by the fact that the maximal tolerated dose (Oki, Aoki et al. 2007).

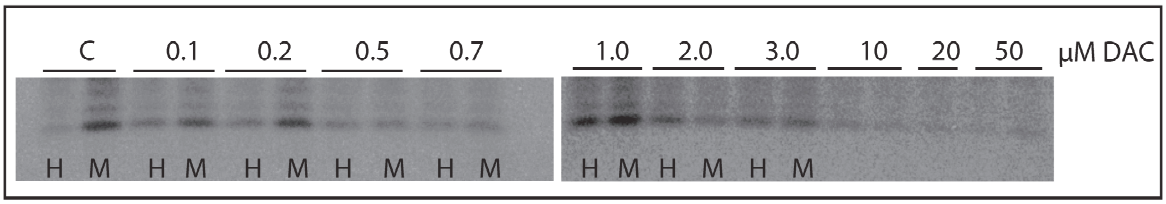

Figure 26: non-continuous treatment of Hs-27 cells of the experiment under Fig. 13 in the result section. A Gain of a band in the HpaII lane is visible onwards up to 3.0µM but disappeared at higher concentrations.

Previous studies have pointed out that Decitabine causes at high doses a cytotoxic effect, whereas at lower doses demethylation of the genomic sequence is the main effect (Jones and Taylor 1980; Creusot, Acs et al. 1982; Jones, Taylor et al. 1982; Oki, Aoki et al. 2007). Therefore, to try and induce demethylation I conducted the non-continuous treatment with 1, 2 and 3µM in respect to single copy regions. The *H19* DMR and the *AIRN* DMR show cautiously explained a partial loss of DNA methylation (Figure 21, Figure 22). This data has to be interpreted with care due to unequal DNA loading. It should be noted that in all experiments which were conducted, measuring accurate DNA concentration seemed to be difficult. Although the ethidium bromide fluorescence often indicated similar loading of the DNA, the DNA blot indicated a decrease in the signal intensity with higher concentrations of DAC. For all experiments the Nanodrop OD_{240nm} measurement was taken accurately measure DNA concentrations for the digestions. Nanodrop measured DNA concen-

tration may have been inaccurate because DAC induces a stress response upon which the RNA level increases, perhaps interfering with measurement of DAC concentrations. A solution of this problem would be to treat DAC treated DNA with RNaseI before measuring the concentration of DNA. Another issue that may have altered the treated samples compared to the control sample is that DAC might have a different UV-vis absorption that may have affected the accuracy of DNA concentration measurements. To examine this I measured the absorption of 1mM CTP and 1mM DAC as well as 1mMCTP/DAC. The result was that 1mM CTP had an absorption at 273nm, 1mM DAC had the absorption at 243nm and both together at 243nm. This leads to the conclusion that there is a slight difference in the absorption between the control (273nm) and the DAC treated samples (243nm). Whether this was responsible for the inaccuracy of measuring DAC treated DNA concentrations remains still unclear.

3.3 Cytotoxicity

Another feature throughout the experiments was that the higher the concentration of DAC the slower the cells divide and more cells died by apoptosis. This is primarily mediated by the cytotoxic effect of DAC. The cytotoxic effect is the result of the trapping of the Dnmt1 (Juttermann, Li et al. 1994). However, the downstream effects of this trapping are not really clear. When the cell gets the signal to divide the cell enters the cell cycle. During this time a cell has to pass a number of checkpoints that measure if the cell is in a healthy state e.g. during G2/M checkpoint a cell gets examined if the replication occurred correctly during S-phase. If DNA damage had occurred the cell may cell may go into apoptosis, if the mistakes were not repaired. The most important molecule that pushes the cell in cell cycle arrest is the transducer p53. It was previously shown that DAC is able to induce p53 (Karpf, Moore et al. 2001). In another study by Karpf et al. they showed that the bulky DNMT1-DAC adducts can induce the expression of p21 through activation of p53. In this study they used human lung cancer cell lines H549 (WT p53) and H1299 (p53- null) cells. p21 is a downstream target of p53 and upon DAC treatment p21 was only activated in H549 cells and not in H1299 cells. In these cell lines the promotor of p21 was unmethylated and therefore this study shows that the primary signal that leads to the

activation of p21 is DNA damage independent of demethylation (Zhu, Hileman et al. 2004). Through the activation of p21 the cell enters G1 arrest. This study also indicated that Decitabine might have other effects than demethylation. Palii et al demonstrated that DAC induces double strand breaks and this activated the main sensors ATM and ATR (Palii, Van Emburgh et al. 2008). In addition, Wang et al have shown that the activation of p21 is dependent on the activation of ATM and ATR which mediate certain posttranslational modifications (Ser15-phosphorylation and Lys320-acetylation) of p53, which only then is able to activate p21 (Wang, Zhao et al. 2008). On the contrary another study has shown that DAC is able to induce p21 independently of p53 (Nieto, Samper et al. 2004). The tumor suppressors p53 and p21 can be induced by treatment independent of its demethylation capacity. As mentioned above DAC has besides its demethylation capacity also the ability to induce cytotoxicity. It was previously published that the demethylation effect is primarily mediated at low concentrations whereas the cytotoxicity effect is initiated at higher concentrations (Jones and Taylor 1980; Creusot, Acs et al. 1982; Jones, Taylor et al. 1982). However, it was published that also lower doses can mediate a cytotoxic effect, albeit to a lower degree (Zhu et al 2004). Therefore to achieve a possible demethylation effect it should be more efficient to work with lower doses. This in turn means that high doses of DAC will lead to an extensive trapping of the DNMT1 and therefore to an extensive damage potential, which in fact the cell cannot deal with. At lower concentrations the cell is able to cope with the DNA damage and exits the cell cycle arrest and enters the cell cycle again. Finally, this decrease in proliferation was also visible by eye. In Figure 20 the control sample was MOCK treated with PBS and they grew to over 90% confluency. In comparison the treated samples with 1-3µM DAC showed a clear decrease in density that can be explained by the induction of cell cycle arrest in G1 or G2 or apoptosis.

In summary for my experiments and published data it appears that non-continuous DAC treatment at lower doses (~1µM) is the best approach to maximize the DNA demethylation effect because cytotoxicity should be kept at a minimal level so that the cells are still able to proliferate and replicate which is necessary to achieve DNA demethylation and also obtain enough DNA for Southern blotting.

3.4 DAC and the induction of gene expression

In addition examining the effect of DAC treatment on DNA methylation, I checked also the expression levels of two candidate genes the *H19* ncRNA and *MAGE-A1*. From the tiling array data as well as from the control of my qPCR assay (SYBR green and TaqMan) I knew that the *H19* ncRNA was not expressed in Hs-27 cells. Nevertheless, upon DAC treatment I induced its expression. The MAGE-A1 gene was previously published not as being expressed in normal somatic cells, but expressed in certain tumors and its transcriptional repression is associated with DNA methylation (De Smet, Lurquin et al. 1999). Also this gene was induced upon DAC treatment (Figure 23). It should be mentioned that up to now no tissue specific gene was found that is directly regulated by DNA methylation. Therefore, if I assume that DAC has only the ability to demethylate the DNA, I would expect for the *H19* ncRNA a 2 fold induction, which was clearly not the case. The induction I observed was 10-100 fold. This is an argument that DAC has also secondary effects besides its de-methylation capacity. One possibility would be that DAC induces repair pathways that might be responsible that the unmethylated maternal allele is affected by in-creasing the expression of ncRNA *H19*, whereas the expression of *H19* from the methylated allele is hindered. This might be an explanation that the results showed in Figure 23 (A, C) do not reveal a 2 fold induction. Moreover, the transcriptional start site of *MAGE-A1* is not associated with a CpG island, but is CpG rich and due to the limited area that I examined upon Southern blotting most HpaII sites were unmethy-lated, although upon DAC treatment *MAGE-A1* was induced. This is another indica-tion that DAC might have secondary effects beside DNA demethylation. Interestingly, a recent study showed that Decitabine induce the expression of 81 out of 22.000 genes. Half of the induced genes had CpG islands and from 5 randomly chosen genes only one was associated with CpG methylation but the expression of all was induced upon DAC treatment (Schmelz, Wagner et al. 2005).

All of this data shows that a complete DNA demethylation effect upon DAC treatment failed to be observed. On the other hand this data shows that DAC is able to induce the expression of 2 genes which are associated with DNA methylation *MAGE-A1* published as being associated with DNA methylation, but in Hs-27 cells the area I look at lacks DNA methylation. To elucidate the methylation state of

MAGE-A1 more clearly other restriction sites should be considered) as well as that secondary effects were involved in the induction of gene expression upon DAC treatment.

3.5 Future directions

The Myelodysplastic Syndrom (MDS) is a clonal-stem cell disorder in the bone marrow and manifests primarily in elderly patients, on average 70 years old who have a 2-40% risk to suffer from acute myeloid leukaemia (AML). Genetic mistakes in a hematopoetic stem cell, causing ineffective hematopoesis, provide the foundation of the disease. The patients display several symptoms like anaemia (low blood cell count), neutrocytopenia (low white cells, neutrophils) thrombocytopenia (low platelet count, thrombocytes). In general, AML and MDS display a reduction of normal cells, but whereas in AML cells of all blood-linages are underrepresented (red blood cells, granulocytes and platelets) in MDS often only one of the three linages displayed a reduction. This reduction is due to the hypercellular bone marrow with effective apoptosis events. This is another point which sets MDS apart from AML because in AML the increased apoptosis events are not present anymore. However, net result is cytopenia like neutrorocytopenia and thrombocytopenia. The first results in a high infectious risk for these individuals and the latter is the cause of bleeding. MDS differs from AML also in genetic and chromosomal aberrations like: inversion, deletion, translocation, monosomie and trisomie of which the most common one that is associated with MDS is the deletion or complete loss of chromosome 5 and/or 7. (Corey, Minden et al. 2007)

The average elderly age of affected individuals prevents an effective treatment strategy. Only a small number of patients, with progessed MDS can be medicated intensively with chemotherapeutic agents or make use of bone marrow transplantation, the latter provides, up to now the only cure. Whereas, the overall health of the majority of patients make such treatment approaches impossible. Due to the fact, that epigenetic aberrations like DNA-methylation associated gene silencing (e.g. $p15^{INK4B}$(Uchida, Kinoshita et al. 1997), CALCA, CDH1 (Vidal, Paixao et al. 2007))

also play a role in the development of the disease, provides an innovative treatment starting point for epigenetic agents, like Decitabine.

Decitabine is FDA (Food and Drug Administration) approved and is used in the treatment of MDS. So far it is known that Decitabine at a low dose is able to reverse DNA methylation pattern and contributes to cell differentiation and proliferation, via the activation of before DNA methylation associated silenced genes. However, the downstream effects of Decitabine after DNA demethylation are still unknown. We would like to know how Decitabine exerts its function(s) in MDS patients and investigate the possibility of the involvement of macro non-coding RNAs.

4. Materials and Methods

4.1 Bioinformatics

Table 1 indicates the name of the analyzed region and their respective sequence coordinates that were retrieved from the UCSC genome browser (http://genome.ucsc.edu/ March 2006 hg18). Interspersed elements were identified with the Repeat Masker software (http://www.repeatmasker.org/), using standard parameters. Moreover, the repeat masked sequences were used for creating gene maps with Gene Construction Kit^{Tm} v 2.5 (Textco, Inc.), and according to these maps DNA blot probes were designed. The following Accession numbers were used to obtain the sequences of the indicated elements: satellite2: X72623 ((Weisenberger, Campan et al. 2005)); HERV: M10976 (Repaske, Steele et al. 1985); LINE M13002 (Bourc'his and Bestor 2004). These sequences were blasted with the option BLAT on UCSC browser (hg18).

Analyzed element	Chromosom:position	Reference
H19 DMR	chr11: 1972987-1975651	(Jinno, Sengoku et al. 1996)
AIR DMR	chr6: 160346236-160347473	(Smrzka, Fae et al. 1995)
KCNQ1OT1DMR	chr11: 2676987-2678663	(Beatty, Weksberg et al. 2006)
DLK1 DMR	chr14: 100333007-100341006	(Geuns, De Temmerman et al. 2007)
PWS DMR	chr15: 22751129-22751302	(Zeschnigk, Schmitz et al. 1997)
OCT4	chr6: 31240093-31246430	(Freberg, Dahl et al. 2007)
MAGE-A1	chrX: 152134716-152139310	(De Smet, Lurquin et al. 1999)
SINE(AluJb)	chr6: 160311821-160312130	-
LINE(L1P3)	chr9: 23095114-23101238	(Bourc'his and Bestor 2004)
HERV (LTR)	chr19: 20721466-20730278	(Repaske, Steele et al. 1985)
Satellite2	chr10: 41799625-41800157	(Weisenberger, Campan et al. 2005)
mt	chrM: 6,119-6,662	-

Table 2: Chromosomal location of the investigated regions (USCS genome browser hg18).

4.2 PCR reaction

Primers for the PCR reaction were designed with the Primer3 programme (http://fokker.wi.mit.edu/primer3/input.htm), using standard parameters and were synthesized by VBC-BIOTECH (Vienna) with standard HPLC purification. The primers were ordered in a lyophilized form and were then dissolved with TE buffer to a final concentration of 100pmol/µl (stock). The PCR reaction was conducted with a 1:10 dilution of the primer stock. Table 2 shows all used primer pairs. The PCR program was as followed: 1. 95°C- 3min, 2. 95°C- 30 sec, 3. 59°C- 30sec, 4. 72°C- 45sec, 5. 72°C-7min (step 2-4: 34 cycles). The PCR reaction was conducted in a 25µl volume using the following ingredients: 5µl of 5xGoTaq Flexi Buffer (Promega), 0.5µl of dNTPs (10mM), 4µl of Betaine (5M), 0.125µl of GoTaq (5U/µl) Polymerase, 1µl of each primer, 1µl of $MgCl_2$ (0.4/0.48/0.60/0.70/0.80/1.0/1.2/1.6 mM for optimization) and 10.875µl of H_2O.

Probe name	Forward primer	Reverse primer	Length
hH19mp	GATATGGCCCGATACGAAGA	AGTTGTGGAATCGGAAGTGG	592bp
hDLK1mp	GTCACCCTAAGGCTGCTGAG	TGAGACAGCAGGAGAGCAGA	582bp
hPWS mp	GTGGAAGGTGCACAAGGAAT	TTCCTAGCCTGCTTTTTGGA	616bp
hAluJbmp	AAACGAGGTCAGGCTGAGAA	AGGCCAGCTGGGTTAATTTC	411bp
hHERV(gag)mp	CCTTCTGGGCTCTCCTCTT	TTTGAGTCCACAGTGCTTGC	574bp
hL1P3mp	AACTTCCAGAGGAGCGATCA	AGTACGCCGTGGTTTTCCAG	606bp
hOCT4mp	CTGGCACTCTCTCAGGCTCT	TTCAGCAAAGGTTGGGAAAC	532bp
hMAGE-A1mp	ACACTTTTCGTATCTTCCAAGG	TGCCAACGTGACAATCAAAT	607bp
hSat2mp	CCATAGGCCACATTGCACTT	TCAGTGAGGCCAAGTTTGAA	533bp
hMTmp	CCATCATAATCGGAGGCTTT	ATTCCGAAGCCTGGTAGGAT	600bp

Table 3: PCR primers in 5' to 3' direction and the length of the PCR products are indicated.

4.3 Gel Elution of PCR fragments

The PCR reactions were loaded on a 0.8-2% agarose gel, run in 1xTAE buffer and stained for 1hr in ethidium bromide (see point 16. chemicals/solutions). The bands of interest were cut out and purified using the Wizard SV Gel and PCR Clean-Up System (Promega), according to manufacturer's protocol.

4.4 Cloning into pGEM -T-Easy vector

The PCR fragments were cloned into the pGEM-T-Easy vector (Promega) according to the manufacturer's protocol. In brief, for each PCR fragment a 1:1 and 1:3 (vector : insert ratio) ligation reaction was conducted. The ingredients were mixed according to the protocol and the whole reaction was incubated for 1 hour at room temperature.

4.5 Transformation

Chemo-competent bacteria from the *E. coli* strain DH5α, stored at -80°C, were thawn for 30 minutes on ice. The whole ligation reaction was added into the tube and incubated on ice for additional 30 minutes. Heat shock was conducted on 42°C for 1 minute followed by 2 minutes of incubation on ice. Afterwards, 250µl of LB media were added. The bacteria were placed on 37°C for 1 hour shaking at 300rpm in the thermo mixer. The whole transformation was plated out on LB/ amp /X-gal/ IPTG (see point 16. chemicals/solutions) plates and left over night on 37°C.

4.6 Mini Prep

White colonies were picked and inoculated in 3ml LB/amp (see point 16. chemicals/solutions) media for the mini prep and incubated on 37°C over night. On the next day, 1.5ml of these cultures were centrifuged (Eppendorf centrifuge 5417C) at 14000rpm for 1min, the supernatant was discarded and the pellet was resuspended in 100µl of P1 solution (resuspension buffer). 200µl of P2 (lysis buffer)

were applied and the tubes were incubated for 5min at RT. 200µl of P3 (neutralization buffer) were added, mixed and 400µl of Chloroform were applied, vortexed and incubated for 15 minutes on ice. The samples were centrifuged for 10 minutes at 14000rpm and the supernatants (~400µl) were transferred into new tubes, containing 1ml of 96% of ethanol (EtOH). Tubes were centrifuged at 13500rpm for 20 minutes at 4°C and the supernatant were discarded. To each pellet 500µl of 70% EtOH were added, incubated for 5 minutes and centrifuged for 5 minutes at 13500rpm at 4°C. This washing step was done two times. After the pellet had been air-dried it was dissolved in 60µl TE buffer, vortexed and placed for over night on 55°C. For confirmation of the right fragment in the vector ~10µg of DNA was digested with an appropriate enzyme, incubated over night on working temperature and loaded on a 0.8% or 2% agarose gel. After 1 hour of staining in ethidium bromide a picture was taken and the digestion pattern was confirmed with the "*in silico"* predicted one that was created with Gene Construction Kit^{Tm} v. 2.5 (Textco, Inc.).

4.7 Amplification (Maxi Prep) and DNA preparation

The amplification of the constructs was conducted in a 2-step-culture procedure. Tubes were prepared with each 3ml LB/amp media. To each tube, 20µl of the miniprep culture were added and placed for 8 hr on 37°C shaking. The 3ml culture was inoculated in 250ml LB/amp media and incubated over night on 37°C.
Plasmid isolation was conducted according to the manufacturer's protocol (Promega PureYield^{TM} Plasmid Midiprep System) either by purification by centrifugation or purification by vacuum. The DNA was eluted from the column with 800µl of TE buffer and was precipitated by standard procedures (Sambrook, Fritsch et al. 1989). 10µg of each construct were sent for sequencing to VBC-BIOTECH (Vienna), using standard primers from T7 promotor.

4.8 Cell culture and DAC treatment

Human-foreskin-fibroblasts (Hs-27 HFF, a primary human differentiated cell line) were quickly thawn up at 37°C. The vial content was transferred to a tube con-

taining 10ml of DMEM media (see point 16. chemicals/solutions/kits). The tube was centrifuged at 1050rpm for 5 minutes, the supernatant was removed and the cells were resuspended in 5ml of DMEM media (see point 16. chemicals/solutions/kits). The cell suspension was transferred to a T80 flask, containing 13ml of DMEM media and cells were grown until they were confluent. For 5-aza-2'deoxycytidine (DAC, Sigma) treatment cells at passage 9, 10, 11, 16 were used. The cell-seeding number in all experiments was $3*10^5$ cells per 10 or 15 cm dishes. DAC (Sigma) treatment started post 24 hours of seeding. The media-change and drug supply was repeated every third, (non-continuous treatment) or every day, (continuous treatment). Concentration range is listed in table 3. Cells were split according to necessity and confluence using Trypsin. DNA and/or RNA was isolated after either 5 or 9 days of drug-treatment.

Con. (µM)	0.05	0.1	0.2	0.5	0.7	1	2	3	10	20
stock	0.1mM	0.1mM	0.1mM	0.1mM	0.1mM	0.1mM	0.1mM	0.1mM	1mM	1mM

Table 4: The concentration (con. µM) range for the treatment of Hs-27 cells is given in the upper panel and the stock either 0.1mM or 1mM is given in the lower panel. The concentration range accords to a final volume of 20ml DMEM media (see point 16. chemicals/solutions/kits).

As DAC is a toxic compound all steps were performed under the cell culture hood and gloves are used all the time. Everything that came into contact with DAC was disposed into the toxic waste.

4.9 DNA isolation

The media containing DAC was taken off and transferred into a bottle and trashed into toxic waste. 2.6ml of lysis buffer (see point 16. chemicals/solutions/kits) were applied and cells were scraped down using a cell scraper. The cells were transferred into a 15ml Falcon tube and incubated on 55°C overnight. On the next day, 300µl of saturated NaCl were applied to each tube and mixed for 1 minute. The suspension was centrifuged at 14.000rpm for 10 minutes. 800µl of supernatant were transferred into a fresh tube. 500µl of isopropanol were added, mixed for 1 minute and centrifuged again for 10 minutes at room temperature. The supernatant was removed and the pellet was washed two times with 70 % EtOH. The pellet was dissolved in 50-70µl of TE buffer, 55°C over night.

4.10 DNA blotting

10-15µg of DAC (Sigma) treated Hs-27 DNA was digested with a suitable enzyme (Fermentas/ Roche) and incubated overnight according to their working temperature. For analyzing the loss of methylation (LOM), methylation sensitive restriction digests were preformed using HpaII (Fermentas) as a methylation sensitive enzyme, which recognizes a CCGG motif and cuts exclusively when the CG is unmethylated. In addition, the methylation insensitive isoschizomere MspI (Fermentas), that recognizes CCGG, but cuts either if CG is methylated or unmethylated, was used. The digestion reactions were mixed with an appropriate amount of loading buffer, loaded on a 0.8% TBE gel together with a 1kb DNA ladder (Fermentas) and run at 5V/cm or 6V/cm. The gels were stained in ethidium bromide (see point 16. chemicals/solutions/kits) and a picture was taken. The gels were denatured in denaturing solution (see point 16. chemicals/solutions/kits). For DNA blotting, a tray with denaturing solution covered by a glass plate was prepared. Before the 3MM Whatman papers (VWR International Gmbh) were placed on the glass plate, they were prewet in denaturing solution. The ends overlapped the bottom and top of the glass plate and reached into the denaturing buffer. A pipette was used for removing residing air bubbles between the papers and glass plate. The gel was then placed upside down on the 3MM Whatman papers and air bubbles were rolled out with a pipette. The gel was then covered with a Hybond-Nylon membrane (Hybond^{TM}-XL blotting membrane (Amersham, GE Healthcare), which was prewet for 1 minute in MQ water and additional 5 minutes in denaturing solution. On top of the membrane three additional 3MM Whatman papers were placed. Paper towel stack was put on the top, covered with a glass plate and weight. DNA transfere was preformed for at least 18 hours.

4.11 DNA Blot re-hybridization ("stripping")

Hybond-Nylon membranes were washed two times for 30 minutes in 40mM NaOH, were washed three times with H_2O and neutralised in 20mM Na_2HPO_4. Thereafter the membranes were pre- hybridized in Church buffer.

4.12 Probe labelling and cleaning

On the same day as the blotting procedure was preformed, probes were radioactively labelled. 20-30ng of the in 14µl of H_2O denatured at 99°C for 5 minutes cooled for 2 minutes on ice. The Cold Mix, containing for 1 approach 6µl CTG/ 20µl LS buffer and 1µl of the Klenow fragment (2U/Fermentas). During the time the probe denatured on ice, 2 µl of $^{32}\alpha$-P-ATP were added to the Cold Mix and to each probe sample 29µl of the radioactive Cold Mix was added. The samples were labelled over night.

On the next day, the probe was cleaned using Sephadex G50 columns. A 1ml plastic syringe was used as a column, the barrel was removed and aquarium wool was placed at the bottom. The column was placed into a 15ml tube. The whole syringe was filled up with Sephadex solution by using a Pasteuris pipette and centrifuged at 3000rpm for 3 minutes at RT (HERAEUS, MEGAFUGE 1.OR). The column was transferred into a new 15ml tube that contained a screw cap tube at the bottom. To the probe 60µl of TE buffer were applied and the whole content of the vial was transferred onto the column and centrifuged at 3000rpm for 3min (HERAEUS, Biofuge primo). A 1:100 dilution of the labelled probe in TE buffer was used to assess the counts per minute with the Scintillation counter (liquid Scintillation Analyzer 1600TR).

After the blot was disassembled and the membrane pre-hybridized for 30 minutes in Church buffer (see point 16. chemicals/solutions/kits), the probe was mixed with ~30ml of Church buffer and applied to the hybridization bottle. Hybridisation was carried out at 65°C for at least 18 hours. The membrane was washed two times with pre-warmed (65°C) Wash Buffer (see point 16. chemicals/solutions/kits).

The membrane was wrapped into plastic foil, and placed into a film cassette and exposed to a PhosphoImager plate (Fuji). After the exposure the plate was scanned on Typhoon 8600 Variable Mode Image scanner. The picture was analyzed with Adobe Photoshop 7.0 and bands were quantified with ImageJ.

4.13 RNA isolation

DAC treated Hs-27 cells were trypsinized and the cell pellet was resuspended in 2ml of TRI reagent (Sigma), incubated for 5 minutes at room temperature and stored at –20°C. The samples were transferred to 1.5ml tubes. 100µl of BCP were added per ml, mixed, incubated for 10 minutes at room temperature and subsequently centrifuged at 13000rpm for 15 minutes. The upper phase was transferred into a fresh tube containing 500µl of isopropanol, mixed, incubated for 10 minutes at room temperature and centrifuged at 13000rpm for 15 minutes. The pellet was washed with 1ml of 70% EtOH (diluted with DPEC treated, autoclaved H_2O), mixed and centrifuged for 10min at 13000rpm. Each pellet was dissolved in 100µl RNA storage solution (Ambion). According to the concentration an appropriate amount of RNA was used for cDNA preparation (see below). The rest of the RNA was stored at –20°C as precipitate, with 2.5 volume of EtOH + 10% 5M NaAc.

4.14 cDNA preparation

cDNA preparation was performed using the DNA-*free* Kit (Ambion) and the Revert Aid Kit (Fermentas). 4µg of RNA were used for cDNA preparation. DNase digest was carried out by adding 1µl of DNase (supplied with the Ambion kit), 3.3µl of 10x DNA-free buffer in a final volume of 33µl. The reaction was incubated 30 minutes in the thermo mixer at 37°C. 5µl of inactivation solution were added, incubated for 2 minutes at room temperature and centrifuged for 90 seconds at 13000rpm on 4°C. After this step, 33µl of the supernatant were transferred into a PCR tube and 3µl of random hexamer primers (supplied with Fermentas kit) were added to each sample. The samples were denatured in the PCR machine at 70°C for 5 minutes and then cooled down for 4°C, and placed on ice. A pre-mix was prepared containing 12µl of 10xbuffer, 6µl of dNTPs (supplied with Fermentas kit) and 3µl of RNase in-

hibitor (supplied with Fermentas kit). Into each PCR tube 21µl of pre-mix were added, which in turn was divided into one tube containing 38µl as total volume (+RT) and one tube containing 19µl in total (-RT). All tubes were then incubated for 5 minutes at 25°C in the PCR machine and thereafter 2µl of Reverse transcriptase (supplied with Fermentas kit) were added to the +RT approach. At last the full RT program was performed including the following steps: 25°C for 10 minutes, 42°C for 60 minutes, 70°C for 10 minutes and 4°C.

4.15 qPCR

Primers and the probe (Table 4) were designed using PrimerExpress® Software v2.0 (Applied Biosystems) and qPCR was conducted using the ABI Prism 7000 Sequence Detection System. Primers were ordered at VBC-BIOTECH (Vienna) with standard HPLC purification, and were obtained in a lyophilized form. Primers were diluted with embryo water to 100pmol/l. The working concentration of the primers was 10µM (dissolved in embryo water). For quantification purpose standard curves were generated using 1:1, 1:4, 1:16 and 1:64 dilutions of the cDNA of Hs-27 cells. The qPCR was normalized to RPLPO (ribosomal protein, large, PO) as well as GAPDH. The qPCR assay for H19, MAGE-A1 and RPLPO was a SYBR green assay and for normalization to GAPDH, a TaqMan Assay was used. In case of the SYBR-assay a master mix was prepared with 2xuMM buffer, forward primer (10µM), reverse primer (10µM) and embryo H_2O. In terms of the TaqMan assay a master mix was prepared with 2xuMM buffer, forward primer (10µM), reverse primer (10µM), embryo H_2O and 50µM GAPDH Taqman probe. In each well of the 96-well plate, which will be used, firstly 20µl of Master mix were applied and then 5µl of template was added. The template for this purpose was the cDNA prepared under the point cDNA preparation. One qPCR approach was conducted using the +RT sample and one approach was conducted using the –RT approach, as a control. In addition three wells were carried out with embryo water as the template serving as a second control. As in the case of the –RT approach also the water approach showed no specific amplification. Conditions for the reaction in the ABI Prism 7000SDS were 5 minutes at 95°C 40 cycles of 95°C 15 seconds and 60°C for 1 minute. qPCR data was ana-

lysed using the manufacturer's protocol (Applied Biosystems). All reactions were conducted in 3 technical replicas.

RNA name	forward primer	reverse primer
H19 ncRNA	GTGTGACGGCGAGGACAGA	TCCGTGGAGGAAGTAAAGAAACA
MAGE-A1	TGAGGGACGGCGTAGAGTTC	GTTGGCCTGTCCCCTGAAA
GAPDH (TaqMan)	TGAAGGTCGGAGTCAACGG	ACCAGAGTTAAAAGCAGCCCT
GAPDH TaqMan probe	TTGGTCGTATTGGGCGCCTGGT	
RPLPO	CCACGCTGCTGAACATGCT	TCGAACACCTGCTGGATGAC

Table 4: qPCR primers for measuring expression levels of H19 ncRNA and MAGE-A1 in DAC treated Hs-27 cells; primers are given in 5' to 3' direction.

4.16 RNA-chip

The RNA expression tilling array experiment was performed by Irena Vlatkovic, a Ph.D. student in the lab.

4.16.1 Sample preparation

6.5µg of total RNA, isolated from Hs-27 cells, was treated with DnaseI and dissolved in 16µl DEPC ddH_2O. For first-strand cDNA synthesis 16.5µl were used as a template by using 5µg Random Hexamer primers in a total volume of 35µl according to Superscript II Reverse Transcriptase standard protocol. Second-strand cDNA synthesis was performed by adding 76µl nuclease-free ddH_2O, 30µl 5× Second strand buffer, 3µl 10mM dNTP, 4µl DNA Polymerase I, 1µl *E. coli* DNA Ligase, 1µl RNase H, followed by 2hour at 16°C. 2µl of T4 Polymerase (5U/µl- Invitrogen) were added and cooled for additional 10min at 16°C. cDNA cleaning was conducted with QIAquick PCR Purification Kit. Precipitation and incubation on -20°C overnight followed and the cDNA was recovered by was recovered by centrifugation at

13,200rpm for 30min at 4°C. The pellet was re-suspended in 14~18µl nuclease-free ddH_2O.

'Input sample' preparation was conducted by isolation of 100µg of Hs-27 genomic DNA followed by treatment with RNase A (final concentration: 25µg/ml) overnight at 37°C. 15µl Proteinase K (10mg/µl) were added for protein digestion at 55°C for 2~3hours. 1ml of genomic DNA, Phenol-Chloroform exacted, was sonicated 5min on the condition of 20% power with 20s on/1min off pulse. The distribution of the sonicated DNA was checked in 2% agarose gel. Each 10µg sonicated genomic DNA was cleanuped with one column from QIAquick PCR Purification Kit according to the manufacturer protocol. After ethanol precipitation, the input DNA was recovered in certain volume of nuclease-free ddH_2O.

4.16.2 Sample quantification and qualification

Concentration was measured on $NanoDrop_{ND1000}$ spectrophotometer and adjusted between 300ng/µl to 500ng/µl. The minimal total amount of each sample was 4.5µg. The 260/280 absorbance ratio of DNA samples was more than 1.6. To measure the distribution of the samples Agilent 2100 Bioanalyzer with Agilent DNA 7500 kit was used according to the manufacturer protocol. The size range of DNA samples was between 100bp to 800bp.

4.16.3 Sample hybridization

The Enriched and Input samples were sent to Imagenes ("Berlin"), hybridization and scanning was performed by the NimbleGen service in the company. For normal hybridization, the Enriched sample (ds-cDNA) labeled with Cy5 Dye and the Input sample (ds-gDNA) labeled with Cy3 Dye were co-hybridized to one NimbleGen HIRTA chip.

4.17 Chemicals, Solutions and Kits

Chemicals/ Materials	
Agarose	Biozym
5-aza-2'deoxycytidine	Sigma
Betaine	Sigma
BCP	Sigma
Chloroform	Sigma
DMEM	Invitrogene
dNTPs 10mM each (dATP, dCTP, dTTP, dGTP)	Fermentas
Ethanol (96%)	Merck
EDTA	Sigma
Ethidium bromide	Fluka
Gentamycin (10mg/ml)	GibcoBRL
L-Glutamine	GibcoBRL
X-gal	Merck
Isopropanol	Merck
IPTG	Merck
LB agar	Roth
MgCl2	Sigma
NaCl	Sigma
Natriumacetate	VWR
PBS	Qbiogene
RNA storage solution (RSS)	Ambion
Sepahdex^{TM}G-50	Amersham
SDS	Applichem
TRI reagent	Sigma
Trypsin	GibcoBRL
Whatman paper	VWR
Enzymes	
HpaII/ MspI/ EcoRI/ BglII/ BstXI/ PvuII/NcoI/RsaI/Cfr421/AluI/DraIII/SphI Buffer: Orange, Red, Green, Tango	Fermentas
Klenow fragment	Roche
ProteinaseK	Qbiogene
Taq polymerase	Roche
Kits	
DNA- *free* Kit	Ambion
Reverta Aid first strand cDNA Synthesis Kit	Fermentas
Pure Yield^{TM} Plasmid Wizard PCR Clean-Up System	Promega
PureYield^{TM} Plasmid Midiprep System	Promega
GoTag Flexi DNA polymerase	Promega
QIAquick PCR purification Kit	Qiagen
Agilent DNA 7500 kit	Agilent
Marker	
1kb DNA ladder	Fermentas
$^{32}\alpha$-P-ATP	New England Nuclear (Perkin Elmer)

Solutions

(All solutions were prepared with MiliQwater)

TE-Buffer pH 8.0: 10ml 1M Tris.HCl pH 8.0 + 2ml 0.5M EDTA up to 1l with H_2O

1M Tris pH 8.5 (for 100ml): 12.1g Tris with HCl to pH 8.5 up to 100ml with H_2O

50x TAE buffer: 242g Tris + 57,1ml Acetic acid + 100ml 0.5 M EDTA pH 8.0 fill up to 1l with H_2O.

10x TBE buffer: 108g Tris, 55g Boric Acid, 0.5M EDTA pH 8.0 up to 1l with H_2O

5xTen9: 250ml Tris pH9.0 + 200ml 0.5M EDTA pH 8.0 + 40ml 5M NaCl

0.5M EDTA pH8.0: 186.1g EDTA pH to 8.0 with NaOH up to 1l with H_2O, autoclave

20% SDS: 200g SDS up to 1l with H_2O

P1 (resusspension buffer): 6.06g Tris base/ 3.72g $Na_2EDTA.2H_2O$ add 800ml H_2O and adjust to pH 8.0 with HCl to 1l with H_2O (RNase: 100mg/l)

P2 (lysis buffer): 8.0g NaOH in 950ml H_2O + 50ml 20% SDS up to 1l with H_2O.

P3 (neutralization solution): 294.5g/500ml H_20 KaAc, adjust to pH5.5 with acetic acid add H_2O to a final volume of 1l

ProteinaseK: 10mg/ml

Na_2HPO_4: (0.5M): 89g $Na_2HPO_42H_2O$/l adjust to pH 7.2 with H_3PO_4

Lysis buffer: (for 20ml) 4ml 5x TEN9 + 1ml 20%SDS + 1.0 ProteinaseK(10mg/ml) + 14ml H_2O

10M NaOH: 800g NaOH in 1600ml H_2O, 4 hour rotating, fill up to 2l with H_2O

40mM NaOH: 4ml of 10M NaOH up to 1l with H_2O

CTG mix: 100µM dTTP + 100µM dCTP + 100µM dGTP + BSA 2mg/ml

LS mix: stock: 25ml 1M HEPES pH6.6 + 25ml 250mM Tris-Cl pH8 / 25mM $MgCl_2$ $6H_2O$/ 50mM beta-mercaptoethanol + 25ml OD U/ml hexameres

Denaturing solution: 50ml 10M NaOH, 300ml 5M NaCl/l

Church buffer: 500ml 0.5M Na_2HPO_4 + 350ml 20%SDS + 2ml 0.5M EDTA

Wash Buffer: 40ml 0.5 $Na_2HPO_4.2H_20$ (pH7.2) + 50ml 20% SDS up to 1l with MQH_2O

DPEC-H_2O: 900ml H2O + 900µl DPEC (shake for 20 seconds, 2 hours on 37°C)

DMEM media: (for 200ml): 177ml DMEM (high glucose) + 20ml FCS + 2ml L-Glutamine (200mM) + 1ml Gentamycin (10mg/ml)

Ethidium Bromide (2mg/ml): 20mg EtBr in 10ml H_2O; 500µl EtBr in 1000ml H_2O

LB media: 10g LB media + 400ml of H_2O

LB/amp plates: 400ml Circlegrow Agar + 400µl Ampicilin (stock: 50mg/ml in H_2O: EtOH / 50:50)

X-gal: 50mg X-Gal in 1ml N,N- dimethylformamid

IPTG: (0.1M) 1g of IPTG dissolved in 41.7ml autoclaved, filter sterile by using a 50ml Syringe + Syringe filter

0.8% agarose gel: 3.2g agarose in 400ml TAE

2.0% agarose gel: 8g agarose in 400ml TAE

Loading buffer: 0.5% Xylenol orange (0.25g) + 30% Glycerol 15ml in 1x TAE up to 50ml

3M NaAc pH 5.2: 246.1g NaAc/l and adjust to pH 5.2 with acetic acid

5. Acknowledgements

First, I would like to thank Denise P. Barlow for her support and let me doing my Diploma in her lab, on this project.

This work would not have been possible without the help of a lot of people. A special thank you goes to Florian who was constantly there throughout this project and gave me lots of suggestions. Thanks to Martha who was there when I had questions and was open and interested in reading and correcting my thesis. Thanks to Quanah, not only for all your invitations to the parties you gave, also for reading and correcting my thesis and helping me whenever I had problems. Thanks to Kasia, Xenia, Angelika and Romana for manging the ordering from companys, preparing nice birthday partys and everything else. Thank you Irena for your help during my starting time, for providing me the Bx probe and preparation of the RNA-expression tiling array. Thanks also to Renping for providing me the hKCNQ1OT1mp probe. I also want to thank Ru and Federica who are great sitting neighbours. Cheers for this great time.

A big thank you goes to my parents Annemarie and Werner Rudigier who supported me the whole time and for their understanding that I'm not so often at home. Especially for the last point I thank my sister Christina, her husband Christian and their daughter Hanna. Not to forget my brother Sebastian.

Thank you my dear friends: Christian Schiller (Shi), Philipp Leissing (Pippo), Ruben Aubrecht (Ruby), Daniel Schmidt (Schmitty), Marcel Milohnic (Marci), Brooke Morriswood, Marco Sealy, Mathew Sloane, Alessandro Carreri, Sarah Himbert, Mads Beich-Frandsen, Philip Gärtner, Michaela Radegger, Christoph und Benedikt Halmer, Klaus Neumueller, ……

6. Curriculum Vitae

Name	Lucas Johannes Rudigier
Date of birth	5th of November, 1981
Place of birth	Feldkirch, Austria
Parents	Annemarie Rudigier - Amann and Werner B. Rudigier
Education:	September 1988 - July 1992 Elementary school in Hard am Bodensee
	September 1992 - July 1994 Secondary school at Benediktinum in Scharnitz
	September 1994 - July 1997 Gymnasium Mehrerau in Bregenz
	September 1997 - June 2001 Gymnasium (BORG) in Lauterach 24th of September: Matura
	October 2001 - December 2001 Internship at Gebrüder Weiss, Lauterach
	January 2002 Univeristy College Dublin (U.C.D) Ireland
	February 2002 - February 2003 Civil service at Lebenshilfe in Hörbranz
	March 2003 Internship at Post in Wolfurt

April 2003 - August 2003
Internship at Pfanner in Lauterach

October 2003 - January 2007
Study of Biology (A437) at the University of Vienna

January 2007 - June 2009
Study of Microbiology and Genetics (A441) at the Univeristy of Vienna

Diploma Thesis

April 2008 - May 2009
“ DNA demethylation effects in normal human fibroblasts”

in the Laboratory of
Denise P. Barlow, PhD
Centre for Molecular Medicine – CeMM
c/o Institut for Microbiology and Genetics
University of Vienna
Dr. Bohrg. 9/4
1030 - Vienna

7. References

Arita, K., M. Ariyoshi, et al. (2008). "Recognition of hemi-methylated DNA by the SRA protein UHRF1 by a base-flipping mechanism." Nature **455**(7214): 818-21.

Barlow, D. P. and M. S. Bartolomei (2007). Genomic Imprinting In Mammals. Epigenetics. Cold Spring Harbor, New York, Cold Spring Harbor Laborartory Press.

Barlow, D. P., R. Stoger, et al. (1991). "The mouse insulin-like growth factor type-2 receptor is imprinted and closely linked to the Tme locus." Nature **349**(6304): 84-87.

Bartolomei, M. S., S. Zemel, et al. (1991). "Parental imprinting of the mouse H19 gene." Nature **351**(6322): 153-5.

Beatty, L., R. Weksberg, et al. (2006). "Detailed analysis of the methylation patterns of the KvDMR1 imprinting control region of human chromosome 11." Genomics **87**(1): 46-56.

Bell, A. C., A. G. West, et al. (2001). "Insulators and boundaries: versatile regulatory elements in the eukaryotic." Science **291**(5503): 447-50.

Bender, C. M., M. L. Gonzalgo, et al. (1999). "Roles of cell division and gene transcription in the methylation of CpG islands." Mol Cell Biol **19**(10): 6690-8.

Bestor, T. H. (1988). "Cloning of a mammalian DNA methyltransferase." Gene **74**(1): 9-12.

Bestor, T. H. (2000). "The DNA methyltransferases of mammals." Hum Mol Genet **9**(16): 2395-402.

Bestor, T. H. and V. M. Ingram (1983). "Two DNA methyltransferases from murine erythroleukemia cells: purification, sequence specificity, and mode of interaction with DNA." Proc Natl Acad Sci U S A **80**(18): 5559-63.

Bird, A. P. (1986). "CpG-rich islands and the function of DNA methylation." Nature **321**(6067): 209-13.

Bourc'his, D. and T. H. Bestor (2004). "Meiotic catastrophe and retrotransposon reactivation in male germ cells lacking Dnmt3L." Nature **431**(7004): 96-9.

Brandeis, M., T. Kafri, et al. (1993). "The ontogeny of allele-specific methylation associated with imprinted genes in the mouse." EMBO J **12**(9): 3669-77.

Brueckner, B., R. Garcia Boy, et al. (2005). "Epigenetic reactivation of tumor suppressor genes by a novel small-molecule inhibitor of human DNA methyltransferases." Cancer Res **65**(14): 6305-11.

Cattanach, B. M. and M. Kirk (1985). "Differential activity of maternally and paternally derived chromosome regions in mice." Nature **315**(6019): 496-8.

Cheng, X. and R. M. Blumenthal (2008). "Mammalian DNA methyltransferases: a structural perspective." Structure **16**(3): 341-50.

Christman, J. K. (2002). "5-Azacytidine and 5-aza-2'-deoxycytidine as inhibitors of DNA methylation: mechanistic studies and their implications for cancer therapy." Oncogene **21**(35): 5483-95.

Corey, S. J., M. D. Minden, et al. (2007). "Myelodysplastic syndromes: the complexity of stem-cell diseases." Nat Rev Cancer **7**(2): 118-29.

Creusot, F., G. Acs, et al. (1982). "Inhibition of DNA methyltransferase and induction of Friend erythroleukemia cell differentiation by 5-azacytidine and 5-aza-2'-deoxycytidine." J Biol Chem **257**(4): 2041-8.

De Smet, C., C. Lurquin, et al. (1999). "DNA methylation is the primary silencing mechanism for a set of germ line- and tumor-specific genes with a CpG-rich promoter." Mol Cell Biol **19**(11): 7327-35.

DeChiara, T. M., E. J. Robertson, et al. (1991). "Parental imprinting of the mouse insulin-like growth factor II gene." Cell **64**(4): 849-59.

Ehrlich, M. (2003). "The ICF syndrome, a DNA methyltransferase 3B deficiency and immunodeficiency disease." Clin Immunol **109**(1): 17-28.

Ehrlich, M., M. A. Gama-Sosa, et al. (1982). "Amount and distribution of 5-methylcytosine in human DNA from different types of tissues of cells." Nucleic Acids Res **10**(8): 2709-21.

Esteller, M. (2008). "Epigenetics in cancer." N Engl J Med **358**(11): 1148-59.

Ewald, B., D. Sampath, et al. (2008). "Nucleoside analogs: molecular mechanisms signaling cell death." Oncogene **27**(50): 6522-37.

Ferguson-Smith, A. C., H. Sasaki, et al. (1993). "Parental-origin-specific epigenetic modification of the mouse H19 gene." Nature **362**(6422): 751-5.

Fournel, M., P. Sapieha, et al. (1999). "Down-regulation of human DNA-(cytosine-5) methyltransferase induces cell cycle regulators p16(ink4A) and p21(WAF/Cip1) by distinct mechanisms." J Biol Chem **274**(34): 24250-6.

Freberg, C. T., J. A. Dahl, et al. (2007). "Epigenetic reprogramming of OCT4 and NANOG regulatory regions by embryonal carcinoma cell extract." Mol Biol Cell **18**(5): 1543-53.

Geuns, E., N. De Temmerman, et al. (2007). "Methylation analysis of the intergenic differentially methylated region of DLK1-GTL2 in human." Eur J Hum Genet **15**(3): 352-61.

Goll, M. G. and T. H. Bestor (2005). "Eukaryotic cytosine methyltransferases." Annu Rev Biochem **74**: 481-514.

Goll, M. G., F. Kirpekar, et al. (2006). "Methylation of tRNAAsp by the DNA methyltransferase homolog Dnmt2." Science **311**(5759): 395-8.

Hashimoto, H., J. R. Horton, et al. (2008). "The SRA domain of UHRF1 flips 5-methylcytosine out of the DNA helix." Nature **455**(7214): 826-9.

Hata, K., M. Okano, et al. (2002). "Dnmt3L cooperates with the Dnmt3 family of de novo DNA methyltransferases to establish maternal imprints in mice." Development **129**(8): 1983-93.

Herman, J. G., J. Jen, et al. (1996). "Hypermethylation-associated inactivation indicates a tumor suppressor role for p15INK4B." Cancer Res **56**(4): 722-7.

Herman, J. G., F. Latif, et al. (1994). "Silencing of the VHL tumor-suppressor gene by DNA methylation in renal carcinoma." Proc Natl Acad Sci U S A **91**(21): 9700-4.

Holliday, R. and J. E. Pugh (1975). "DNA modification mechanisms and gene activity during development." Science **187**(4173): 226-32.

Howlett, S. K. and W. Reik (1991). "Methylation levels of maternal and paternal genomes during preimplantation development." Development **113**(1): 119-27.

Jenuwein, T. and C. D. Allis (2001). "Translating the histone code." Science **293**(5532): 1074-80.

Jinno, Y., K. Sengoku, et al. (1996). "Mouse/human sequence divergence in a region with a paternal-specific methylation imprint at the human H19 locus." Hum Mol Genet **5**(8): 1155-61.

Jones, P. A. and S. M. Taylor (1980). "Cellular differentiation, cytidine analogs and DNA methylation." Cell **20**(1): 85-93.

Jones, P. A., S. M. Taylor, et al. (1982). "Cell cycle-specific reactivation of an inactive X-chromosome locus by 5-azadeoxycytidine." Proc Natl Acad Sci U S A **79**(4): 1215-9.

Jones, P. L., G. J. Veenstra, et al. (1998). "Methylated DNA and MeCP2 recruit histone deacetylase to repress transcription." Nat Genet **19**(2): 187-91.

Juttermann, R., E. Li, et al. (1994). "Toxicity of 5-aza-2'-deoxycytidine to mammalian cells is mediated primarily by covalent trapping of DNA methyltransferase rather than DNA demethylation." Proc Natl Acad Sci U S A **91**(25): 11797-801.

Kafri, T., M. Ariel, et al. (1992). "Developmental pattern of gene-specific DNA methylation in the mouse embryo and germ line." Genes Dev **6**(5): 705-14.

Kaneda, M., T. Sado, et al. (2004). "Role of de novo DNA methyltransferases in initiation of genomic imprinting and X-chromosome inactivation." Cold Spring Harb Symp Quant Biol **69**: 125-9.

Kapranov, P., J. Cheng, et al. (2007). "RNA maps reveal new RNA classes and a possible function for pervasive transcription." Science **316**(5830): 1484-8.

Kapranov, P., A. T. Willingham, et al. (2007). "Genome-wide transcription and the implications for genomic organization." Nat Rev Genet **8**(6): 413-23.

Karpf, A. R., B. C. Moore, et al. (2001). "Activation of the p53 DNA damage response pathway after inhibition of DNA methyltransferase by 5-aza-2'-deoxycytidine." Mol Pharmacol **59**(4): 751-7.

Koerner, M. V., F. M. Pauler, et al. (2009). "The function of non-coding RNAs in genomic imprinting " Development(136): 1771-1783.

Lei, H., S. P. Oh, et al. (1996). "De novo DNA cytosine methyltransferase activities in mouse embryonic stem cells." Development **122**(10): 3195-205.

Lemaire, M., L. F. Momparler, et al. (2009). "Inhibition of cytidine deaminase by zebularine enhances the antineoplastic action of 5-aza-2'-deoxycytidine." Cancer Chemother Pharmacol **63**(3): 411-6.

Leonhardt, H., A. W. Page, et al. (1992). "A targeting sequence directs DNA methyltransferase to sites of DNA replication in mammalian nuclei." Cell **71**(5): 865-73.

Lerchner, W. and D. P. Barlow (1997). "Paternal repression of the imprinted mouse Igf2r locus occurs during implantation and is stable in all tissues of the post-implantation mouse embryo." Mech Dev **61**(1-2): 141-9.

Li, E. (2002). "Chromatin modification and epigenetic reprogramming in mammalian development." Nat Rev Genet **3**(9): 662-73.

Li, E., C. Beard, et al. (1993). "Role for DNA methylation in genomic imprinting." Nature **366**(6453): 362-5.

Li, E., T. H. Bestor, et al. (1992). "Targeted mutation of the DNA methyltransferase gene results in embryonic lethality." Cell **69**(6): 915-26.

Li, L. H., E. J. Olin, et al. (1970). "Cytotoxicity and mode of action of 5-azacytidine on L1210 leukemia." Cancer Res **30**(11): 2760-9.

Liang, G., F. A. Gonzales, et al. (2002). "Analysis of gene induction in human fibroblasts and bladder cancer cells exposed to the methylation inhibitor 5-aza-2'-deoxycytidine." Cancer Res **62**(4): 961-6.

Lyle, R., D. Watanabe, et al. (2000). "The imprinted antisense RNA at the Igf2r locus overlaps but does not imprint Mas1." Nat Genet **25**(1): 19-21.

Lynch, C. A., B. Tycko, et al. (2002). "Reactivation of a silenced H19 gene in human rhabdomyosarcoma by demethylation of DNA but not by histone hyperacetylation." Mol Cancer **1**: 2.

McGrath, J. and D. Solter (1984). "Completion of mouse embryogenesis requires both the maternal and paternal genomes." Cell **37**(1): 179-83.

McGrath, J. and D. Solter (1984). "Maternal Thp lethality in the mouse is a nuclear, not cytoplasmic, defect." Nature **308**(5959): 550-1.

Menendez, L., B. B. Benigno, et al. (2004). "L1 and HERV-W retrotransposons are hypomethylated in human ovarian carcinomas." Mol Cancer **3**: 12.

Merlo, A., J. G. Herman, et al. (1995). "5' CpG island methylation is associated with transcriptional silencing of the tumour suppressor p16/CDKN2/MTS1 in human cancers." Nat Med **1**(7): 686-92.

Mikkelsen, T. S., M. Ku, et al. (2007). "Genome-wide maps of chromatin state in pluripotent and lineage-committed cells." Nature **448**(7153): 553-60.

Miranda, T. B. and P. A. Jones (2007). "DNA methylation: the nuts and bolts of repression." J Cell Physiol **213**(2): 384-90.

Monk, D., P. Arnaud, et al. (2006). "Limited evolutionary conservation of imprinting in the human placenta." Proc Natl Acad Sci U S A **103**(17): 6623-8.

Monk, M., M. Boubelik, et al. (1987). "Temporal and regional changes in DNA methylation in the embryonic, extraembryonic and germ cell lineages during mouse embryo development." Development **99**(3): 371-82.

Neumann, B., P. Kubicka, et al. (1995). "Characteristics of imprinted genes." Nat Genet **9**(1): 12-3.

Nieto, M., E. Samper, et al. (2004). "The absence of p53 is critical for the induction of apoptosis by 5-aza-2'-deoxycytidine." Oncogene **23**(3): 735-43.

Norris D.P., P., Kay G.F., Penny G.D., Brockdorff N., Sheardown S.A., and Rastan S. (1994). "Evidence that random and imprinted Xist expression is controlled by preemptive methylation." Cell(77): 41-51.

Oka, M., A. M. Meacham, et al. (2005). "De novo DNA methyltransferases Dnmt3a and Dnmt3b primarily mediate the cytotoxic effect of 5-aza-2'-deoxycytidine." Oncogene **24**(19): 3091-9.

Okano, M., S. Xie, et al. (1998). "Cloning and characterization of a family of novel mammalian DNA (cytosine-5) methyltransferases." Nat Genet **19**(3): 219-20.

Oki, Y., E. Aoki, et al. (2007). "Decitabine--bedside to bench." Crit Rev Oncol Hematol **61**(2): 140-52.

Olek, A. and J. Walter (1997). "The pre-implantation ontogeny of the H19 methylation imprint." Nat Genet **17**(3): 275-6.

Oswald, J., S. Engemann, et al. (2000). "Active demethylation of the paternal genome in the mouse zygote." Curr Biol **10**(8): 475-8.

Oudejans, C. B., B. Westerman, et al. (2001). "Allelic IGF2R repression does not correlate with expression of antisense RNA in human extraembryonic tissues." Genomics **73**(3): 331-7.

Palii, S. S., B. O. Van Emburgh, et al. (2008). "DNA methylation inhibitor 5-Aza-2'-deoxycytidine induces reversible genome-wide DNA damage that is distinctly influenced by DNA methyltransferases 1 and 3B." Mol Cell Biol **28**(2): 752-71.

Pastor-Anglada, M., P. Cano-Soldado, et al. (2005). "Cell entry and export of nucleoside analogues." Virus Res **107**(2): 151-64.

Paulsen, M., O. El-Maarri, et al. (2000). "Sequence conservation and variability of imprinting in the Beckwith-Wiedemann syndrome gene cluster in human and mouse." Hum Mol Genet **9**(12): 1829-41.

Pinto, A., V. Attadia, et al. (1984). "5-Aza-2'-deoxycytidine induces terminal differentiation of leukemic blasts from patients with acute myeloid leukemias." Blood **64**(4): 922-9.

Rai, K., S. Chidester, et al. (2007). "Dnmt2 functions in the cytoplasm to promote liver, brain, and retina development in zebrafish." Genes Dev **21**(3): 261-6.

Regha, K., M. A. Sloane, et al. (2007). "Active and repressive chromatin are interspersed without spreading in an imprinted gene cluster in the mammalian genome." Mol Cell **27**(3): 353-66.

Reik, W. and J. Walter (2001). "Genomic imprinting: parental influence on the genome." Nat Rev Genet **2**(1): 21-32.

Repaske, R., P. E. Steele, et al. (1985). "Nucleotide sequence of a full-length human endogenous retroviral segment." J Virol **54**(3): 764-72.

Rhee, I., K. E. Bachman, et al. (2002). "DNMT1 and DNMT3b cooperate to silence genes in human cancer cells." Nature **416**(6880): 552-6.

Riggs, A. D. (1975). "X inactivation, differentiation, and DNA methylation." Cytogenet Cell Genet **14**(1): 9-25.

Salem, C. E., I. D. Markl, et al. (2000). "PAX6 methylation and ectopic expression in human tumor cells." Int J Cancer **87**(2): 179-85.

Sambrook, J., E. F. Fritsch, et al. (1989). Molecular cloning : a laboratory manual. Cold Spring Harbor, N.Y., Cold Spring Harbor Laboratory.

Santi, D. V., A. Norment, et al. (1984). "Covalent bond formation between a DNA-cytosine methyltransferase and DNA containing 5-azacytosine." Proc Natl Acad Sci U S A **81**(22): 6993-7.

Schmelz, K., M. Wagner, et al. (2005). "5-Aza-2'-deoxycytidine induces p21WAF expression by demethylation of p73 leading to p53-independent apoptosis in myeloid leukemia." Int J Cancer **114**(5): 683-95.

Seidl, C. I., S. H. Stricker, et al. (2006). "The imprinted Air ncRNA is an atypical RNAPII transcript that evades splicing and escapes nuclear export." EMBO J **25**(15): 3565-75.

Shemer, R., Y. Birger, et al. (1997). "Structure of the imprinted mouse Snrpn gene and establishment of its parental-specific methylation pattern." Proc Natl Acad Sci U S A **94**(19): 10267-72.

Simpson, A. J., O. L. Caballero, et al. (2005). "Cancer/testis antigens, gametogenesis and cancer." Nat Rev Cancer **5**(8): 615-25.

Sleutels, F., R. Zwart, et al. (2002). "The non-coding Air RNA is required for silencing autosomal imprinted genes." Nature **415**(6873): 810-3.

Smrzka, O. W., I. Fae, et al. (1995). "Conservation of a maternal-specific methylation signal at the human IGF2R locus." Hum. Mol. Genet. **4**(10): 1945-1952.

Sorm, F., A. Piskala, et al. (1964). "5-Azacytidine, a new, highly effective cancerostatic." Experientia **20**(4): 202-3.

Spahn, L. and D. P. Barlow (2003). "An ICE pattern crystallizes." Nat Genet **35**(1): 11-2.

Stegmann, A. P., M. W. Honders, et al. (1995). "De novo induced mutations in the deoxycytidine kinase (dck) gene in rat leukemic clonal cell lines confer resistance to cytarabine (AraC) and 5-aza-2'-deoxycytidine (DAC)." Leukemia **9**(6): 1032-8.

Stoger, R., P. Kubicka, et al. (1993). "Maternal-specific methylation of the imprinted mouse Igf2r locus identifies the expressed locus as carrying the imprinting signal." Cell **73**(1): 61-71.

Stresemann, C., B. Brueckner, et al. (2006). "Functional diversity of DNA methyltransferase inhibitors in human cancer cell lines." Cancer Res **66**(5): 2794-800.

Stresemann, C. and F. Lyko (2008). "Modes of action of the DNA methyltransferase inhibitors azacytidine and decitabine." Int J Cancer **123**(1): 8-13.

Surani, M. A., S. C. Barton, et al. (1984). "Development of reconstituted mouse eggs suggests imprinting of the genome during gametogenesis." Nature **308**(5959): 548-50.

Szabo, P. E. and J. R. Mann (1995). "Allele-specific expression and total expression levels of imprinted genes during early mouse development: implications for imprinting mechanisms." Genes Dev **9**(24): 3097-108.

Szabo, P. E. and J. R. Mann (1995). "Biallelic expression of imprinted genes in the mouse germ line: implications for erasure, establishment, and mechanisms of genomic imprinting." Genes Dev **9**(15): 1857-68.

Tada, T., M. Tada, et al. (1998). "Epigenotype switching of imprintable loci in embryonic germ cells." Dev Genes Evol **207**(8): 551-61.

Takai, D. and P. A. Jones (2002). "Comprehensive analysis of CpG islands in human chromosomes 21 and 22." Proc Natl Acad Sci U S A **99**(6): 3740-5.

Taylor, S. M. and P. A. Jones (1979). "Multiple new phenotypes induced in 10T1/2 and 3T3 cells treated with 5-azacytidine." Cell **17**(4): 771-9.

Uchida, T., T. Kinoshita, et al. (1997). "Hypermethylation of the p15INK4B gene in myelodysplastic syndromes." Blood **90**(4): 1403-9.

Verhaagh, S., N. Schweifer, et al. (1999). "Cloning of the mouse and human solute carrier 22a3 (Slc22a3/SLC22A3) identifies a conserved cluster of three organic cation transporters on mouse chromosome 17 and human 6q26-q27." Genomics **55**(2): 209-18.

Verona, R. I., M. R. Mann, et al. (2003). "Genomic imprinting: intricacies of epigenetic regulation in clusters." Annu Rev Cell Dev Biol **19**: 237-59.

Vidal, D. O., V. A. Paixao, et al. (2007). "Aberrant methylation in pediatric myelodysplastic syndrome." Leuk Res **31**(2): 175-81.

Walsh, C. P., J. R. Chaillet, et al. (1998). "Transcription of IAP endogenous retroviruses is constrained by cytosine methylation." Nat Genet **20**(2): 116-7.

Wang, H., Y. Zhao, et al. (2008). "An ATM- and Rad3-related (ATR) signaling pathway and a phosphorylation-acetylation cascade are involved in activation of p53/p21Waf1/Cip1 in response to 5-aza-2'-deoxycytidine treatment." J Biol Chem **283**(5): 2564-74.

Wang, Z. Q., M. R. Fung, et al. (1994). "Regulation of embryonic growth and lysosomal targeting by the imprinted Igf2/Mpr gene." Nature **372**(6505): 464-7.

Weisenberger, D. J., M. Campan, et al. (2005). "Analysis of repetitive element DNA methylation by MethyLight." Nucleic Acids Res **33**(21): 6823-36.

Wutz, A., O. W. Smrzka, et al. (1997). "Imprinted expression of the Igf2r gene depends on an intronic CpG island." Nature **389**(6652): 745-9.

Xu, Y., C. G. Goodyer, et al. (1993). "Functional polymorphism in the parental imprinting of the human IGF2R gene." Biochem Biophys Res Commun **197**(2): 747-54.

Yamasaki, Y., T. Kayashima, et al. (2005). "Neuron-specific relaxation of Igf2r imprinting is associated with neuron-specific histone modifications and lack of its antisense transcript Air." Hum Mol Genet **14**(17): 2511-20.

Yoder, J. A. and T. H. Bestor (1998). "A candidate mammalian DNA methyltransferase related to pmt1p of fission yeast." Hum Mol Genet **7**(2): 279-84.

Yoder, J. A., N. S. Soman, et al. (1997). "DNA (cytosine-5)-methyltransferases in mouse cells and tissues. Studies with a mechanism-based probe." J Mol Biol **270**(3): 385-95.

Yoo, C. B. and P. A. Jones (2006). "Epigenetic therapy of cancer: past, present and future." Nat Rev Drug Discov **5**(1): 37-50.

Zeschnigk, M., B. Schmitz, et al. (1997). "Imprinted segments in the human genome: different DNA methylation patterns in the Prader-Willi/Angelman syndrome region as determined by the genomic sequencing method." Hum Mol Genet **6**(3): 387-95.

Zhu, W. G., T. Hileman, et al. (2004). "5-aza-2'-deoxycytidine activates the p53/p21Waf1/Cip1 pathway to inhibit cell proliferation." J Biol Chem **279**(15): 15161-6.

Zwart, R., F. Sleutels, et al. (2001). "Bidirectional action of the Igf2r imprint control element on upstream and downstream imprinted genes." Genes Dev **15**(18): 2361-6.